



저작자표시-비영리-변경금지 2.0 대한민국

이용자는 아래의 조건을 따르는 경우에 한하여 자유롭게

- 이 저작물을 복제, 배포, 전송, 전시, 공연 및 방송할 수 있습니다.

다음과 같은 조건을 따라야 합니다:



저작자표시. 귀하는 원저작자를 표시하여야 합니다.



비영리. 귀하는 이 저작물을 영리 목적으로 이용할 수 없습니다.



변경금지. 귀하는 이 저작물을 개작, 변형 또는 가공할 수 없습니다.

- 귀하는, 이 저작물의 재이용이나 배포의 경우, 이 저작물에 적용된 이용허락조건을 명확하게 나타내어야 합니다.
- 저작권자로부터 별도의 허가를 받으면 이러한 조건들은 적용되지 않습니다.

저작권법에 따른 이용자의 권리는 위의 내용에 의하여 영향을 받지 않습니다.

이것은 [이용허락규약\(Legal Code\)](#)을 이해하기 쉽게 요약한 것입니다.

[Disclaimer](#)

**A DISSERTATION
FOR THE DEGREE OF DOCTOR OF PHILOSOPHY**

**The suppression of oncogenic activity under the influence of BRM270
in stem like cancer initiating cells mediated carcinogenesis**

Raj Kumar Mongre

**GRADUATE SCHOOL
JEJU NATIONAL UNIVERSITY**

June, 2016

**The suppression of oncogenic activities under the
influence of BRM270 in stem like cancer initiating
cells mediated carcinogenesis**

Raj Kumar Mongre

(Supervised by Professor Dong Kee Jeong)

A dissertation submitted in the partial fulfillment of the requirement for the degree
of
Doctor of Philosophy

2016. 06

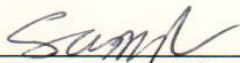
This dissertation has been examined and approved by



Professor Dong Sun Lee, Chairman, Department of Biotechnology, Jeju National University



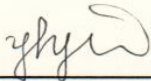
Professor Dong Kee Jeong, Vice Chairman, Department of Animal Biotechnology, Jeju National University



Professor Ki-Duk Song, Department of Animal Biotechnology, Chonbuk National University



Professor Somi Kim Cho, Department of Biotechnology, Jeju National University



Professor Young-Heun Jee, College of Veterinary Medicine, Jeju National University

GRADUATE SCHOOL
JEJU NATIONAL UNIVERSITY

THIS WORK IS DEDICATED TO MY BELOVED PARENTS

“An the attempt to make scientific discoveries, every problem is an opportunity and the more difficult the problem, the greater will be the importance of its solution”

(E.O. Wilson)

ACKNOWLEDGMENTS

This work was carried out during September, 2013 to June, 2016 at the Laboratory of Animal Genetic Engineering and Stem Cell Biology, Department of Animal Biotechnology and Advance Next Generation Convergence Technology, Faculty of Biotechnology, Jeju National University, Jeju, Republic of Korea.

First and foremost I would like to express my gratitude to my esteemed supervisor Professor Dong Kee Jeong for giving me the opportunity to work in such an interesting motivating field as cancer stem research and for being inspiring and guiding me in right directions within a high degree of freedom. His overly enthusiasm and integral view on research and his mission for providing only high quality work and not less, has made a deep impression on me. I owe him lot of gratitude for having me shown this way of research. Besides of being an excellent supervisor, Prof Jeong was as close as a relative and a good friend to me. I am really glad that I have come to get know Prof. Dong Kee Jeong in my life.

Also, I wish to offer my humble gratitude to professors of my department, Animal Biotechnology Prof. Oh Sung Jong, Prof. Youg Hoon Yang, Prof. Min Soo Kang, Prof. Wang Shik Lee, Prof. Ryu Youn-Chul, Do, Kyoung-tag. From the Department of Advance Next Generation Convergence, Prof. Dong Sun Lee, Prof. Somi Kim Cho and Prof. Young-Heun Jee (College of Veterinary Medicine) for their inspiring and encouraging way to guide me to a deeper understanding of knowledge, and their invaluable comments during the course work.

I also would like to thank Prof. Ki-Duk Song, Department of Animal Biotechnology, Chonbuk National University, Republic of Korea for his guidance and valuable suggestions.

My heartiest thanks to our lab members Dr. Neelesh Sharma, Dr. Simrinder Sodhi, Dr. Mrinmoy Ghosh, Dr. Taeho-Kwon, Nam-Eun Kim, Hyun-Ju Kang, Jeong-Hyun Kim, Do Luong Huynh, Zhang Ziao Ziao, Dr. Meeta Gera, Mr. Pradeep Adhikari and Miss. TAN Chandimali for love, timely support and for a pleasant working atmosphere during my stay in laboratory of Animal Genetic Engineering and Stem Cell Biology.

Special thanks to my friends and seniors Dr. Prashant Sharma, Dr. Anil Khambampati, Dr. Mayank Anand, Mr. Rajveer Joshi, Dr. Nagmalleswara Rao Alluri, Dr. Markandan Ganeshan, Dr. Ganesh Kumar Veerasubramani, Dr. Chandra Bhushan Mishra, Dr. Sikha Kumari,

Dr. Namrata Kumari, Miss Shama Rukhshar Khan and Mr. Adiya Raj Kaushal for encouragement, help and all kind of support. I am also thankful to Prof. Vinod Singh for constant moral support. I thank them all for giving me so many memories to cherish during my stay in Jeju. I also thank all the members of JISO who has been very cooperative and supportive.

Many thanks to institute for School of Applied Biotechnology funded by Korean government for supporting me during my stay in Korea. Also, Graduate school of Jeju University has been grateful to wave the tuition fee for my doctoral studies. I thank RDA and BRM which provided the funds for presenting the research work held in Korea and abroad.

I am also thankful to my teacher's Prof. Anil Bajpai, Prof. Jaya Bajpai, Prof. Prashant Selot, Prof. PL Ahirwal, Prof. Vinoy Shrivastava, Prof. Manisha Tiwari, and Prof. Pratibha Mehta Luthra, India.

I am fortunate enough to have chance to thank to Mrs. Chitrlekha Thakur (Maa Ji), Mr. Deepak Singh Thakur (Dada ji) and Mr. Vivek Singh Thakur, Sri Genda Lal Kewat for your extremely all kind of support and helps.

Finally, I will never find words enough to express the gratitude that I owe to my parents and family members. Their tender love and affection has always been the cementing force for building the blocks of my academic career. The all round support rendered by them provided the much needed stimulant to sail through the phases of stress and strain.

I would like to thank all those whom I have not mentioned above but helped me in numerous ways to my success.

ABSTRACT

The discovery and development of anticancer drugs, especially cytotoxic agents are a challenging task and differ drastically from the drug development process for any other diseases. Current therapy of cancer is suffering from numerous obstacles such as severe side effect, normal cell cytotoxicity as well as anticancer drug resistance. Therefore, discovery of novel agent which may provide better option to control cancer is always appreciable. Herbal products are always a better choice to explore as anticancer agents because these products do not exerts side effects like synthetic molecules. Phyto-products a have been considered as conducive for cancer anticipation. Numerous preclinical and clinical studies have established plant derived substances as suitable and effective candidates for treating various types of cancers due to their broad chemical diversity. Such phyto-products can block the action of carcinogens on target tissues thereby suppressing cancer progression. Hence, the risk of cancer can be repressed by taking more fruits, vegetables and other related plant products. Meta-analyses of cohort and case control studies show significant confirmation for cancer defensive effects with fruit use as they are good sources of vitamins and minerals. In this regards, we have investigated anticancer efficacy along with the mechanism of action of a natural super cocktail BRM270

In our investigation, Phyto-drug BRM270 appeared as a potent cytotoxic agent against osteosarcoma cells. In the first chapter, we have proved that BRM270 is a inhibitor of NF- κ B. The nuclear factor kappa B (NF- κ B) and interleukin-6 (IL-6) contribute to multiple drug resistance (MDR) in tumor chemotherapy. The essential phenomenon of oncogenic activation of NF- κ B in cancer-initiating cells showing MDR resulting from increased IL-6 expression is still unclear. Cancer stem cells (CSCs) have been the objective of intensive study. The aim of this study was to investigate the selective and potential efficacy of BRM270 against stem like cancer-

initiating cells (SLCICs) via the molecular mechanisms of its anti-cancerous effects. Co-regulation of NF- κ B and Cdk6 might be a new arena to mitigate the tumorigenesis. In the current study phyto-drug based approach has provided a new avenue in understanding the amelioration and regulatory mechanisms in CSCs. In the present study, an *in-vivo* tumor metastasis model of osteosarcoma was established by injecting Cal72 and SaOS-2 SLCICs into the right lower flank of nude mice. Later the development of tumor was analyzed by LICOR Biosciences (pearl image analyzer). Significant suppression of the activation of NF- κ B and LPS-induced gene expression and apoptosis by BRM270 was confirmed by FACS, western blot and qPCR. Further, both p65 and Cdk6 significantly ($P < 0.05$) overexpressed in BRM270 non-treated Cal72 SLCICs than treated group. BRM270 directly dephosphorylated RelA and selectively inhibited NF- κ B transcriptional activity, resulting in decreased expression of interleukin-6, cytokines implicated in cancer metastasis. BRM270 mediated cell shrinkage, pyknosis, karyorrhexis and programmed cell death (PCD) were observed by Hoechst 33342 staining while flow cytometry analysis showed the significant ($P < 0.05$) decrease in cell population from G0-G1 phases. These findings suggest that activation of the oncogenic Cdk6-NF- κ B pathway, resulting from increased IL-6 expression, plays a central role in CD133 expressing SLCICs augmented MDR and neoplasia. This study proposes the insight of targeting of NF- κ B, Cdk6 with IL-6 as potential targets for PCD and treatment of chemotherapeutic resistance of CSCs to design novel therapies to eliminate them. For more confirmation, we next conducted *in-vivo* model of adenolung carcinoma via epigenetic modulation of epithelial to mesenchymal transition which is abrogated by BRM270.

Moreover, in the chapter 2 our investigations have shown that BRM270 plays a significant role in the mesenchymal transition EMT reversal by inhibiting NF- κ B. To induce

tumor metastasis by induction EMT, we transfected oncogenic *hLCN2* gene to A549 tumor initiating cells. Tumor initiating cancer stem like cells (TICSCs) have recently become the object of intensive study. Human-Lipocalin-2 (*hLCN2*) acts as a biomarker for cancers. The aim of the current study was to explore new insights regarding the potential role of *LCN2* in inducing epithelial to mesenchymal transition (EMT) by transfecting *LCN2* into CD133⁺-A549-TICSCs and its cross talk with the NF- κ B signaling pathway in adeno-carcinoma of lung which has blocked by BRM270. Further EMT was confirmed by transcriptomic analysis, immuno-blotting and immunocyto/histochemical analyses. Tumorigenesis and metastasis were further confirmed by molecular therapeutics tracer 2DG infrared optical probe in BALB/cSic-nude mice. It was observed that the CD133⁺-expressing-*LCN2*-A549 TICSCs population increased in adeno-carcinoma of lung than in the normal lung tissue. The expressions of genes involved in stemness, adhesion, motility and drug efflux were higher in these cells than in their non-*LCN2* expressing counterparts. The current study revealed that elevated expression of *LCN2* significantly induced metastasis via EMT. Over-expression of *LCN2* has significantly increased stemness and tumor metastasis by modulating NF- κ B cellular signaling. BRM270, a novel inhibitor of NF- κ B plays a significant role in the EMT reversal. BRM270, a naturaceutical induces cell shrinkage, karyorrhexis and programmed cell death (PCD) which were observed by Hoechst 33342 staining while flowcytometry analysis showed significant ($P<0.05$) decrease in cell population from G0-G1 phases. Also, 2DG guided *in vivo* model revealed that BRRM270 significantly ($P<0.0003$) reduced tumor metastasis and increased percent survival in real time with complete resection. An elaborated work on the novel concept with respect to linking of naturaceuticals as selective and potential anticancer agent that eliminates the elevated *LCN2* induced EMT and tumor dissemination through cooperation with the NF- κ B signaling as the baseline data for the planning

of new therapeutic strategies has been conducted for the first time. Our results also illustrate a molecular mechanistic approach for 2DG-guided molecular imaging based cancer therapy using BRM270 as a novel cancer therapeutic drug to enhance the effect of Doxorubicin (Dox) resistant *LCN2* induced metastasis of solid tumors in nude mice. After this metastasis model, next we confirmed the efficacy of BRM270 against hepatocellular carcinoma.

Hepatocellular carcinoma (HCC) is a major threat to human health worldwide and development of novel antineoplastic drug is urgently needed. BRM270, a natural plant product, is a proprietary combination of different phytochemical extracts, has been shown to be effective against a wide range of tumors. In this study, the antitumor effect of BRM270 on human hepatoma cell line, CD133⁺ expressing stem-like cancer-initiating cells (MSCICs) HepG-2 and SNU-398, and the mechanism involved have been investigated. Multistep intervention models including EZ-CyTox-WST assay, cell cycle regulation and apoptosis were analyzed using Hoechst 33342 staining and flow-cytometric Annexin-VI/PI double staining method. Gene expression profiling by qPCR and specific cellular protein expressions were measured using immunocytochemistry and western blot analysis. *In vivo* imaging in mice model using 2DG-(2-Deoxy-D-Glucose) optical-probe was performed to delineate the size and extent of metastasized tumor. Cellular and molecular traits revealed a typical CyclinD1-dependent DNA-fragmentation, cell cycle arrest and Casp-3-mediated apoptosis after treatment with BRM270. Moreover, qPCR/blot analysis and *in-vivo* imaging study revealed significant attenuation ($P < 0.05$) of c-Myc, Bcl2 and c-Jun involved in HCC metastasis. The present study indicates that BRM270 can effectively inhibit proliferation and induce apoptosis in hepatoma HepG-2 and SNU -398 cells and the apoptosis induction is related with down-regulation of CyclinD1 mediated c-Jun-JNK

apoptotic pathway. Lastly, BRM270 effectively inhibits cells proliferation by induction of Let-7 miRNA.

MicroRNA (miRNA) is a post transcription modulator and its abnormal expression has been observed in various types of cancers. Here we show that the *let-7* miRNA negatively regulates *LIN28*. Elevated level of *LIN28* simultaneously suppresses *let-7* and activates mitochondrial intrinsic apoptotic gene expression in a *let-7*-dependent manner. Both transcriptomic and translational analysis showed the efficacy of BRM270 as prominent anticancer agents to augment apoptosis by upregulation of *Let-7* mRNA while the simultaneously inversely *LIN-28* expression. In addition, proteome microarray also revealed that BRM270 significant induces expression of intrinsic apoptotic proteins. The *Let-7* expression is lower in SLCICs tumors than in normal cells, while *LIN-28* MRNA is significantly higher in tumor samples, providing a possible mechanism to *let-7* in SLCICs induced carcinogenesis. A greater understanding of what controls *let-7* expression might enable the development of treatments to fight or prevent many cancers.

Thus, our series of experiment in various *in-vitro* as well as *in-vivo* model successfully established BRM270, as a potent anticancer agent without showing significant toxicity in normal cells. Hence, these explorations open a new door to slow down cancer progression by use of safe drug BRM270 and might be save more and more mankind with this phyto-drug.

초 록

항암제 개발은 도전적인 일이며, 다른 종류의 질병에 대한 치료약을 개발하는 것과는 분명하게 구별되는 일이다. 최근 들어, 항암치료는 정상 세포에 대한 독성과 약제에 대한 암세포에서의 내성 등 부작용으로 인해 한계에 부딪히고 있다. 이에 암에 대하여 더 효과적으로 조절할 수 있는 효율적인 약제의 발견과 개발은 항상 주목되어왔다. 약초와 같은 천연물 유래의 물질은 합성 물질로부터 기인할 수 있는 부작용을 나타내지 않는다는 점에서 항암제로써의 가능성을 탐색하는데 우선적으로 선택된다. 이러한 식물유래의 물질들은 암 예방에 효과가 있는 것으로 여겨지고 있으며, 많은 전임상 및 임상 연구에서 식물 유래의 물질들이 갖는 화학적인 다양성을 바탕으로 여러 종류의 암을 치료하거나 예방하는데 효과적임이 증명되었다. 이러한 식물유래 물질들은 다양한 종류의 원암 전사 조절인자나 원암 단백질들의 작용을 억제함으로써 특정 조직에서 작용할 수 있는 발암 물질의 기능을 막을 수 있다. 이러한 연구 결과들에 근거하여, 암에 의한 위험은 더 많은 과일이나 채소, 혹은 관련된 식물 유래의 물질을 섭취함으로써 억제될 수 있다고 여겨진다. 더불어, 특정 집단에 대한 메타분석과 사례 연구에서는 비타민과 무기질의 훌륭한 섭취원인 과일이 암 발생을 억제하는데 매우

효과적임을 확연하게 증명하고 있다. 이와 같은 식물 유래 물질의 효과에 근거하여, 본 연구에서는 천연물 유래의 조성물인 BRM270의 항암 효과와 기작에 대해 규명하고자 하였다.

본 연구에서 사용된 phyto-drug인 BRM270은 인간 골육종 세포에 대하여 잠재적인 암세포독성 효과를 나타내었다. 이러한 BRM270이 갖는 암세포독성 효과에 대하여 논문 발표의 첫 번째 chapter에서는 BRM270이 NF- κ B의 억제제로 작용하는 것을 증명하였다. Nuclear factor kappa B(NF- κ B)와 interleukin-6(IL6)는 암에 대한 화학적요법(항암제 요법)에서 다약제 내성(multi drug resistance, MDR)을 일으키는데 작용하는 것으로 알려져 있다. IL-6의 발현이 증가됨에 따라 MDR이 나타나는 cancer-initiating cell에서 NF- κ B가 활성화되는 것으로부터 기인하는 중요한 현상에 대해서는 아직까지 정확히 규명되지 않았다. 암줄기세포(Cancer stem cells, CSCs)는 최근 많은 연구를 통해 주목받고 있는 주요 키워드이다. 이에, 본 연구에서는 BRM270이 stem like cancer-initiating cells(SLICs)에 대한 잠재적이고 선택적인 활성화에 대한 분자적 수준의 기작을 밝힘으로써 BRM270이 갖는 항암효과에 대해 규명하고자 하였다. NF- κ B와 Cdk6를 동시에 조절하는 것은 종양이 형성되는 것을 억제하는 또 하나의 관점이 될 수

있다. 더불어, phyto-drug에 근거한 연구를 진행함에 따라 CSCs 내에서의 조절 기작과 이를 치료할 수 있는 기작에 대한 새로운 안목을 제안할 수 있었다. CSCs의 기작 연구에 대한 *in-vivo* 모델로써 Cal-72과 SaOS-2 SLCIC를 누드 마우스에 이식함으로써 종양조직을 형성시키고 시간 경과에 따른 마우스 내의 암 진행 형상을 LICOR Biosciences (pearl image analyzer)를 통해 분석하였다.

활성화와 LPS 유도의 유전자 발현 정도가 BRM270에 의해 효율적으로 억제되고 세포예정사인 apoptosis가 유도되는 것을 FACS analysis, Western blot analysis, qPCR analysis를 통해 확인하였다. 더 나아가 BRM270을 처리하지 않은 Cal-72 SLCIC 세포 대비 BRM270을 처리한 Cal-72 SLCIC 세포에서 p65와 Cdk6의 발현양이 두드러지게 감소한 것을 확인하였다. BRM270은 RelA의 인산기를 직접적으로 제거하고 NF- κ B의 전사 활성을 억제하는 것으로 여겨지며, 결과적으로 암의 전이와 관련되어 있는 IL-6와 cytokine의 발현을 감소시켰다. BRM270 처리로 인한 cell shrinkage, pyknosis, karyorrhexis, programmed cell death(PCD)는 Hoechst 33342 staining를 통해 확인하였으며, flow cytometry analysis를 통해 G0-G1기의 세포 수가 현저하게 감소하는 것을 확인하였다. 이러한 결과들을 통해 Cal-72 이나 SaOS-2 SLCICs와 같이

CD133가 과발현 되어있는 SLCIC에서는 IL-6의 발현양 증가로 인한 Cdk6-NF- κ B pathway의 활성화가 일어나며, 이러한 활성화는 결과적으로 다약제내성과 종양형성을 증가시키는데 핵심적인 역할을 하는 것으로 판단된다. 결론적으로, 본 연구의 결과를 종합하였을 때, CSC에 대한 약제 내성을 치료하고 PCD를 일으키는데 NF- κ B, Cdk6, IL-6를 치료를 위한 표적 단백질로 제안할 수 있었으며, BRM270이 해당 단백질들을 효과적으로 조절할 수 있음을 증명하였다. 이러한 항암제로서의 가능성에 근거하여, 추가적인 연구를 통해 폐선암의 상피세포-간엽세포전환(epithelial to mesenchymal transition, EMT)에 대한 후성유전적 조절(epigenetic modulation)로서 억제되는 효과를 *in-vivo* 모델에서 수행하였다.

두 번째 chapter에서는 BRM270이 NF- κ B를 억제함에 따라 EMT 현상이 확연하게 회복되는 데에 기여함을 증명하였다. 암의 전이성과 EMT 현상에 대한 연구의 모델을 구축하기 위하여, A549 tumor initiating 세포에 hLCN2 유전자를 주입하였다. 본 연구에서 주목한 Tumor initiating cancer stem like cells(TICSCs)는 최근 주요 연구에서 각광받고 있는 주제이며, Human-Lipcalin-2(hLCN2)는 암에 대한 지표로서 사용되는 유전자이다. 이에 본 연구에서는 BRM270의 조절 작용에 근거하여 LCN2를 주입한

CD133⁺-A549-TICSCs에서 EMT가 일어날 때 *LCN2*가 갖는 역할과 *LCN2*와 NF- κ B pathway 간의 상호작용에 대해 규명하고자 하였다. *LCN2*를 삽입함에 따라 나타나는 EMT 현상은 transcriptomic analysis, immune-blotting, immunocyto/histochemical analysis를 통해 확인하였다. 더 나아가, 종양 형성능과 전이성은 누드 마우스 모델에 2DG(2-Deoxy-D-Glucose)를 적외선 광학 지표로써 사용함으로써 측정하였다. 이러한 실험 결과들을 통해 CD133⁺-expressing-*LCN2*-A549 TICSCs는 정상적인 폐 조직에서보다 폐선암이 형성되어 있는 군집에서 관찰됨을 알 수 있었다. 더불어, 줄기세포성(stemness), 부착성(adhesion), 이동능(motility), 약물분비능(drug efflux)에 관련된 유전자들 또한 non-*LCN2* expressing 군집보다 CD133⁺-expressing-*LCN2*-A549 TICSCs에서 더 많이 전사되고 있었다. 최근의 연구에서 *LCN2*의 과발현은 EMT를 통한 전이성을 증가하는 것을 밝혀냈다. *LCN2*의 과발현은 줄기세포성(stemness)와 종양 전이성(tumor metastasis)를 확연하게 증가시키는데, 이러한 증가는 NF- κ B에 대한 신호 전달 체계를 세포 수준에서 조절함으로써 나타나는 것으로 판단된다. 앞서 언급된 바와 같이 NF- κ B의 억제제로 작용하는 BRM270은 이러한NF- κ B 매개로 일어나는 EMT를 효과적으로 회복시키는데 작용하는 것이 확인되었다. 2DG를 활용한 *in vivo* 모델에서 BRM270이 암세포의 전이를 확연하게 감소시키고 생존율을 증가시킴을 관찰할 수

있었다. 천연 유래의 물질을 항암 치료의 가능성을 가진 새로운 후보물질로써 제안하기 위하여 치료 기작에 대한 기초적인 정보를 제공할 때에, NF- κ B 신호 전달 체계와 LCN2간의 상호 작용에 의한 EMT 및 종양 전이(tumor dissemination)을 후보 물질이 억제할 수 있다는 정보는 처음으로 본 연구에서 수행되고 확인된 사항이다. 이와 같이 잘 확립된 기틀을 바탕으로 수행된 연구결과들은, BRM270이 효과적이면서 새로운 항암 약제로써 Doxorubicin(Dox)에 대한 내성을 보이며 LCN2에 의한 전이성을 보이는 암에 대한 효과를 보인다는 사실을 분명하게 설명하고 있다.

세 번째 Chapter에서는 간암 세포주에 대한 BRM270의 항암 효과를 확인한 연구 결과에 대해 기술하였다. 간암(Hepatocellular carcinoma, HCC)은 전세계적으로 많은 인류의 건강을 위협하는 대표적인 암이며, 간암을 효과적으로 치료할 수 있는 약제의 개발이 절실한 상황이다. 이에 앞서 언급된 여러 종류의 암에 대하여 항암 작용에 효과를 보인 BRM270이 HCC에 대하여 가질 수 있는 항암작용에 대한 연구를 추가로 진행하였다. 본 연구에서 CD133+ expressing stem-like cancer initiating cells(MSCICs)인 HepG-2와 SNU-398세포에 대하여 BRM270은 항암 효과를 보이고 있음을 확인하고 작용하는 기작에 대한 탐색을 수행하였다. Multistep intervention model인 EZ-CyTOx-

WST assay를 포함하여 세포주기 분석과 세포자살에 대한 확인은 Hoechst 33342 staining, flow-cytometric Annexin-V/PI double staining 방법을 통해 확인하였다. 유전자 발현에 대한 프로파일링은 qPCR을 통해 이루어졌으며 특정한 단백질의 발현 정도는 immunocytochemistry와 western blot analysis를 통해 측정되었다. In vivo 마우스 모델에서 암 형성 정도와 전이 정도의 관찰은 2DG optical-probe를 이용하여 수행되었다. 세포분자적 수준의 탐색을 통해 BRM270에 의한 간암에서의 세포자살은 CyclinD1 의존적인 DNA 분절화, cell cycle arrest, Capase-3 매개의 경로를 통해 일어남을 증명하였다. 더 나아가, qPCR/blot analysis와 in-vivo imaging study를 통해 간암의 전이에 관여하는 c-Myc, Bcl2, c-Jun의 발현이 유의할 수준으로 감소함을 확인하였다. 본 연구를 통해 BRM270dl HepG-2와 SNU-398 세포에 대하여 세포자살을 일으키고 성장을 효과적으로 억제할 수 있다는 것을 확인하였는데, 이 때 일어나는 세포자살은 CyclinD1의 발현 감소를 매개로 나타나는 c-Jun-JNK 세포자살 결로를 통하는 것임을 증명할 수 있었다.

마지막으로, 추가적인 연구를 통해 BRM270이 암세포 내에서 microRNA를 통한 세포자살을 조절하는 기작에 대한 연구가 진행되었다. MicroRNA(miRNA)는 전사 후

단계에 대한 조절자로서 miRNA의 비정상적인 발현은 여러 종류의 암에서 발견되어지는 현상이다. 본 연구를 통해 *let-7* miRNA가 *LIN28*을 음성적으로 조절하는 것을 추가적으로 확인하였다. *LIN28*의 발현이 증가되어 있는 것은 *let-7*을 억제하면서 동시에 *let-7*에 의존적인 미토콘드리아를 통한 내재적 세포자살 경로의 유전자 발현을 활성화시키는 현상을 확인하였다. mRNA 수준과 단백질 수준 모두에서 BRM270은 *let-7*의 발현을 증가시킴으로써 세포자살을 일으키는 것을 확인하였다. 더불어, proteome microarray를 통해 BRM270이 내재적 세포자살 경로의 단백질들의 발현을 유도하는 것으로 확인되었다. *let-7*의 발현은 정상 세포보다 SLCICs에서 더 낮은 상태로 유지되고 있는 반면, *LIN-28*의 mRNA는 암세포에서 더욱 높은 상태로 유지되고 있었다. 추가적인 연구를 통해 무엇이 *let-7*의 발현을 조절하는지에 대해 밝히는 것이 필요하며, 이러한 연구는 더 많은 종류의 암을 치료하고 암을 이겨내는데 기여할 수 있을 것으로 여겨진다.

모든 결과를 종합하였을 때, *in-vitro*와 *in-vivo* 모델을 포함하는 일련의 연구들을 통해 BRM270이 정상세포에 대한 특정한 세포 독성이 없는 효과적인 항암 약제로써 활용될 수 있음을 증명할 수 있었다. 더불어, 본 연구의 결과들을 기초로 하여

BRM270을 암의 진행을 늦추는데 기여하는 안전한 약제로서 사용할 수 있는 새로운
기회의 창을 열었으며, 궁극적으로는 BRM270과 같은 phyto-drug으로 인해 더 많은
인류가 암에 대한 공포를 줄이고 오랜 삶을 누리는데 기여할 수 있을 것이다.

TABLE OF CONTENTS

ABSTRACT.....	iii
초 록	viii
TABLE OF CONTENTS.....	xvii
LIST OF TABLES.....	xix
LIST OF FIGURES	xx
ABBREVIATIONS	xxii
CHAPTER 1	1
INTRODUCTION	1
AIMS OF THE STUDY	5
CHAPTER 2	6
REVIEW AND LITERATURE: CANCER	6
1. Cancer: The brief keynote.....	6
2. Cancer: Prevalence.....	7
3. “Drivers” of Cancer	9
4. Pathophysiology of Cancer	9
5. Targets of Cancer Therapy.....	11
5. 1. The Extrinsic Pathway	13
5. 2. The Intrinsic Pathway	13
5. 3. Regulation of Intrinsic and extrinsic pathway	14
5. 4. p53 tumoricidal proteins and its signaling cascades	14
5. 5. NF- κ B cellular signaling pathway	15
5. 6. PI3K signal transduction.....	17
5. 7. Proteosome.....	19
6. Current Treatment of Cancer	19
7. Pitfalls in Cancer Therapy	21
8. Hypothesis and Work Plan.....	23
CHAPTER 3	26
NOVEL INHIBITOR BRM270 DOWN-REGULATES TUMORIGENESIS BY SUPPRESSION OF NF-KB SIGNALING CASCADE IN MDR-INDUCED STEM LIKE CANCER-INITIATING CELLS	26
ABSTRACT.....	26
1. INTRODUCTION	28

2. MATERIALS AND METHODS	30
3. RESULTS	38
4. DISCUSSION AND CONCLUSION	52
CHAPTER 4	60
EPIGENETIC INDUCTION OF EPITHELIAL TO MESENCHYMAL TRANSITION BY <i>LCN2</i> MEDIATES METASTASIS AND TUMORIGENESIS, WHICH IS ABROGATED BY NF-KB INHIBITOR BRM270 IN A XENOGRAFT MODEL OF LUNG ADENOCARCINOMA	60
ABSTRACT	60
1. INTRODUCTION	62
2. MATERIALS AND METHODS	65
3. RESULTS	72
4. DISCUSSION AND CONCLUSION	88
CHAPTER 5	95
CHEMOPREVENTIVE AND ANTICANCER POTENTIAL OF NOVEL NATURACEUTICAL BRM270 IN METASTATIC STEM LIKE CANCER INITIATING CELLS OF HEPATOCELLULAR CARCINOMA	95
ABSTRACT	95
1. INTRODUCTION	97
2. MATERIALS AND METHODS	101
3. RESULTS	110
4. DISCUSSION AND CONCLUSION	127
CHAPTER 6	132
BRM270 INHIBITS TUMORIGENESIS BY UPREGULATION OF <i>LET-7</i> MICRORNA THROUGH ACTIVATION OF MITOCHONDRIAL INTRINSIC APOPTOSIS PATHWAY	132
ABSTRACT	132
1. INTRODUCTION	133
2. MATERIALS AND METHODS	136
3. RESULTS	141
4. DISCUSSION AND CONCLUSION	148
REFERENCES	151

LIST OF TABLES

Table 3.1. Primer sequence used in quantitative real-time PCR.....	35
Table 5.1. Primer Sequence Used in Quantitative Real-Time PCR (qPCR)	107
Table 5.2. Influences of BRM270 and Doxorubicin on cell cycle progression in liver HepG-2 and SNU-398 cells	116
Table 5.3. Quantitative apoptosis assay of hepatocellular carcinoma MSCICs using Annexin- V/PI dual staining method by FACS.....	119
Table 5.4. Dose response to BRM270 administered on hepatoma cell line induced carcinoma in CRJORI: CD-1-5WM mice.	122
Table 6.1. Nucleotide sequence used in quantitative real-time PCR	138

LIST OF FIGURES

Figure 2.1. Cancer Mortality in men worldwide.....	8
Figure 2.2. Cancer mortality in women worldwide	8
Figure 2.3. Potential causes of Cancer.....	10
Figure 2.4. Outline of Carcinogenesis. Various environmental factors involving to induce oncogenesis in stem like cells or normal cells.	12
Figure 2.5. Crosstalk between NF- κ B and various biochemical regulators in different cellular processes as a master key regulator	16
Figure 2.6. Diagrammatic showing of mechanism of cancer inhibition by major apoptotic pathway.	18
Figure 3.1. CD133 is a novel biomarker of SLCICs in tumorigenesis with multidrugs resistance (MDR).....	39
Figure 3.2. CD133 expressing Cal72 cells are efficient to induce tumor in BALC nu	40
Figure 3.3. CD133 expressing tumorigenic subpoulation in SLCICs	40
Figure 3.4. BRM270 does not affect normal human cells while it suppresses the stem-ness to induce mitotic DNA damage catastrophe, DNA condensation and shrinkage and is highly cytotoxic on SLCICs.....	43
Figure 3.5. Influence of BRM270 on cell cycle progression/distribution in stem SLCICs and normal hBMCs.....	46
Figure 3.6. BRM270 induced IL-6 mediated apoptosis in CD133+ Cal72 SLCICs via down-regulation of chromatin SMC2.....	47
Figure 3.7. IL-6 augmented neoplasia chemotherapeutic drug resistance ameliorated via co-suppression of p65 and Cdk6 by BRM270 in SLCICs	50
Figure 3.8. De-phosphorylation of NF- κ B by CDK6/cyclin complexes by BRM270 in dose dependent manner.	51
Figure 3.9. Diagrammatic representation of BRM270 as a novel inhibitor.....	56
Figure 4.1. LCN2 modulates epigenetic switching in CD133+-A549-TICSCs induce tumorigenesis.	73
Figure 4.2. NF- κ B novel inhibitor BRM270 abrogates metastatic TICSCs via DNA fragmentation and cell shrinkage	75
Figure 4.3. Novel NF- κ B inhibitor BRM270 inhibits cell proliferation via targeting of Condensin (SMC2)-I complex in CD133+ over-expressing LCN2-A549 TICSCs by dose dependent manner	77
Figure 4.4. Influence of BRM270 on cell cycle progression and apoptosis in TICSCs.	80
Figure 4.5. LCN2 augments SNAI2/ Twist1 mediated EMT and phenotypic reversion in lung adenocarcinoma.....	81
Figure 4.6. 2DG-guided molecular imaging based in vivo model of adeno-carcinoma of lung. .	83
Figure 4.7. BRM270 reduced tumor extent in dose and time dependent manner.	84

Figure 4.8. LCN2 enhances EMT and cross talk with the NF- κ B signaling cascade.....	86
Figure 4.9. Schematic representation of epigenetic induction of EMT and their cross talk with NF- κ B signaling cascade in lung adenocarcinoma.	92
Figure 5.1. CD133+ overexpressing heterogeneity of liver HepG-2 and SNU-398 MSCICs are highly tumorigenic	111
Figure 5.2. Natural drug BRM270 inhibits proliferation of Hepatocellularcarcinoma stem like cancer cells.	113
Figure 5.3. Cell Influence of BRM270 on cell cycle progression/distribution in HCC	115
Figure 5.4. Novel naturaceutics BRM270 induces nuclear condensation, fragmentation and apoptosis on hepatocellularcarcinoma	118
Figure 5.5. BRM270 recruits Casp-3 to negatively attenuate cell proliferation by Cyclin-D1 mediated early and late apoptosis.	120
Figure 5.6. Phyto-drug BRM270 reduces metastatic dissemination to the lung in a CRJORI:CD-1-5WM mice.	123
Figure 5.7. BRM270 reduces metastatic dissemination and mitigates tumor progression in IRDye® -2DG guided molecular imaging xenograft model.....	124
Figure 5.8. Overexpression of c-Myc and Bcl-2 associated with metastasis and poor prognosis, which abrogated by BRM270 via suppression of JUN interaction.....	126
Figure 6.1. BRM270 inhibits proliferation and tumorigenic colony sphere forming capacity...	142
Figure 6.2. BRM270 induced apoptosis in Proteome Micro Array profiling.....	143
Figure 6.3. Antineoplastic efficacy of BRM270 by collapsing the mitochondrial membrane potential ($\Delta\Psi_m$) and inducing ROS generation in Cal72 cancer cells.....	144
Figure 6.4. BRM270 enhanced p53 via suppression of anti-apoptotic Bcl-2.....	146
Figure 6.5. BRM270 downregulated LIN-28 by induction of Let-7.	147
Figure 6.6. Proposed mechanism of action of BRM270 by which it produces anticancer efficacy via mitochondrial intrinsic apoptosis pathway.....	149

ABBREVIATIONS

CSCs	Cancer stem cells
SLCICs	stem like cancer-initiating cells
NF- κ B	Nuclear factor of kappa B
EMT	Epithelial to mesenchymal transition
ANOVA	Analysis of Variance
JNK	c-Jun N-terminal kinases
DRs	death receptors
TRAIL R	tumor necrosis factor related apoptosis-inducing ligand receptor
APAF1	Apoptotic protease activating factor 1
MMP	mitochondrial membrane potential
PI3K	Phosphatidylinositol-4,5-bisphosphate 3-kinase
IL-6	Interleukin -6
XIAP	X-linked inhibitor of apoptosis protein
RT	radiation therapy
BSA	body surface area
BRM	Biological Response Modifier
CDK6	cell division kinase-6
MDR	multidrug resistance
hLCN2	Human Lipocalin2
2DG	2-Deoxy-D-Glucose
qPCR	Qualitative real time polymerase chain reaction
DMEM	Dulbecco's Modified Eagle Medium
LPS	lipopolysaccharide
EDTA	Ethylenediaminetetraacetic acid
Dox	Doxorubicin
MTT	Thiazolyl Blue Tetrazolium Blue
PBS	phosphate-buffered saline
FITC	Fluorescein isothiocyanate

FACS	fluorescence-activated cell sorting
SMC-2	structural maintenance of chromosomes protein 2
DAPI	4', 6-diamidino-2-phenylindole
PMSF	phenylmethane sulfonyl fluoride
BCA	The bicinchoninic acid assay
PVDF	polyvinylidene difluoride membranes
ICC	Immunocytochemistry
FSC	forward scatter
SSC	side scatter
MCD	mitotic cell death
PCD	programmed cell death
EtBr	ethidium bromide
TJP-1	Tight Junction Protein 1
PET	positron emission tomography
NIRF	near-infrared fluorescence
hBMCs	Human bone marrow cells
HCC	Hepatocellular carcinoma
HBV	Hepatitis C Virus
GFP	Green fluorescent protein
miRNA	MicroRNA
FBS	fetal bovine serum
ROS	Reactive Oxygen Species
$\Delta\Psi_m$	mitochondrial membrane potential

CHAPTER 1

INTRODUCTION

Cancer is one of the most serious health problems and leading cause of death over the world. In 2012, cancer was responsible for 8.2 million deaths and it is expected that annual cases will rise from 14 million in 2012 to 22 within the next two decades (Siegel *et al.*, 2016). These statistics may be linked to population growth, the process of industrialization and changes in life style. Apart from that poor survival rate is attributed to high frequency of local recurrence and distant metastasis. Interestingly, most of the cancer cases revealed that tumor initiating cells have merit of self renewable and multiple drug resistance which governs neoplasia with stemness. Cancer stem-like cells (CSCs) have been implicated in tumor recurrence and confer resistance to anti-cancer therapy treatment (Dean M *et al.*, 2005, Shrivastava *et al.*, 2015). Cancer is regarded as complex disorder in which dysfunction of numerous signaling pathways of cell division and growth. Currently treatment of cancer is heavily based on chemotherapy, radiotherapy, surgical removal, hormone therapy as well as immunotherapy.

The Cancer stem cells (CSCs) or stem like cancer-initiating cells (SLCICs) are thought to be responsible for cancer initiation, progression, drug resistance, recurrence and metastasis (Chen *et al.*, 2013). SLCICs have multiple unique features which make them to be vital for tumor formation and self-renewal (Chen *et al.*, 2013; Schober *et al.*, 2011). Specific surface biomarkers for distinct phenotypes can be used to distinguish SLCICs from other tumor and normal stem cells (Woodward *et al.*, 2008). However, cancer stem cells are mediators of recurrence which can be proliferated to any type of neoplasia. Therefore, methods to identify and targeting such cells will represent a significant advancement in cancer therapy. Conceptually,

SLCICs are known as tumor stem cells (TSCs) and tumor initiating cells (TICs) (Dou et al., 2012). CD133 molecule (a trans-membrane protein Prominin 1) is a common and ubiquitous biomarker for endothelial progenitor cells, hematopoietic stem cells, glioblastoma, neuronal glial stem cells and different body organs (Horn *et al.*, 1999; Sanai *et al.*, 2005; Shmelkov *et al.*, 2005; Mizrak *et al.*, 2008). In addition, apart from CD133, 11 proteins have been proposed as potential differentiated biomarkers for SLCICs (Khan *et al.*, 2013). On the basis of these glycoprotein cell surface biomarkers, we had established new paradigm to eliminate the stem like cancer cells inducing carcinoma by both naturaceutical BRM270 and chemopreventive approaches.

Phytochemicals have been considered as advantageous option in cancer therapy. Various preclinical and clinical studies have proven that plant derived dietary substances are suitable candidates for treating various types of cancers due to their broad chemical diversity (Cragg *et al.*, 2015; Gullett *et al.*, 2010). Such phytochemicals may block the action of carcinogens on target tissues thus suppressing cancer progression. Hence, the risk of cancer can be subdued by eating more fruits, vegetables and other plant products. Meta-analyses of cohort and case control studies have shown noteworthy confirmation for cancer prevention with phytochemicals containing fruit consumption (Schuurman *et al.*, 1998). Numerous plant products have studied in various *in-vitro* as well as *in-vivo* model of cancer and these plant products gave fruitful result towards cancer inhibition. In the current study, we had developed natural super cocktail from more than ten herbal plants then performed their specific ration that is BRM270. BRM270 is a one of the promising anti-cancerous medicinal plant extract. It is widely distributed in Northeast Asia mainly China, South Korea and Japan (Zhang *et al.*, 2012). It's a well-known traditional chinese medicine, which is used to treat variety of diseases and cancers (CPC, 2010; Cao *et al.*, 2013).

On the other hand chemically synthesized molecule also impart crucial role in treatment of cancer and today chemotherapy has placed in center for cancer therapy (DeVita et al., 2008). Identification of cytotoxic compounds led the development of anticancer therapeutics is key point of anticancer drug discovery. To continuing our anticancer drug development agenda and enthused by diverse anticancer property of the triazole and piperazine moieties (Ma et al., 2015; She et al., 2013), we have designed a novel series of triazole-piperazine hybrid molecules to evaluate their anticancer activity *in vitro* as well as *in vivo*.

The current progress in molecular sciences and the advances in genomics and proteomics have produced several potential new drug targets to control malignancies, leading to changes in the paradigms of anticancer drug discovery toward specific targeted therapeutics (Roti et al., 2012). Both small and large molecular compounds continue to be investigated as anticancer agents.

Selection of suitable molecular targets for inhibition or modification, such that the target is tumor specific, non-redundant, and able to influence the outcome of tumor progression, is a significant confront given the difficulty of molecular signaling pathways in cells. However, induction of apoptosis in cancer cells is main target to control cancer (Sellers et al., 1999).

Apoptosis or programmed cell death is a key regulator of physiological growth control and regulation of tissue homeostasis which initially define by its morphological characteristics such as cell shrinkage, membrane blebbing, chromatin condensation and DNA nuclear fragmentation (Dini et al., 1996). The stimulation of apoptosis has been considered as a standard and best approach in anticancer therapy. In the multiple intervention model for treatment of cancer apoptosis is a major way to follow by most of the anticancer drugs to kill stem like tumor cells (Signore et al., 2013). Consequently, in order to develop novel therapeutic strategies,

apoptosis must be inhibited by novel drugs inhibitors, active biomolecules or naturaceutics as BRM270 via various cellular signaling mechanisms. In addition, mitototic catastrophe can also be induced in number of malignancies by targeting abnormal mitosis checkpoints and apoptosis (Castedo et al., 2004). In our study, we have conducted the apoptosis mediated antitumor activity via both TNF-augmented extrinsic and mitochondrial dysfunction regulated intrinsic apoptosis signaling pathways in stem like cancer initiating cells.

In our anticancer drug development agenda, we have taken plant derived material (chapter 3, 4, 5) as well as synthetic molecules (Chapter 6, 7) to study their extensive mechanism of action associated with anticancer activity. In this regards various molecular target has been chosen which is responsible to control tumor genesis and action of our natural drug as well as synthetic molecule on those target has been studied in detail. In this project we strive to discover potent chemotherapeutic agent from natural sources as well as synthetic sources.

Finally our project gave fruitful result and we able to discover mechanism of action of plant derived product BRM270. Moreover, we also discovered potent anticancer agents from synthetic sources. In this line, we have found various potent synthetic molecules which showed excellent *in vitro* as well as *in-vivo* anticancer activity. Additionally, their mechanism of action which governs anticancer activity has been also discovered.

AIMS OF THE STUDY

The overall objective of this study was to establish a zero footprint based multistep intervention paradigm for cancer eradication through the targeting of various cellular signaling cascades in the disease environment for prevention of uncontrol neoplastic cancers. Present study was concentrated on the following objectives:-

1. Molecular mechanism elucidation and anticancer activity of novel phyto-drug BRM270 against stem like cancer initiating cells via cellular signal trafficking - NF- κ B pathways (Chapter 3).
2. Efficacy of BRM270 in the mitigation of adenolung carcinoma metastasis through blocking of epithelial to mesenchymal transition (EMT) as an epigenetic modulation model (Chapter 4).
3. Anticancer activity of BRM270 in hepatocellular carcinoma (Chapter 5).
4. *In-vitro* and *in-vivo* anti cancer activity assessment of novel BRM270 in inhibition of tumorigenesis by upregulation of Let-7 microRNA through activation of mitochondrial intrinsic apoptosis pathway (Chapter 6).

CHAPTER 2

REVIEW AND LITERATURE: CANCER

1. Cancer: The brief keynote

Cancer is derived from a Latin word ‘crab’. The ancients used the word to mean a malignancy, doubtless because of the crab-like tenacity a malignant tumor sometimes seems to show in grasping the tissues it invades. Cancer means “New Growth” and is a deadly disease of the “gene” in which abnormal growth of cells takes place in an uncontrolled way and eventually leads to form new growth known as tumor or neoplasm (NIH, 2007). Therefore, cancer may also be called malignancy, a malignant tumor, or a neoplasm (literally, a new growth). Two types of tumors are reported till date, first is the benign tumor, which is generally not considered as cancerous and second is a malignant tumor which is cancer itself. The benign tumor grows slowly and does not spread or invade surrounding tissue, and once it is remove, doesn’t usually recure.

On the other hand, a malignant tumor invades surrounding tissue and spreads to other parts of the body. Moreover, if the malignant tumor cells spread to the surrounding tissues, it usually recurs even after its removal. Cancer is not a single disease, but it is a large group of nearly 100 types. Malignant neoplastic disease can affect any tissue of the body and induce many different configurations in each body region (Lodish et al. 2000). Most cancers are named for the type of cell or organ in which they start, for example, lung, colon, mouth, prostate, bone, stomach, breast, brain, ovarian, pancreatic, cervical, liver, kidney, skin, thyroid, uterine cancer. Cancers of the blood such as leukemia generally do not form solid tumors. Cancer cells reveal a

comprehensive spectrum of genetic changes that include gene rearrangements, point mutations, and gene amplifications, leading to disturbances in molecular pathways regulating cell growth, survival, and metastasis (Bhatt et al. 2010).

2. Cancer: Prevalence

More than 11 million people are diagnosed with cancer every year. It is calculated that there will be 16 million new lawsuits every year by 2020. In 2012, an estimated 14.1 million new cases of cancer occurred worldwide (de Moor et al. 2013). More than half of cancers occurring worldwide are in less developed parts. The four most common cancers occurring worldwide are lung, female breast, intestine and prostate cancer (Rebecca et al. 2015). These four accounts for around 4 in 10 of all cancers diagnosed worldwide. Lung cancer is the most usual cancer in humans worldwide (Molina et al. 2008). More than 1 in 10 of all cancers diagnosed in men are lung cancers. Figure 2.1 and 2.2 shows the cancer mortality in men and women, respectively. Worldwide, about 32.5 million people diagnosed with cancer within the five years previous were alive at the close of 2012. An approximated 169.3 million years of healthy life were lost globally because of cancer in 2008. In 2012, an estimated 8.2 million people perished from cancer worldwide (Cancer Research UK 2014). More than 6 in ten cancer deaths worldwide occur in less developed areas of the globe. Lung, liver, abdomen, and bowel are the most usual reasons of cancer death worldwide, accounting for about half of all cancer deaths. Lung cancer causes the most cancer deaths worldwide. About a fifth of all cancer deaths worldwide are lung cancers (Ferlay et al. 2010).

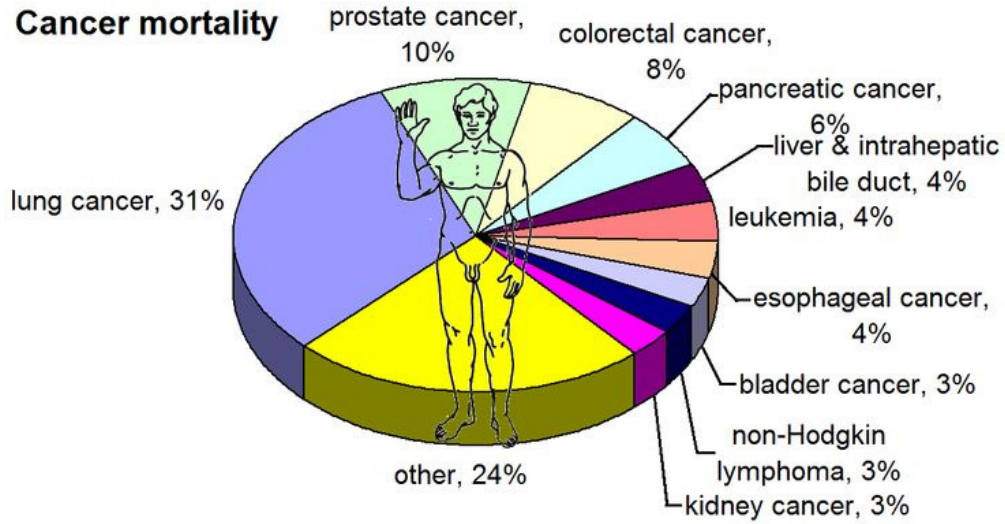


Figure 2.1. Cancer Mortality in men worldwide

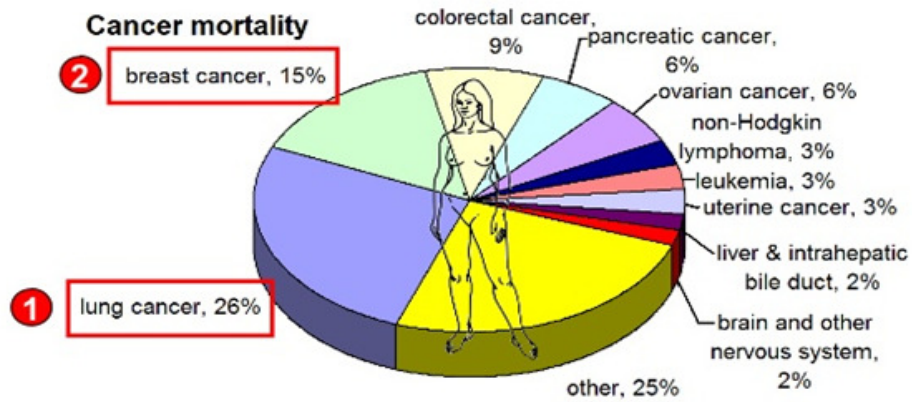


Figure 2.2. Cancer mortality in women worldwide

3. “Drivers” of Cancer

Cancer arises from a change in one single cell. The transformation from a normal cell into a tumor cell is a multistage process, typically a progression from a pre-cancerous lesion to malignant tumors (Yokota 2000). There are several causes which significantly contribute to the development of cancer. Figure 2.3 summarizes potential causes which lead to cancer onset and progression. These changes are the outcome of the interaction between a person's genetic factors and 3 categories of external factors, including:

- Physical carcinogens, such as UV and ionizing irradiation;
- Chemical carcinogens, such as asbestos, components of tobacco smoke, aflatoxin (a food contaminant) and arsenic (a drinking water contaminant); and
- Biological carcinogens, such as infections from certain viruses, bacteria or parasites.

4. Pathophysiology of Cancer

The uncontrolled cell growth is a characteristic of cancer. Cellular growth rates are regulated by proteins produced by the genetic material in cells (Salem 2015). Genetic material can be altered or mutated by environmental factors, errors in gene replication or repair processes, or by tumor viruses. Altered or mutated genes are called oncogenes, and it is these oncogenes that allow uncontrolled growth in cells. Therefore, cancer cells differ from normal cells in size, structure, function, and growth rate. These malignant cells lack the normal controls of development experienced in healthy cells, and grow uncontrollably (Thorat et al. 2012). Carcinogenesis is a multistage process and Figure 2.4 is a pictorial view of the process of carcinogenesis.

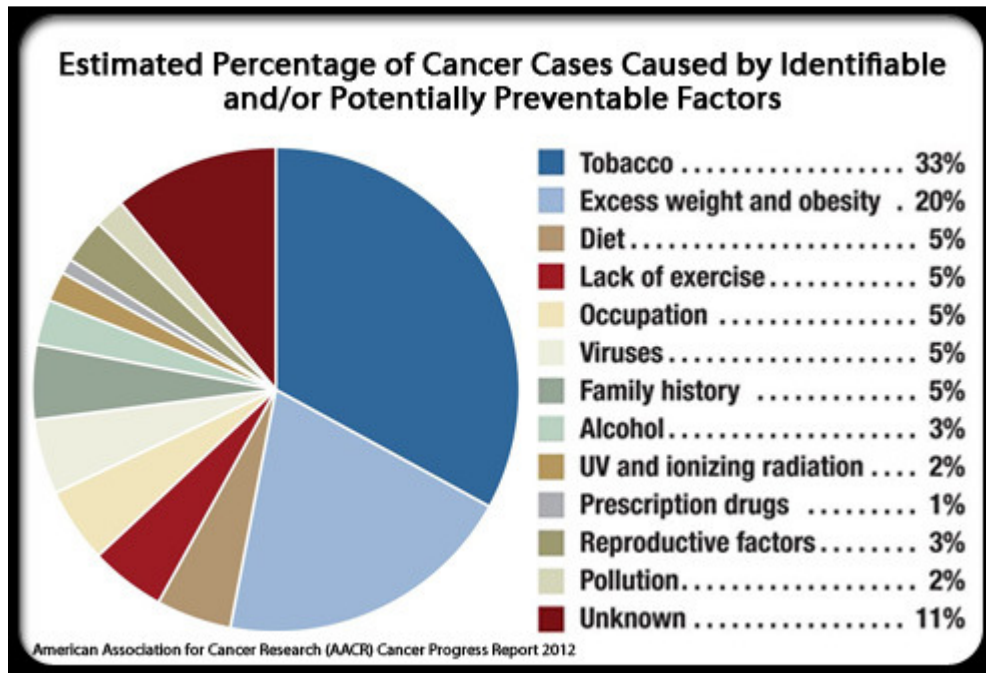


Figure 2.3. Potential causes of Cancer

The process of carcinogenesis gets initiated by various factors such as genetic mutations, carcinogens, radiation and by invasion of certain viruses like Epstein Barr virus, Human papilloma virus, hepatitis B virus (McMillan 1992). All these factors lead to initiation of various biological cascades which results into development of cancer. Moreover, the phenomenon of glycolysis in cancer tissue has been identified as one of the fundamental questions of tumor biochemistry “not yet fully understood.” It has been described as the chief means of energy production in cancer cells (known as the Warburg effect) and as part of a whole-body metabolic circuit important in the production of cancer cachexia (Demetrius et al. 2010).

5. Targets of Cancer Therapy

Cancer is a multifactorial disease in which numerous molecular pathways involve to induce uncontrolled proliferation of cells. From past decades extensive efforts have been made to understand the role of different target to control unrestrained tumor progression. Current cancer therapies such as chemotherapy, immunotherapy or suicide gene therapy primarily produce their antitumor effect by triggering apoptosis in cancer cells. Apoptosis is described by cell morphological alteration including cell shrinkage, membrane blebbing and nuclear DNA fragmentation (Elmore 2007). Chemotherapeutic agents which produce anticancer efficacy by inducing apoptosis, mainly targets intrinsic or extrinsic or both pathway of apoptosis (Fulda et al. 2006).

Overview of Carcinogenesis

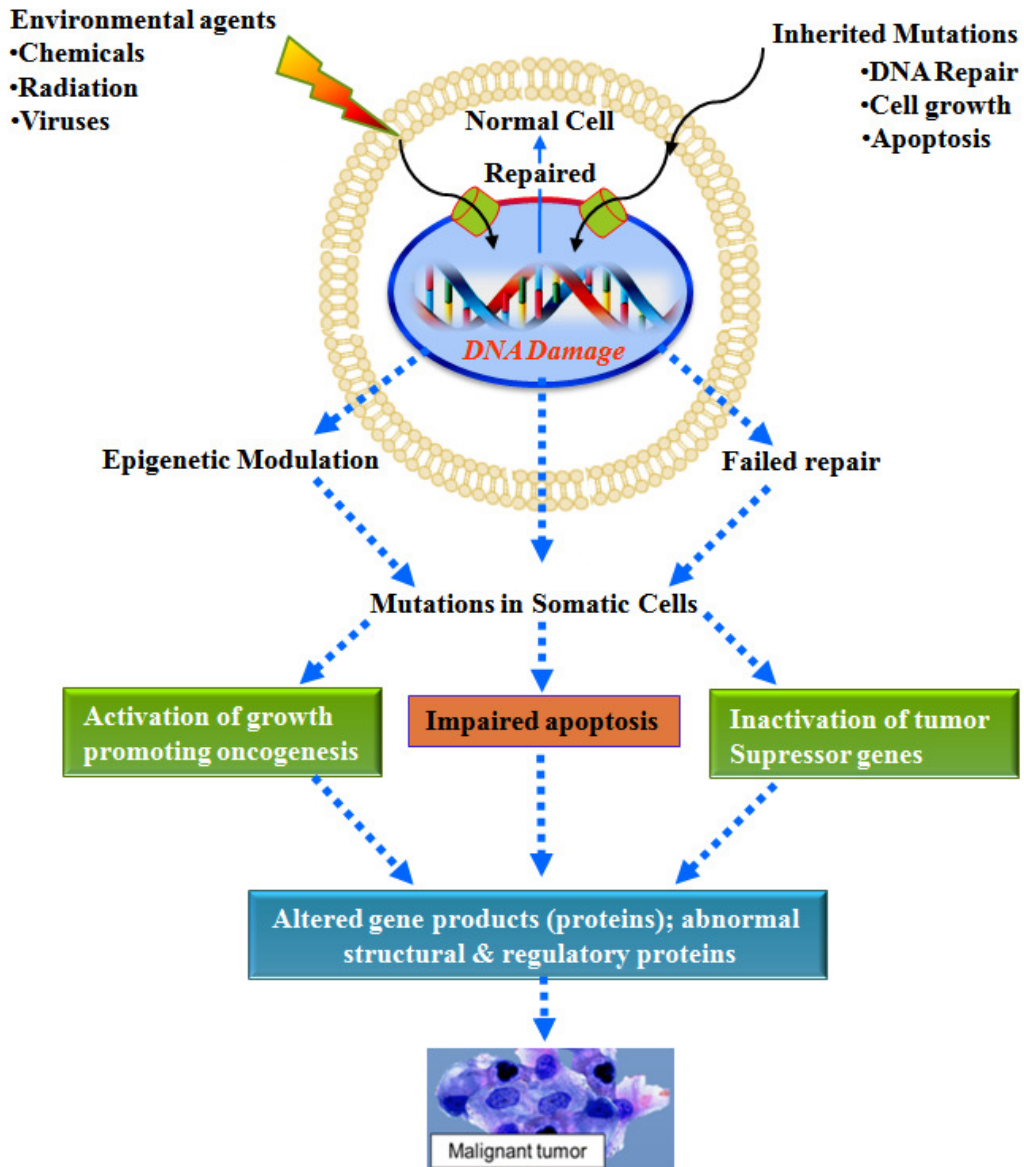


Figure 2.4. Outline of Carcinogenesis. Various environmental factors involving to induce oncogenesis in stem like cells or normal cells.

5. 1. The Extrinsic Pathway

Commencement of the extrinsic pathway is beginning with the ligation of cell surface receptors called death receptors (DRs). Fas is a member of the tumor necrosis factor superfamily and also known as Apo-1 or CD95 (Peter et al. 2003). Other TNF receptors include TNF R1, DR3 (Apo 2), DR4 (tumor necrosis factor related apoptosis-inducing ligand receptor 1 TRAIL R1), DR5 (TRAIL R2), and DR6 (Kalimuthu et al. 2013). Fas signaling plays crucial role in immune surveillance of virus infected cells and in the elimination of self-reactive lymphocytes. Therefore, imperfections in this pathway have been implicated in many malignancies. When a death stimulus activates this pathway, membrane-bound FasL forms death-inducing signaling complex by interacting inactive Fas complexes. This complex activate caspase which leads to activate rest of downstream caspases. In some cases, caspase 8 interacts with intrinsic pathway by cleaving Bid and decreased mitochondrial potential which lead to release of cytochrome c (Parrish et al. 2013).

5. 2. The Intrinsic Pathway

This the common pathway triggered by most of anticancer drug to stop/ slow down cell over growth. Most important regulators of this pathway are the Bcl-2 family of proteins and it's over expression cause resistance of chemotherapeutic agents. Decreasing BCL-2 level may help the anticancer drug to induced apoptosis in cancer cells (Ricci et al 2006).

The Bcl-2 family comprises proapoptotic members such as Bax, Bad, Bak, Bid, Bcl-Xs Bim, and Bik and antiapoptotic members like Bcl-2, Bcl-W, Bcl-XL, and Mcl-1. Antiapoptotic Bcl-2 members take action as suppressor of apoptosis, whereas proapoptotic members act as

promoters (Delbridge et al. 2015). In response to apoptotic stimuli, the mitochondrial membrane becomes permeable which lead to release proapoptotic proteins including cytochrome c in cytosol. Release cytochrome c binds with protease activating factor 1 (APAF1) and forming apoptosome complex by conformational changing (Saelens et al. 2004). These apoptosome complex activate caspase 9 which lead to activate caspase 3 as well as caspase 7 and finally cells apoptosis happen. Change in mitochondrial potential (MOMP) is regulated phenomena and mainly controlled by BCl-2 family (Nikoletopoulou et al. 2013).

5. 3. Regulation of Intrinsic and extrinsic pathway

The intrinsic and extrinsic apoptotic pathways are mainly regulated by p53, NF-KB, eubiquitin proteosome system, and the PI3K pathway.

5. 4. p53 tumoricidal proteins and its signaling cascades

p53 is the most extensively studied tumor suppressor which control apoptosis by regulating the intrinsic as well as extrinsic pathway and may also trans activate numerous components of the apoptotic effectors machinery. p53 serve as a transcription factor which regulating downstream genes essential in DNA repair, cell cycle arrest and apoptosis (Fridman et al. 2003). Defeats of p53 in many cancers make spoil cell cycle regulation, and reticence of apoptosis. P53 also play crucial role in DNA damage and its repair and grasps the cell at a checkpoint until the damage is completely repaired. The mechanism by which p53 promotes apoptosis is still under investigation (Haupt et al. 2003).

5. 5. NF- κ B cellular signaling pathway

Bio-signal trafficking is the pivotal functional mechanism acquired in the differentiation, proliferation, growth and survival of the cells (Lin et al., 2008). During histeotypic neoplasia normal cells follow altered ways to proliferate independently due to growth promoting conditions (Iliopoulos et al., 2009). At the same time, growth inhibitory signals with respect to metastasis, elicit an angiogenic responses as well as to evade mechanism that arrest cell growth cycle and proliferation (Martin, 2003). Inhibition of kappa B kinase blocks the induction of nuclear factor-kappaB (NF- κ B) signaling and makes bridge between inflammation and cancer (Lin et al., 2008; Oeckinghaus et al., 2011). Ghosh et al. (2002) reported regulation of the wide variety of genes encoding cytokines (e.g., IL-1, IL-2, IL-6, IL-12, TNF-, LT, LT, and GM-CSF), chemokines (e.g., IL-8, MIP-1, MCP1, RANTES, and eotaxin), adhesion molecules (e.g., ICAM, VCAM, and E-selectin) acute phase proteins (e.g., SAA), and inducible effector enzymes (e.g., iNOS and COX-2) by NF- κ B. Moreover, consequently NF- κ B-dependent transcription is not only tightly controlled by positive and negative regulatory mechanisms but also closely coordinated with other signaling pathways such as JNK, Akt, and MAPK (Oeckinghaus et al., 2011; Baker et al., 2011). NF- κ B is well-known nuclear factor stimulated by various carcinogens and tumor promoters and it is crucial player in tumor progression (Karin 2006). NF- κ B activation encourages cell proliferation and its suppression led to the stopping of proliferation. NF- κ B also maintains the regulation of the Bcl-2 family proteins and sustains the mitochondrial integrity that is desirable for the survival of cancer cells. Hence, suppression of NF- κ B activity is helpful for induction of apoptosis and it is an important target to produce apoptosis in cancer cells (Hoesel et al. 2013).

NF- κ B is stimulated by numerous stimuli that include growth factors, lymphokines, cytokines, radiation and pharmacologic agents (Ghobrial et al. 2005). Inactive NF- κ B is sequestered in the cytoplasm and bound by inhibitor I- κ B family proteins. When NF- κ B is stimulated by stimuli cause phosphorylation of I- κ B, which is followed by its degradation. This results in exposure of the nuclear localization signals on NF- κ B subunits which leads to translocation of the molecule to the nucleus. Under physiologic conditions, the activation of NF- κ B encourages resistance to apoptotic stimuli by the activation of numerous proteins such as IAP, TNF receptor-associated factor, and X-linked IAP. NF- κ B activation govern apoptosis may be explained by the activation of some proapoptotic proteins like interferon-regulated factor-1, p53, c-myc, and caspases (Chen et al. 2001). In viral infections, initiation of apoptosis by the virus relies on NF- κ B activation. Lastly, major apoptotic pathways govern cellular programmed death via both the extrinsic and intrinsic signaling mechanism (Figure 2.6).

5. 6. PI3K signal transduction

PI3K is a kinase that plays an important role in signaling pathways involved in cell survival, proliferation, and motility (Liu et al. 2009). It is well studied that PI3K is unregulated in many cancers. When phosphatidylinositol 4,5-bisphosphate 3 signals activate the kinase 3-phosphoinositide-dependent protein kinase-1, which leads to activate the kinase Akt (Castellano et al. 2011). Akt activation directs to phosphorylation of certain proteins that lead to cell survival. Bad phosphorylation by Akt leads to its inactivation which resulting blocking of the apoptotic signal. Moreover, phosphorylation of caspase 9 inhibits the induction of apoptosis.

Thus, numerous proteins important in human cancers can be regulated in the PI3K pathway (Arcaro et al. 2007).

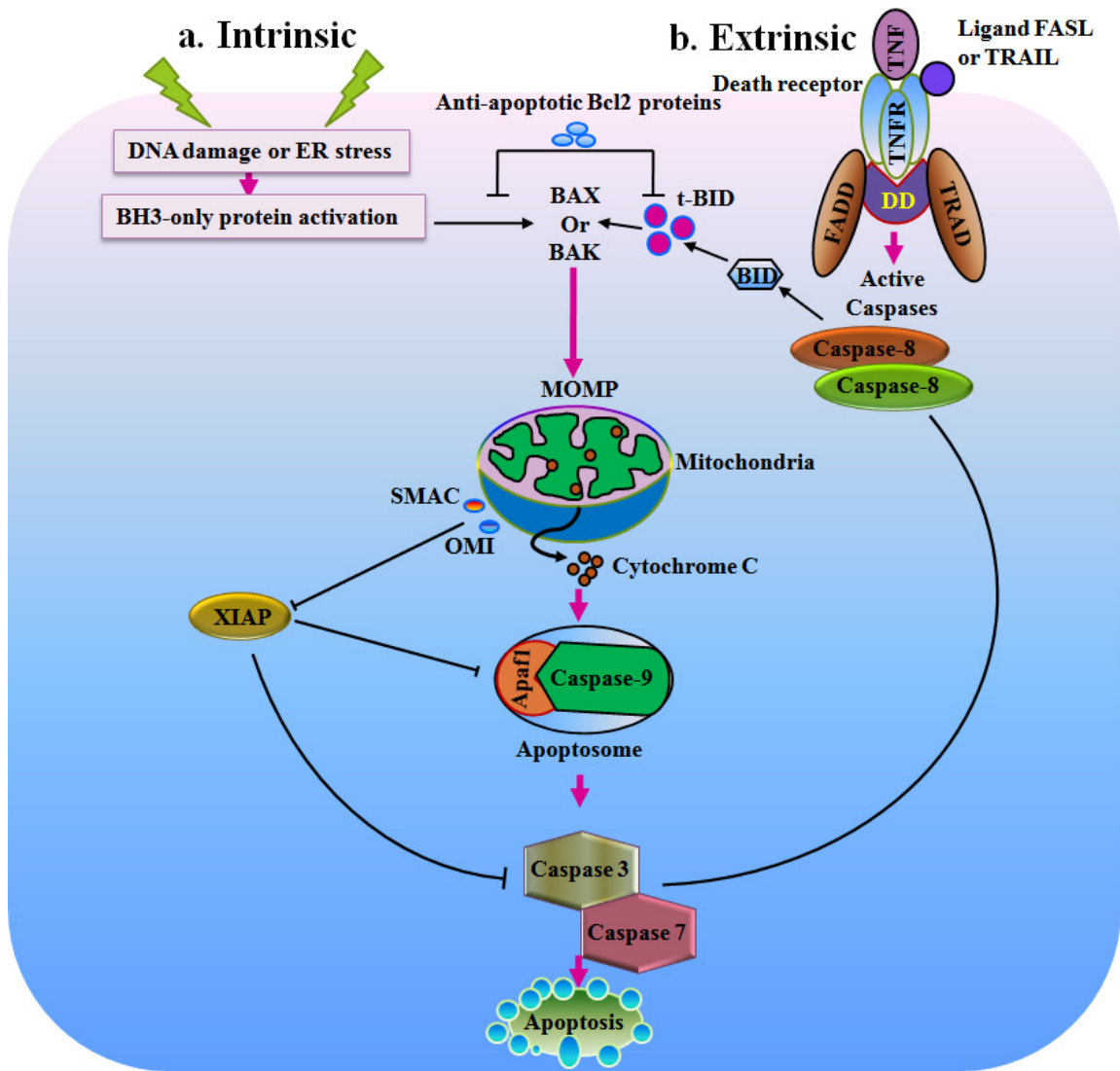


Figure 2.6. Diagrammatic showing of mechanism of cancer inhibition by major apoptotic pathway.

5. 7. Proteosome

The proteosome system serves as an important regulator of cell proliferation and apoptosis (Chen et al. 2010). Proteosome inhibitors have been shown excellent apoptosis in numerous cancer cell lines and also exhibit in vivo antitumor activity. They have also been shown to slow down angiogenesis and metastasis in vivo. Proteosome inhibitor may selectively kill cancer cells because studies have shown that such inhibitor only induced apoptosis (Fan et al. 2001). Experiments have proven that high expression of the *c-myc* oncogene directs cancer cells more susceptible to proteosome inhibitor induced apoptosis. Numerous natural product based protease inhibitor such as lactacystin, MG132, ALLN, and MG115 running in preclinical stage for therapy of cancer (Li Lue et al. 2011). Additionally, recently, FDA approved a protease inhibitor bortezomib for therapy of refractory multiple myeloma (Chen et al. 2011).

6. Current Treatment of Cancer

There are many types of cancer treatment. Some people with cancer will have only one treatment. But most people have a combination of treatments, such as surgery with chemotherapy and/or radiation therapy (RT). Surgery is most effective in the treatment of localized primary tumor and associated regional lymphatics (Tai 2013). When used as a single treatment, surgery cures more patients than any other individual form of cancer therapy because surgery operates by zero-order kinetics, in which 100% of excised cells are killed. With the advent of RT in the 1920s and chemotherapy after the 1940s, cancer surgery has become conservative. In contrast to surgery, chemotherapy and radiation therapy are only capable of killing a fraction of tumor cells by each treatment. Both processes are complementary to each

other. A more common use of RT is in combination with surgery and/or chemotherapy. Preoperative RT is used today in a limited number of tumour locations such as rectal and esophageal carcinomas while postoperative RT is used in many tumor sites including breast and central nervous system tumors among others. Intraoperative RT, the delivery of a single large fraction during surgery with either electrons or low energy photons, is occasionally used (Hindy et al. 2014). Chemoradiotherapy approaches [the administration of chemotherapy prior to (neoadjuvant), during (concomitant) or following RT (maintenance)] have been shown to improve local control and eradicate micrometastatic disease. RT is an important means of providing rapid and effective palliation due to local and/or metastatic disease such as bone or cerebral metastases. Chemotherapy is the use of drugs to treat cancer by destroying or slowing the growth of fast-growing cancer cells. Chemotherapy remains mainstay for the treatment of cancer and several anticancer drugs are available clinically (Gascoigne et al. 2009).

Anticancer drugs can be loosely categorized into cytotoxic and biological factors (Wu, 2006). Cytotoxic agents are alkylating agents, anti-metabolites, plant alkaloids, DNA linking agents and several biological agents. Alkylating agents directly damages DNA by adding methyl or other alkyl groups onto nucleotide bases and thereby inhibit their correct use by base pairing led to a mutation, DNA fragmentation as well as suppression of DNA reproduction and transcription. They also disrupt cell respiration and intermediary metabolism by alkylation of proteins and enzymes. Inhibitors of DNA synthesis inhibit essential bio-synthetic processes or are incorporated into DNA, RNA, proteins and other macromolecules (Warwick, 1963). These drugs are either structural analogues for heterocyclic bases or agents interfering with folate metabolism. DNA building blocks include heterocyclic bases and folic acid. They inhibit main steps in the formation of purine and pyrimidine bases as well as nucleotides. This category of

drugs includes antifolates (methotrexate, pemetrexed), antipyrimidines (5-fluorouracil, capecitabine, eniluracile, hydroxyurea) and antipurines (6-mercaptopurine, 6-thioguanine). Antitumor antibiotics and topoisomerase inhibitors are obtained from the cultures of various microorganisms. Furthermore, topoisomerase inhibitors have been utilized to interpose with the action of topoisomerase I and II enzymes. These enzymes regulate the changes in DNA structure which includes DNA replication, transcription, recombination, and chromatin remodeling (Kathiravan et al., 2013; Pommier et al., 2010). The important inhibitors are camptothecin, irinotecan, topotecan for Topoisomerase I; Etoposide (VP-16), teniposide, doxorubicin, daunorubicin, ellipticine etc, for Topoisomerase II (Pommier, 2006; Nitiss, 2009). These drugs suppress the ability of the topoisomerase to cleave nucleic acid particles. Although these types of drugs have important clinical efficacy, they have undesired and/or adverse effects such as drug resistance, poor bioavailability problems and myelosuppression. Furthermore, some of them lead to disruption or stabilization of DNA, so that these are likewise called as topoisomerase poisons. The other inhibitors of topoisomerase bind to enzyme or DNA and interrupt the catalytic activity of the enzyme and prevent the enzyme binding actions. Etoposide VP-16 (Vepesid), an effective anticancer drug, is applied to treat a broad spectrum of human cancers for more than two decades (Evans et al., 1985). Other examples of herbal medicines are vincristine, vinblastine, podophyllotoxin, teniposide and vindesin.

7. Pitfalls in Cancer Therapy

Chemotherapeutic drugs are working on the basis of their killing ability of fast growing cancer cells. However, chemotherapeutic drugs also produced cytotoxic effect on normal cells

that divide; e.g. bone marrow cells, gut cells, etc. For this reason, the range and effectiveness of chemotherapy becomes restricted (Vriesendorp et al., 1987).

The rising capacity of cancer cells to resist the chemotherapeutic drug is one of the major drawbacks of conventional chemotherapy (Holohan et al., 2013). In drug-resistant cancer cells, expression of surface minute pump like p- glycoprotein and intercellular antioxidant efflux put off the chemotherapeutic agents from entering into the cells. Over-dosage in chemotherapy is also generates much harmful effects in the patients. Several factors like body surface area (BSA) formula, mathematical calculation on the basis of the patient's weight and height had been permitted in early 1950s for calculating individual chemotherapeutic dosage (Levêque et al., 2007).

Diverse side-effects arise depending on the nature of the drug (Vriesendorp et al., 1987). For example, the Alkalyting agents and anti metabolites directly damage DNA to prevent the cancer cells from reproducing; thus they can cause long-term damage to the bone marrow, which can ultimately lead to acute leukemia (Reimer et al., 1977). Similarly, Anthracyclines produce anticancer effect by interfering with enzymes involved in DNA replication. A major drawback of anthracyclines is permanently damage the heart if given in high doses for a long time (Hortobágyi et al., 1997).

Plant alkaloids and other compounds originated from natural products are often known to be mitotic inhibitors also produce several side effects. These drugs cause peripheral nerve damage in pro long time use. Topoisomerase inhibitors that cause DNA damage to cancer cells produce harmful side effects like allergic reaction including fast heartbeat, itching or hives, swelling in the face or hands, chest tightness, and wheezing.

Immune-suppression during chemotherapy causes various side effects such as Bone marrow suppression, caecitis-infection of the gut- includes diarrhea, nausea, vomiting, fever and distended abdomen etc. Lengthened autoinfection manifests as systemic disease conditions like sepsis. Another drawback of some chemotherapeutic agents is infertility exerts in both female and male patients by some gonad toxic chemotherapeutic agents.

Many chemotherapeutic agents cause neuro-cognitive deficiency in which patients suffer from inability to concentrate and loss of memory. One of the crucial draw back during chemotherapy is damages inflicted on normal organs. Therefore, Discovery of potent chemotherapeutic agents from natural source or synthetic source which free from normal cell toxicity is necessarily required to mange cancer.

8. Hypothesis and Work Plan

Phytochemicals have been considered as advantageous option in cancer therapy. Various preclinical and clinical studies have proven that plant derived dietary substances are able to halt progression of various types of cancers due to their broad chemical diversity. Hence, the risk of cancer can be subdued by eating more fruits, vegetables and other plant products¹. Meta-analyses of cohort and case control studies have shown noteworthy confirmation for cancer prevention with fruit consumption ⁴. Numerous plant products have studied in various in-vitro as well as in-vivo model of cancer and these plant products gave fruitful result towards cancer inhibition.

On the other hand chemically synthesized molecule also impart crucial role in treatment of cancer and today chemotherapy has placed in center for cancer therapy. Identification of cytotoxic compounds led the development of anticancer therapeutics is key point of anticancer

drug discovery. The current progress in molecular sciences and the advances in genomics and proteomics have produced several potential new drug targets to control malignancies, leading to changes in the paradigms of anticancer drug discovery toward specific targeted therapeutics. Both small and large molecular compounds continue to be investigated as anticancer agents. Selection of suitable molecular targets for inhibition or modification, such that the target is tumor specific, non-redundant, and able to influence the outcome of tumor progression, is a significant confront given the difficulty of molecular signaling pathways in cells. However, induction of apoptosis in cancer cells is main target to control cancer.

In our anticancer drug development agenda, we have taken plant derived material. To studies plant derived material as anti-cancer agent we have chosen a mixture of pant material BRM270. BRM270 is a highly popular and promising anti-cancerous medicinal plant among North-East Asian countries. Its super cocktail product was procured from the Biological Response Modifier (BRM) International Heath Town Corp., Republic of Korea. Extensive anticancer activity of BRM270 has been carried out along with its mechanism of action finding *in vitro* as well as *in-vivo* model. We planned to know the efficacy of BRM270 to inhibit the cyclin-dependent cell division kinase-6 (CDK6). Moreover, the role of BRM270 in IL-6 mediated activation of multidrug resistance (MDR) in NF- κ B signaling cascade of SLCICs was studied to judge its role as an inhibitor of NF- κ B. Additionally, Our studies potentially targeted on the establishment of a novel therapeutic strategy linking 2DG to LCN2-induced EMT and growth promotion of lung cancer cells through cooperation with the NF- κ B signaling with zero cytotoxicity to normal tissue against adenocarcinoma of lung through the use of BRM270 as a novel anticancer naturaceutics with 2DG optical probe.

In this study, the antitumor effect of BRM270 on human hepatoma cell line, CD133⁺ expressing stem-like cancer-initiating cells (MSCICs) HepG-2 and SNU-398, and the mechanism involved have been investigated. Multistep intervention models including EZ-CyTox-WST assay, cell cycle regulation and apoptosis were analyzed using Hoechst 33342 staining and flow-cytometric Annexin-VI/PI double staining method. Gene expression profiling by qPCR and specific cellular protein expressions were measured using immunocytochemistry and western blot analysis. *In vivo* imaging in mice model using 2DG-(2-Deoxy-D-Glucose) optical-probe was performed to delineate the size and extent of metastasized tumor.

Parallel, we also strive to discover potent chemotherapeutic agent from synthetic sources and this line we have screened pyrazolo-pyrimidine-urea derivatives and triazole-piperazine derivative against various cancer cell line. To indentify mechanism of action of this series we performed Cell cycle inhibition assay, Apoptosis assay and apoptotic as well as anti-apoptotic biomarker has been quantify by real time qPCR and western blot analysis. *In vivo* efficacy of these derivatives has been also elucidated in lung adenocarcinoma nude mice model.

Triazole-piperazine derivatives have been also tested in various cancer cell line *in vitro* studies to identify their anticancer potential. Further mechanism of action which governs its anticancer activity has been also explored. In this regards expression of proteins involve in intrinsic apoptosis pathway has quantify by running real time qPCR and western blot analysis. Action of these derivatives on mitochondria has been studied by measuring Mitochondrial potential, ROS generation and cytochrome c migration. Finally, *in-vivo* potential of these derivatives has been explored in osteosarcoma nude mice model. Whether these derivatives stop tumor metastasis in osteosarcoma nude mice model, a 2DG optical probe guided monitoring has been performed.

CHAPTER 3

NOVEL INHIBITOR BRM270 DOWN-REGULATES TUMORIGENESIS BY SUPPRESSION OF NF- κ B SIGNALING CASCADE IN MDR-INDUCED STEM LIKE CANCER-INITIATING CELLS

ABSTRACT

The nuclear factor kappa B (NF- κ B) and interleukin-6 (IL-6) contribute to multiple drug resistance (MDR) in tumor chemotherapy. The essential phenomenon of oncogenic activation of NF- κ B in cancer-initiating cells showing MDR resulting from increased IL-6 expression is still unclear. Cancer stem cells (CSCs) have been the objective of intensive study. The aim of this study was to investigate the selective and potential efficacy of BRM270 against stem like cancer-initiating cells (SLCICs) via the molecular mechanisms of its anti-cancerous effects. Co-regulation of NF- κ B and Cdk6 might be new arena to mitigate the tumorigenesis. In the current study phyto-drug based approach has provided a new avenue in understanding the amelioration and regulatory mechanisms in CSCs. In the present study, an *in-vivo* tumor metastasis model of osteosarcoma was established by injecting Cal72 and SaOS-2 SLCICs into the right lower flank of nude mice. Later the development of tumor was analyzed by LICOR Biosciences (pearl image analyzer). Significant suppression of activation of NF- κ B and LPS-induced gene expression and apoptosis by BRM270 was confirmed by FACS, western blot and qPCR. Further, both p65 and

Cdk6 significantly ($P<0.05$) overexpressed in BRM270 non-treated Cal72 SLCICs than treated group. BRM270 directly dephosphorylated RelA and selectively inhibited NF- κ B transcriptional activity, resulting in decreased expression of interleukin-6, cytokines implicated in cancer metastasis. BRM270 mediated cell shrinkage, pyknosis, karyorrhexis and programmed cell death (PCD) were observed by Hoechst 33342 staining while flow cytometry analysis showed the significant ($P<0.05$) decrease in cell population from G0-G1 phases. These findings suggest that activation of the oncogenic Cdk6-NF- κ B pathway, resulting from increased IL-6 expression, plays a central role in CD133 expressing SLCICs augmented MDR and neoplasia. This study proposes the insight of targeting of NF- κ B, Cdk6 with IL-6 as potential targets for PCD and treatment of chemotherapeutic resistance of CSCs to design novel therapies to eliminate them.

Keywords: SLCICs, PCD, mitotic catastrophe, MDR, pyknosis, karyorrhexis and cytoplasm shrinkage.

1. INTRODUCTION

The Cancer stem cells (CSCs) or stem like cancer-initiating cells (SLCICs) are thought to be responsible for cancer initiation, progression, drug resistance, recurrence and metastasis (Chen *et al.*, 2013). SLCICs have multiple unique features which make them to be vital for tumor formation and self-renewal (Chen *et al.*, 2013; Schober and Fuchs, 2011). Specific surface biomarkers for distinct phenotypes can be used to distinguish SLCICs from other tumor and normal stem cells (Woodward and Sulman, 2008). However, cancer stem cells are mediators of recurrence which can be proliferated to any type of neoplasia. Therefore, methods to identify and targeting such cells will represent a significant advancement in cancer therapy. Conceptually, SLCICs are known as tumor stem cells (TSCs) and tumor initiating cells (TICs) (Dou and Gu, 2012). CD133 molecule (a trans-membrane protein Prominin 1) is a common and ubiquitous biomarker for endothelial progenitor cells, hematopoietic stem cells, glioblastoma, neuronal glial stem cells and different body organs (Horn *et al.*, 1999; Sanai *et al.*, 2005; Shmelkov *et al.*, 2005; Mizrak *et al.*, 2008). In addition, apart from CD133, 11 proteins have been proposed as potential differentiated biomarkers for SLCICs (Khan *et al.*, 2013).

Multistep phenomenon of carcinogenesis exhibits that it is fragmented into constitutive cell division, proliferation, growth and survival stages (Hahn *et al.*, 2002; Vogelstein *et al.*, 2004). The molecular diatomous mechanisms are mediated through the inactivation of many tumor suppresser genes and oncogenic mutations. Pathophysiology of tumorigenesis has manifested that several transcription factors are involved in tumor progressions. One of the most important transcription factor (TF), NF- κ B plays a causative role but meager information is

available about its mechanisms. NF- κ B, a transcription factor significantly regulates the expression of anti-apoptotic genes, activates different pro-inflammatory cytokines and chemokines including IL-6 (Iliopoulos *et al.*, 2009; Urashima *et al.*, 1997). It is a key molecular link between inflammation, initiation and progression of oncogenesis (Iliopoulos *et al.*, 2009). Moreover, IL-6 is also known to have significant role in the cell cycles (Urashima *et al.*, 1997; Sansone *et al.*, 2012).

Recent studies on phyto-drugs based approaches have opened a new avenue for the understanding of the amelioration and regulatory mechanisms in SLCICs. BRM270 is a one of the promising anti-cancerous medicinal plant extract. It is widely distributed in Northeast Asia mainly China, South Korea and Japan (CPC, 2010; Cao *et al.*, 2013; Cao *et al.*, 2013). It's a well-known traditional Chinese medicine, which is used to treat variety of diseases and cancers (CPC, 2010; Cao *et al.*, 2013; Cao *et al.*, 2013; Zhang *et al.*, 2012). Therefore, the current study was planned to know the efficacy of BRM270 to inhibit the cyclin-dependent cell division kinase-6. Further, the role of BRM270 in IL-6 mediated activation of multi drug resistance (MDR) in NF- κ B signaling cascade of SLCICs was studied to judge its role as noble inhibitor of NF- κ B. To best of author's knowledge this is a one of the pioneer studies where efficacy of BRM270 as an anti- cancerous product under *in-vitro* and *in-vivo* conditions has been studied.

2. MATERIALS AND METHODS

2.1. *Animal preparation and bioethics statement*

For the current study, 10 (6 weeks old) male NOD-SCID (BALB/cSlc (nu/nu), nude mice were procured from Japan SLC, Inc. They were housed in similar environmental and nutritional conditions. Mice were slaughtered at 11 weeks age, according to the standard protocols of Jeju National University, Jeju –si, Jeju- do, South Korea. The research proposal and the relevant experimental procedures were approved by the institutional review board of the Department of Animal Biotechnology, Jeju National University, Jeju –si, Jeju- do, South Korea. All animal studies were conducted to induce tumor. In order to design tumorigenesis induction experiment, the mice were divided into three groups. Two mice were grouped as a negative control (NC). Rest of the mice were distributed in two treatment groups that is Cal72 group (n = 4) and SaOS-2 group (n = 4). Furthermore, 4×10^6 /ml of SLCICs were suspended in Matrigel and injected subcutaneously into right lower flank of nude mouse in both the treatment groups.

2.2. *Cell line*

Human osteosarcoma Cal72 and SaOS-2 cell lines were purchased from Korean Cell Bank (Seoul, South Korea). These cell lines were routinely cultured in Dulbecco's Modified Eagle's Medium (DMEM) supplemented with 10% Fetal Bovine Serum (FBS) (Hyclone, South Logan, UT, USA), 1% antibiotic-antimycotic (Gibco, Invitrogen, Carlsbad, CA, USA) at humidified 37°C and 5% CO₂ atmosphere. The cells were sub-cultured after attaining confluency

level of 80%. For the current study, the cells in passage 9 and 12 were used. Human bone marrow cells (hBMCs) were also used as control.

2. 3. Isolation and characterization of Cal72, SaOS-2 SLCICs and hBMCs

The population of CD133 expressing in Cal72 and SaOS-2 cells was isolated by anti-human CD133 MicroBead kit (Miltenyi Biotec Corp., Auburn, CA, USA) using Midi MACS separator (Miltenyi Biotec Corp.) by following the user instruction manual. The hBMCs were isolated from the adult human bone marrow (Jeju National University Hospital, Jeju, South Korea) and were separated by Ficoll-paque density gradient centrifugation (GE Healthcare Life Science, Piscataway Township, NJ, USA). The potential hBMCs were cultured in DMEM supplied with 10% FBS, 1% antibiotic-antimycotic and 10nM epithelial growth factor (Sigma-Aldrich Corp., St Louis, MO). The hBMCs from 3rd and 4th passage were confirmed as normal control cells against the efficacy of BRM270.

2. 4. Preparation of nuclear and cytosolic protein extracts

A pellet of 1×10^7 cells was cultured and at 80 % confluency, cells were treated with BRM270. Later, BRM270-treated or non-treated vs lipopolysaccharide (LPS) + BRM270 treated samples of Cal72 and SaOS-2 SLCICs were lysed with 400 μ l of 10 mM KCl, 0.2 mM EDTA, 1.5 mM MgCl₂, 0.5 mM DTT, and 0.2 mM PMSF at 4°C for 10 minutes. The lysate was centrifuged for 5 minutes at 12,000 X g and supernatants were stored as cytosolic extract at -80°C. The resulting pellet was re-suspended in 100 μ l of ice-cold 20 mM HEPES (pH 7.9), 420 mM NaCl, 1.5 mM MgCl₂, 20% (v/v) glycerol, 0.5 mM DTT, 0.2 mM EDTA and 0.2 mM PMSF. After incubation at 4°C for 20 minutes, the lysate was centrifuged for 10 minutes at

12,000 X g and the supernatant was stored as a nuclear extract at -80°C . The concentration of cytosolic and nuclear extract was determined using a BCA kit (Bio Rad, Richmond, CA).

2. 5. Cytotoxicity assay

Total 100 μl of suspended cell at density of 5000 cells/well were seeded in 96-well plate (NuncTM, Wiesbaden, Germany). After 24 h of recovery the cells incubated in the humid atmosphere at 37°C and 5% CO_2 were treated with BRM270. The BRM270 was procured from the Biological Response Modifier International Heath Town Corporation, South Korea. The cells were treated with varying concentrations of BRM270 such as 15.6 $\mu\text{g}/\text{ml}$ to 125 $\mu\text{g}/\text{ml}$ and Doxorubicin (Dox) 5 $\mu\text{M}/\text{ml}$ in MTT assay while 125 $\mu\text{g}/\text{ml}$ in rest of the trials and were incubated for 24 h. The enhanced cell viability assay was conducted with EZ-CyTox kit (Daeil Lab Service Co., Seoul, South Korea) to measure the viable cells. 10 μl of EZ-CyTox solution was added to each well and then cells were incubated for 4 h at 37°C and 5% CO_2 . The light absorbance was determined at 450 nm by the Model 680 microplate-reader (Bio-Rad, Berkeley, California USA).

2. 6. DNA fragmentation assay

CD133 expressing Cal72 and SAOS2 cells (1×10^6 cells) were seeded in 6-well microtitre plate (Nunc NunclonTM Delta, USA). Then the cells were treated with the 125 $\mu\text{g}/\text{ml}$ concentrations of BRM270 for 24 h. For analysis of genomic DNA, attached and floating cells in the supernatant were harvested and collected together. Genomic DNA was extracted by AccuPrep[®] Genomic DNA Extraction Kit (Bioneer). 5 μg of DNA was separated on a 1.2%

agarose gel. DNA in the gel was stained with ethidium bromide and was visualized under UV light.

Apoptotic morphological changes in the nuclear chromatin of the cancer stem cells were stained by Hoechst 33258 staining. The cells were seeded in the sterile 6-well plates (Nunc Nunclon™ Delta, USA). After overnight growth, cells were treated with BRM270. Later, the cells were washed with 1X phosphate-buffered saline (10X PBS Gibco, life technologies™ USA) and were fixed with 4% paraformaldehyde for 10 min followed by incubation with 50 μM Hoechst 33258 staining solution for 5 min. After three washes with cold PBS, the cells were viewed under a fluorescence microscope (Olympus, IX-70, and Japan).

2. 7. Apoptosis assay by flow cytometry

1 X 10⁵ cells suspended in 2 ml fresh media were seeded in each well of a 6-well flat-bottomed microtiter plate and incubated overnight. Then BRM270 with 125μg/ml was added. After 24 h, cells were harvested and washed twice with pre-cold PBS followed by re-suspension in 1X binding buffer at a concentration of 1 × 10⁶ cells/ml. 100 μl of such solution (1 X 10⁵ cells) was mixed with 5 μl of annexin V-FITC and 5 μl of Propidium Iodide (PI, BD Biosciences, San Jose, CA, USA) according to the manufacturer's instructions. The mixed solution was incubated at room temperature (25°C) in dark for 15 minutes. Then 400 μl of 1X dilution buffer was added to each tube. Analysis was performed by Beckman Coulter FC500 Flow Cytometry System with CXP Software (Beckman Coulter, Fullerton, CA, USA) within 1 hour of the treatment of cells with dilution buffer.

2. 8. Cell cycle analysis

The analysis of cell cycle was detected by PI staining and analysis was performed by flow cytometry using a fluorescence-activated cell sorting (FACS) caliber (Becton Dickinson, San Jose, CA, USA). Subsequent to the treatment with 125µg/ml and 5µM/ml concentrations of BRM270 and Dox for 24 h, the hBMCs, CD133 expressing Cal72 and SaOS-2 SLCICs were harvested at concentration of 1×10^6 cells/ml. The cells were fixed in 70% ethanol and incubated at 4°C for overnight. The fixed cells were washed twice with cold PBS and then incubated for 30 min with Ribonuclease A (# R-5125, SIGMA, 8 µg/ml) and PI (10 µg/ml). Then the cell samples were transferred to meshed blue capped falcon tubes (BD Falcon™ Tubes # 352235). Later, the fluorescent signals were detected through the FL2 channel and the proportion of DNA that was present in the various phases was analyzed using ModfitLT Version 3.0 (Verity Software House, Topsham, ME, USA).

2. 9. Quantitative real time polymerase chain reaction (qPCR)

The cells were detached by 0.5% Trypsin-EDTA (Gibco, USA) and total RNA was extracted by easyBlue (Intron Biotech, Seongnam-si, Gyeonggi-do, South of Korea). The purified RNA was quantified by using Photometer (Biorad *Hercules*, CA, USA). 1µg of purified RNA was subjected to first strand cDNA synthesis using Superscript III first-strand cDNA synthesis kit and Oligo dT primer (Invitrogen, USA). The cDNA was subjected to qPCR for the quantification of the relative transcript levels of NF-κB (p65) and its inhibitor (IκBα), structural maintenance of chromosomes protein 2 (SMC-2), inflammatory cytokine IL-6 as well as pro-apoptotic gene/anti-apoptotic gene Caspase-8 (Casp-8) using the specific primers (Table 3.1.).

Table 3.1. Primer sequence used in quantitative real-time PCR.

Gene	Sequence	T _m °C	Accession number
<i>β-actin</i>	F- GGA ^{CT} T ^{CG} A ^{GCA} A ^{GAG} A ^{TGG}	57.50	NM_001101
	R- AGCA ^{CT} GT ^{GT} T ^{GG} CG ^{TAC} AG		
<i>Cdk6</i>	F – AGAGACAGGAGTGGCCTTGA	55.40	NM_001145306
	R – GAAAGCAAGCAAACAGGTG		
<i>NF-κB (p65)</i>	F- CTGAACCAGGGCATACTGT	56.45	NM_001243984
	R- GAGAAGTCCATGTCCGCAAT		
<i>IL-6</i>	F – TACCC ^{CC} CAGGAGAAGATTCC	55.45	NM_000600.3
	R – TTTTCTGCCAGTGCCTCTTT		
<i>Casp-8</i>	F- TATGGCACTGATGGACAGGA	54.40	NM_001228
	R- GCAGAAAGTCAGCCTCATCC		
<i>SMC2</i>	F- CACCACCAGAGGGTCAA ^{ACT}	57.50	NM_001042551
	R- TGAGTACGCAGCATCTGTCC		
<i>Oct4</i>	F- TATGGGAGCCCTCACTT ^{CAC}	57.50	NM_002701
	R- CAAAAACCCTGGCACA ^{AACT}		
<i>Prominin1 (CD133)</i>	F- GCCAGCCTCAGACAGAAA ^{AC}	57.50	NM_001145848
	R- CCAAGCCTTAGGAGCATCTG		
<i>IκBα</i>	F-TTGGGTGCTGATGTCAATGC	56.45	NM_020529
	R- CTCACTCTCTGGCAGCATCT		

2. 10. Immunofluorescence staining

CD133 expressing Cal72 and SaOS-2 SLCICs were grown in 4-well chambered slide with glass coverslips (SPL Life Sciences Co., Ltd Korea, 30104 PS/Glass/PP). The cells were cultured along with BRM270 (125µg/ml) and as non-treated (negative control) in DMEM high glucose medium for 24 h. Next day cells were washed with cold 1X PBS and were fixed with 4% paraformaldehyde for 15 min. Following this step the cells were permeabilized with 0.2% Triton X-100 for 10 minutes. After washing with the PBS, cells were blocked with 1% bovine serum albumin (BSA) for 30 minutes. Further, the cells were incubated with primary antibodies for anti-p-NF-κB/p65 Ser536, anti-rabbit-CD133 (Prominin 1), SMC2 and Cdk6 (rabbit IgG, Santa Cruz Biotechnology, Inc., Santa Cruz, CA). All these antibodies were used at 1:200 dilutions. Subsequently, the cells were incubated with Alexa Fluor 488 (donkey anti-rabbit) secondary antibodies (both from Santa Cruz Biotechnology) for 1 hour at room temperature in the dark. Cells were then washed with cold PBS and were counterstained with 4', 6-diamidino-2-phenylindole (DAPI, Invitrogen, USA). After incubation with DAPI for 5 minutes again cells were washed with cold 1X PBS. After addition of 1ml mounting media, cells were observed under the fluorescence microscope (Olympus, Milan, Italy) with adaptable filter consistent with Alexa Fluor 488, FITC or PE.

2. 11. Western blot

Total proteins were isolated by ice-cold RIPA buffer supplied PMSF (Sigma-Aldrich Corp., USA) and ready to use protein inhibitor cocktails (Fermentas, Thermo Scientific, Rockford, IL USA). Protein concentrations were calculated by using Pierce[®] BCA

Protein Assay Kit (Thermo Scientific, IL USA) following the manufacturer's instruction. Sixteen micrograms of protein were then loaded per well. Proteins were separated on 12% polyacrylamide gel and transferred to polyvinylidene difluoride membranes (PVDF, Sigma-Aldrich Corp., USA) in the Bio-rad western blot system (Bio-rad, Berkeley, California, USA). The membrane was incubated with the primary antibodies β -actin (1:1000), 1:200 diluted anti-p-NF- κ B antibody, anti-human-IL-6 antibody (rabbit IgG), Pro-apoptotic protein Casp-8 was detected using 1:200 anti-casp-8 antibody (rabbit IgG), Cdk6 (C-21) (rabbit IgG) and structural maintenance chromosomes protein-2 (SMC-2) (sc-10709 rabbit polyclonal IgG). All of the antibodies used were procured from, Santa Cruz Biotechnology, Inc. CA. The interested proteins were detected by an enhanced chemiluminescence detection kit following manufacturer's instructions using LAS4000 machine (GE Healthcare, Piscataway Township, NJ, USA).

2. 12. Statistical Analysis

After 6 days of injection tumor were visible. The tumor was measured with Vernier's calipers and the volume of the tumor (mm^3) was calculated by the following formula:

$$\text{Volume} = (\text{width})^2 \left(\frac{\text{length}}{2} \right)$$

Further, the size and the extent of metastasis of tumor under *in-vivo* conditions was detected using LI-COR pearl animal image analyzer (LI-COR Biosciences, USA). All the mice were sacrificed for the collection of tumor.

The relative quantitative expressions of the genes by real-time qPCR and western blotting were analyzed by the analysis of variance (ANOVA). The significant differences between the mean expressions of different genes at $P < 0.05$ were analyzed by Tukey's b-test. The values have been expressed as mean \pm SEM.

3. RESULTS

3.1. Promonin 1 is a novel SLCICs marker in various carcinomas those are involved in tumorigenesis with MDR

In an attempt to identify SLCICs, CD133 expressing in Cal72 cells were analyzed. The cells were characterized on the basis of expression of CD133⁺ on their cell surface which is found in number of malignancies. To verify the CD133⁺ as a SLCICs marker, cells were stained with monoclonal antibody human anti-CD133-FITC with iso-control and showed overexpression in Cal72 cells (Figure 3.1). Similarly, Oct4 with higher invasiveness and proliferative rate overexpressed during immunocytochemistry of SLCICs in tumor sphere assay *in-vitro*. Formation of tumor spheroids of high grade was also confirmed by the Oct4 expressing in SLCICs by both *in-vitro* (Figure 3.1) and *in-vivo* (Figure 3.2). Moreover, the CD133⁺ expressed on the cell surface of cancer cells can proliferate and metastasize in *in-vivo*. Palpable tumors were visible after 7 days of injection and to endorse the tumorigenesis capability of CD133⁺ expressing SLCICs, the tumors were visualized by LI-COR Biosciences Pearl impulse IR-fluorophore, IRDye® 800CW 2-deoxyglucose optical imaging system. In this approach the size, grade as well as their metastasization of tumor has been distinctly observed (Figure 3.2). In contrast, the SLCICs are often characterized by a high metabolic rate exemplified by a dramatically elevated glucose uptake. The IRDye 800CW 2DG was used for its ability to target several different tumor types for example solid tumors, colon tumors and soft tumors. This biological activity has been exploited by noninvasive imaging system using infrared pseudo-colored fluorescent signals.

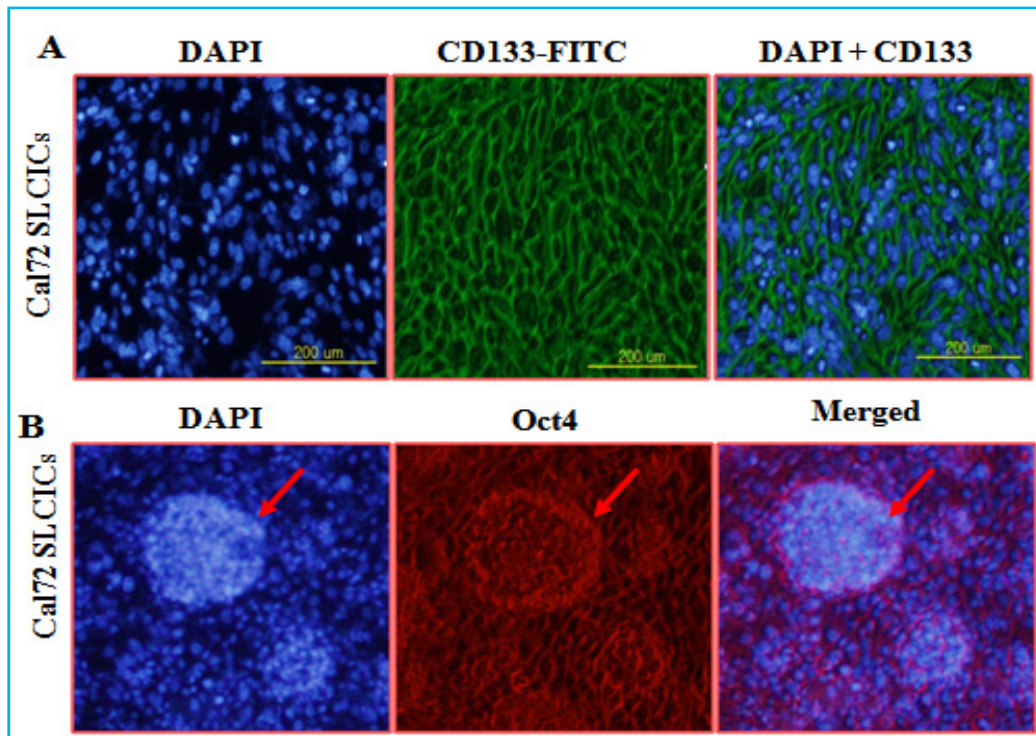


Figure 3.1. CD133 is a novel biomarker of SLCICs in tumorigenesis with multidrug resistance (MDR). A. Immunocytochemistry of Cal72 SLCICs exert the over expression of CD133, blue staining is showing nuclear DAPI, CD133 overexpressed in green followed by their merged expression. B. *In-vitro* immunocytochemistry based tumor sphere forming assay showing the over expression of Oct3/4 in CD133 expressing Cal72 SLCICs.

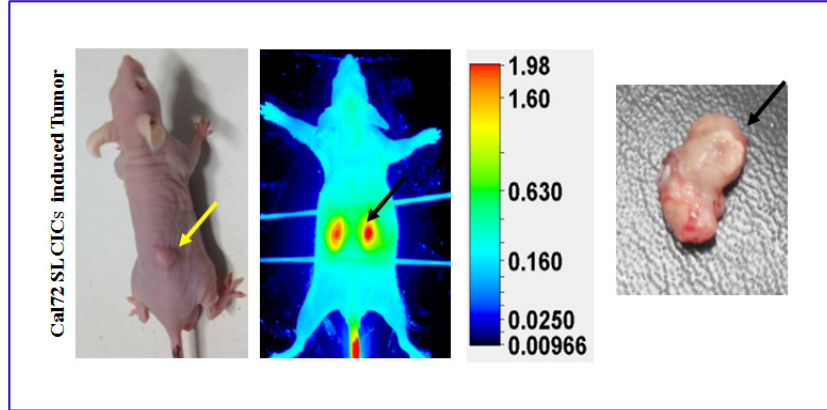


Figure 3.2. CD133 expressing Cal72 cells are efficient to induce tumor in BALB nude mouse and showed high grade of tumor using LI-COR pearl image analyzer (LI-COR Biosciences, USA).

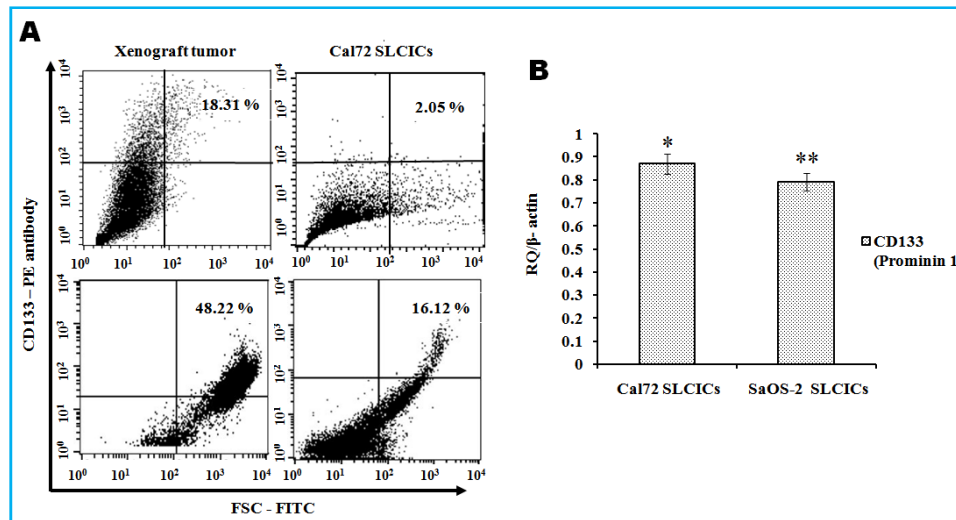


Figure 3.3. CD133 expressing tumorigenic subpopulation in SLCICs. D. To characterize the CD133 expressing Cal72 SLCICs stained with CD133-FITC and analyzed by flow cytometry which are showing CD133 rich subpopulation in gated region. E. Quantitative expression of CD133 in both SaOS-2 and Cal72 SLCICs by qPCR. The data are expressed as mean±S.E.M. (* $P < 0.05$).

Further, pseudo-colored fluorescent signals were superimposed on a white light image using glucose analogues such as 18F-2-deoxy-D-glucose (due to high glucose metabolism in tumor sites) to generate a tumor-localized signal. Higher intensity signals are in red, while lower signal intensity is in blue color (Figure 3.2). For more valid confirmation, cells from solid subcutaneous tumor and CD133 expressing SLCICs were stained with anti-human CD133-FITC conjugate after one day of their isolation and were further assessed by FACS. The CD133⁺ rich SLCICs were selected according to forward scatter (FSC) and side scatter (SSC) property using the gated region R4 to remove the cell debris, residual platelets and red cell contamination. FACS analysis showed the presence of a variable fraction of CD133⁺ cell populations in tumor bearing nude mouse samples, 18.31% and 48.22% respectively. However, 2.05 % and 16.12 % CD133⁺ were observed in Cal72 SLCICs. (Figure 3.3). Moreover, these SLCICs are CD133⁺ rich tumor initiating populations which can be characterized by flow cytometry. A significant ($P<0.05$) quantitative transcript levels of CD133 in both Cal72 (0.87%) and SaOS-2 (0.79%) SLCICs respectively were analyzed by qPCR, (Figure 3.3. B).

3.2. BRM270 does not affect normal human cells while it suppresses the stem-ness to induce mitotic DNA damage catastrophe and G1 to S/G2M transition during premature apoptosis

Cell cycle progression is highly regulated at several checkpoints to ensure proper DNA synthesis and chromosome segregation. It has become increasingly clear that the deregulation of CDK pathways causes unscheduled proliferation that contributes to oncogenic transformation. In the present study, we showed that efficacy of BRM270 is effectively kill the Dox-resistance cancer stem cell in dose and time dependent manner which induced morphological cell shrinkage and DNA and apoptosis (Figure 3.5A). BRM270 selectively inhibits cell proliferation by

inducing programmed cell death (PCD) and mitotic cell death (MCD) due to unrepaired DNA damage during premature apoptosis (Figure 3.5B). Initially the morphology of chromatin condensed in the cultured cells undergoing apoptosis was compared with that of *in-vitro* triggered DNA fragmentation in nuclei isolated from the corresponding non-apoptotic cells (Figure 3.5). Therefore after 24 h of exposure, cells treated with BRM270 and Dox in dose dependent manner, were observed for DNA fragmentation and chromatin condensation by confocal fluorescence microscope (Figure 3.5B). Further, the genomic DNA was extracted and was separated on 2% agarose gel. To confirm the extent of genomic DNA fragmentation by BRM270, the DNA was run in the gel stained with ethidium bromide (EtBr) and was visualized under UV light (Figure 3.5).

It showed that hallmark of apoptotic cell death is the cleavage of chromosomal DNA at inter-nucleosomal sites into fragments of multiples sizes (Figure 3.5). For confirmation of DNA damage-induced mitotic cell death, CD133⁺ expressing SLCICs treated with BRM270 and Dox, were stained with Hoechst 33258 stain. It was observed that BRM270 interrupt the microtubule cytoskeletal formation in Dox resistance SLCICs, formed chromosomal condensation (pyknosis), nuclear fragmentation (karyorrhexis) (Figure 3.5, red arrows) and cytoplasmic shrinkage (Figure 2B-2 and 5 yellow arrows). BRM270 displayed potent cytotoxicity in Dox resistance cancer stem cells by changed morphology of cells (Figure 3.5). In addition, BRM270 has shown selective inhibition of neoplasm. Cytotoxicity was analyzed by colorimetric assay 3-(4, 5-dimethylthiazol-2-yl)-2, 5-diphenyltetrazolium bromide (MTT assay) (Figure 3.5) where it showed its ability to kill the CD133⁺ expressing SLCICs. MTT assay analysis showed that at the concentration of 125µg/ml, after the exposure of 24 h with BRM270, 4.51% (CD133⁺ expressing Cal 72 SLCICs) and 7.253% (SaOS-2 SLCICs) viability has been recorded.

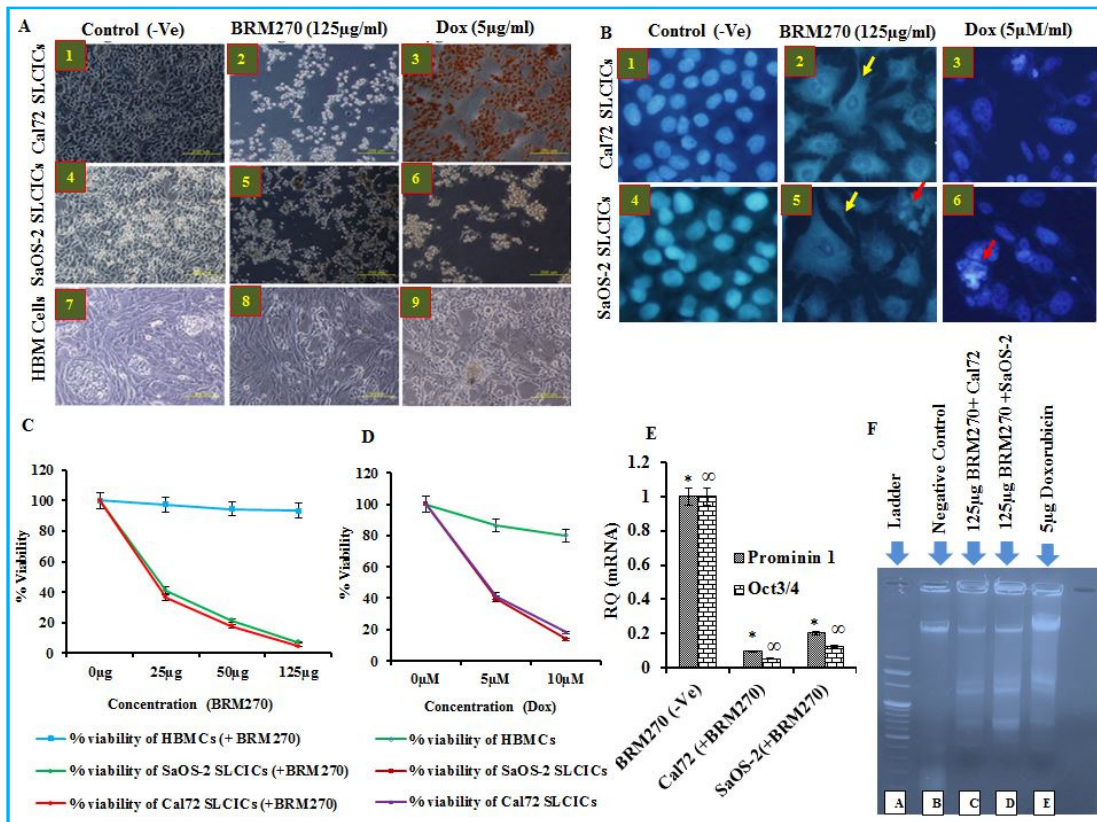


Figure 3.4. BRM270 does not affect normal human cells while it suppresses the stem-ness to induce mitotic DNA damage catastrophe, DNA condensation and shrinkage and is highly cytotoxic on SLCICs. A. Morphological changes of SLCICs and hBMCs are treated with 125µg/ml concentration of BRM270 while 5µM/ml Dox treated as a positive control for 24 h. **B.** Confirmation of the DNA fragmentation apoptosis, condensation and shrinkage of cells with Hoechst 33342 staining (Blue DNA). **C.** Confirmation of cytotoxicity of BRM270 by cell viability test (MTT assay). **D.** Higher toxicity of Dox in neoplasia was confirmed by MTT assay **E.** Relative qPCR analysis of CD133 and Oct4 gene expression. **F.** Genomic DNA fragmentation of Cal72 SLCICs exposed to BRM270 with different concentration for 24 h exposure. DNA laddering formation was viewed on ethidium bromide-stained gel (1.2%). The data are mean±S.E.M. (* $P < 0.05$).

Further, to know the cytotoxic effect of BRM270 on normal human cell line, hBMCs were used. At the similar conditions as those of cancer cell lines, hBMCs showed 93.41% viability with respect to control (Figure 3.5). Similarly, in Dox treated group 17.95%, 13.56% and 79.99% viability observed in Cal72, SaOS-2 and hBMCs respectively. It showed that Dox is more toxic in normal cells compare with BRM270 (Figure 3.5).

Furthermore, CD133⁺ and Oct3/4 in Cal72 SLCICs have indicated towards the high stemness while after treatment with BRM270 a significant ($P<0.05$) decrease in their levels has been reported (Figure 3.5). The cell cycle progression in both parental and Dox-resistant SLCICs after 24 h exposure of BRM270 has been observed (Figure 3.5). Flow cytometry analysis showed the significant ($P<0.05$) decrease in cell population from G0-G1 phases (Figure 3.5). A significant decrease (17.09%) has been recorded in the Cal72-SLCICs population after their treatment with BRM270 as compared to 6.77% decrease in the cell population after their exposure to Dox. The 15.49% (BRM270 treated) and 5.88% (Dox treated) concomitant accumulation or transit of cells in the G2/M checkpoint (BRM270-15.49%, Dox-5.88%) was in both CD133⁺ expressing Cal72 SLCICs has been recorded. Again, the SaOS-2 SLCICs cell samples were collected and cells were stained with Propidium Iodide to analyze cell cycle arrest which divulged transition from G0-G1 (lost 4.82 %) into G2/M phase (transit 15.09 %) while in normal hBMCs, checkpoints for transition of G2/M are G0-G1 (loss very less 0.2 %) into G2/M phase (transit 4.31 %) while in Dox treated G0-G1 (loss 6.63 %) to G2/M (6.47 %) respectively (Figure 3.6). This finding suggests that anti-cancer drug Dox arrest cells at G0. Further it is also observed that transit to G2/M checkpoint by Dox is lesser than NF- κ B noble inhibitor BRM270 in both SaOS-2 and Cal72 SLCICs while Dox showed more cytotoxicity to normal hBMCs with respect to BRM270.

3.3. BRM270 induced IL-6 mediated apoptosis in CD133⁺ SLCICs via down-regulation of SMC2.

BRM270 induced IL-6 mediated apoptosis and the expression of pro-apoptotic proteins was observed in SLCICs. Apoptotic cell death was measured with fluorescein isothiocyanate-conjugated Annexin V and PI staining at 12 h and 24 h after treated with BRM270. The apoptosis induced by BRM-270 was studied in Cal72 SLCICs and SaOS-2 SLCICs. The lower right quadrant in Figure 4A indicates early apoptotic cells. In addition, the number of apoptotic cells (Annexin V-positive cells) increased in both CD133⁺ expressing Cal72 and SaOS-2 SLCICs after 24 h exposure of BRM270. The annexin V-FITC assay showed that approximately 16.75% and 12.14% in 12 h while 33.39% and 29.32% in 24 h underwent apoptosis with the exposure of BRM270 in both Cal72 and SaOS-2 SLCICs respectively. No significant ($P < 0.05$) difference in the necrotic cells (PI-positive and annexin-V-negative cells) was observed between the groups (Figure 3.7). On the basis of time of exposure of BRM270 to both cell lines, significant differences have been observed. The number of early apoptotic cells (Annexin V-positive and PI-negative cells) was approximately two folds greater in the both cell lines at 24 h exposure than the 12 h of exposure (Figure 3.7). Similarly, qPCR revealed the relative quantitatively down-regulated levels of IL-6 and SMC2 whereas increased transcript levels of Casp-8 were observed in both Cal72 SLCICs and SaOS-2 SLCICs (Figure 3.7). These results suggest that down-regulation of IL-6 and SMC2 increased Casp-8 activity and enhanced BRM270-induced apoptosis in CD133 expressing Cal72 and SaOS-2 SLCICs.

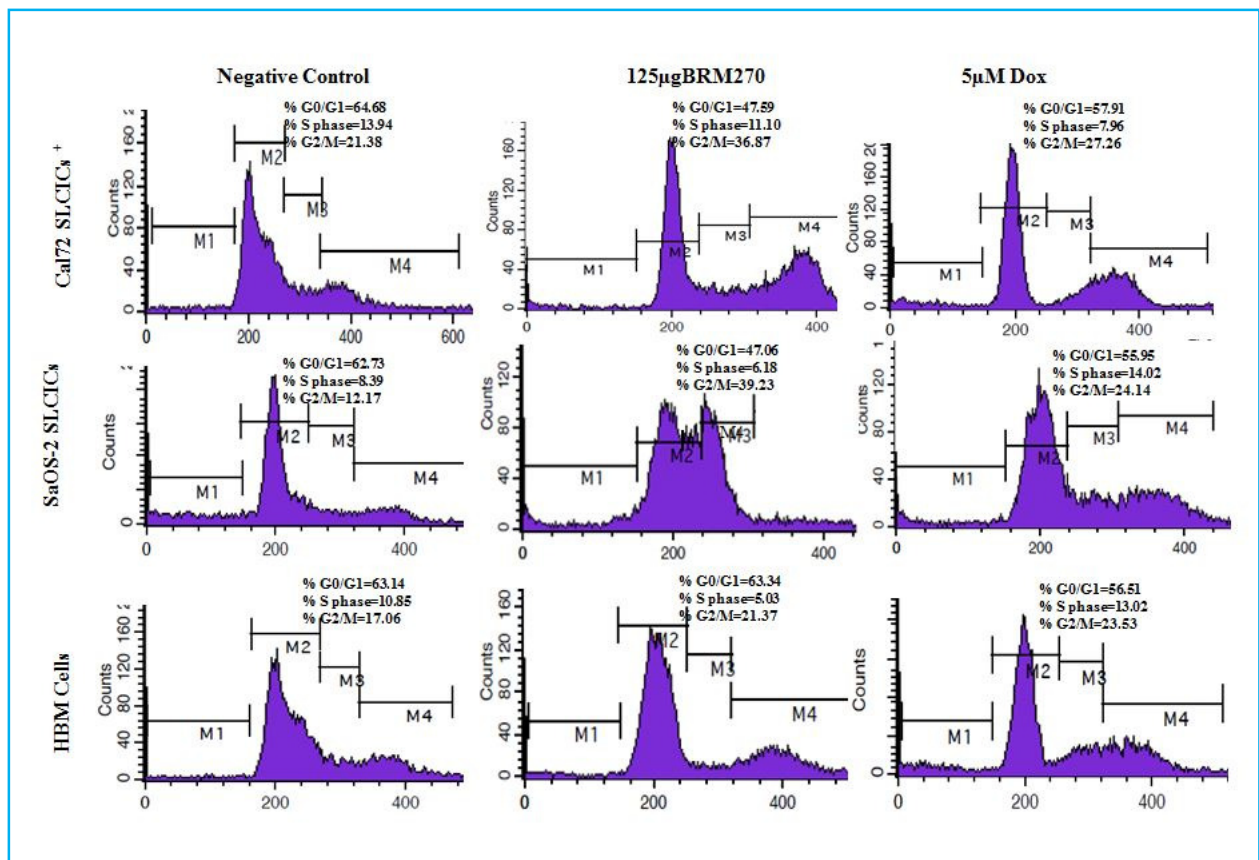


Figure 3.5. Influence of BRM270 on cell cycle progression/distribution in stem SLCICs and normal hBMCs. Cell cycle analysis of Cal72 SLCICs, SaOS-2 and normal hBMCs after being cultured with BRM270 for 24 h, BRM270 induced an increase in G2/M phase cells (%). The data are mean±S.E.M. (* $P < 0.05$).

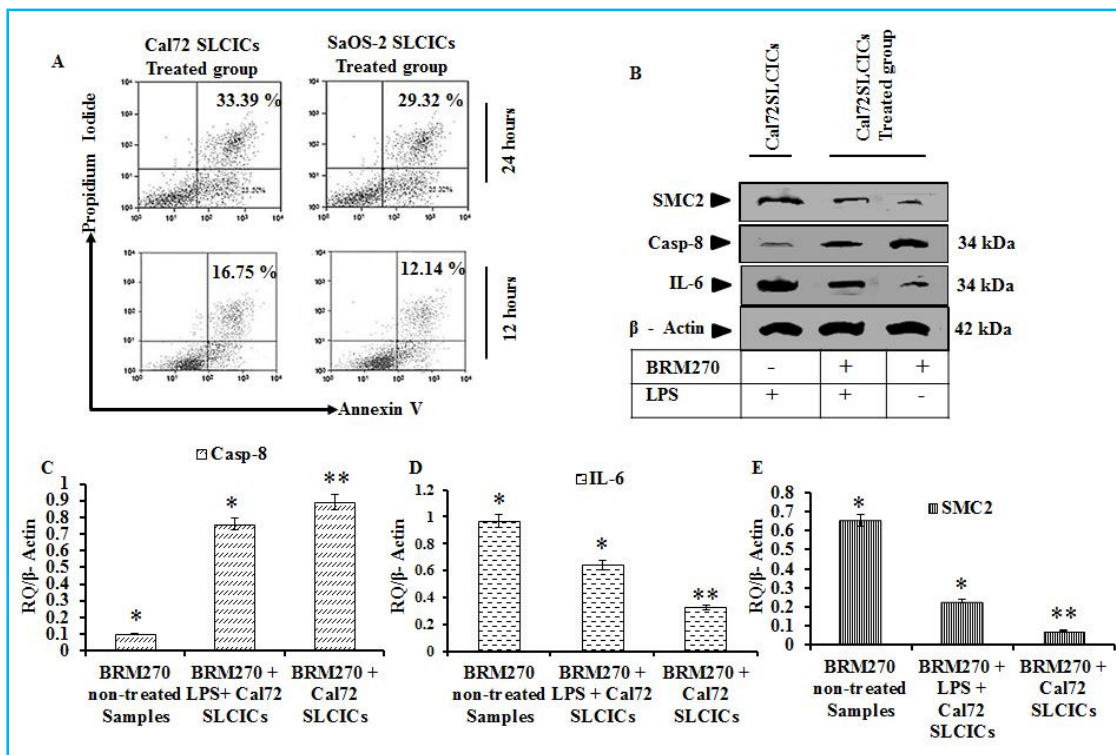


Figure 3.6. BRM270 induced IL-6 mediated apoptosis in CD133+ Cal72 SLCICs via down-regulation of chromatin SMC2. **A.** Apoptotic cell death was measured by flow-assisted cytometry analysis with fluorescein isothiocyanate-conjugated Annexin V/PI staining at 24 h after BRM270 to determine phytodrug-induced apoptosis in Cal72 SLCICs and SaOS-2 SLCICs. The lower right quadrant indicates early apoptotic cells. The early apoptotic cells are represented by a quantitative analysis. **B.** Protein lysates were analyzed by western blot analysis using IL-6 mediated regulation of anti-apoptosis gene Casp-8 and chromatin structure condensing gene SMC2 (Condensin-2) antibodies in Cal72 SLCICs with LPS or without LPS at 24 h after BRM270 exposure. **C.** Significant expression of Casp-8 increased after exposure of BRM270 treated Cal72 SLCICs than LPS with BRM270 treated group. **D.** Simultaneous decrease in IL-6 expression in BRM270 and LPS with BRM270 groups. **E.** Expression of chromatin structure forming gene SMC2 is more down-regulated in BRM270 treated group with respect to LPS with BRM270 in Cal72 SLCICs. The data are mean \pm S.E.M. (* P <0.05).

Furthermore, protein lysates were analyzed by western blot using IL6-mediated regulation of Pro-apoptosis protein Casp-8 and SMC2 in Cal72 SLCICs. To demonstrate the direct effects of BRM270 to regulate NF- κ B signal trafficking, before exposure to BRM270 the cells were given treatment with LPS. Later, the blot expressions of Casp-8 and SMC2 were studied in the cells treated with and without LPS after 24 h exposure of BRM270. However, there is significant difference ($P<0.05$) in the blot expressions of both LPS + BRM270 versus only BRM270 groups (Figure 3.7). Moreover, the relative transcriptomic levels of apoptotic gene Casp-8 increased significantly ($P<0.05$) in Cal72 SLCICs than LPS treated group after treatment with BRK270. At the same time, a significant ($P<0.05$) decrease in the transcriptomic levels of IL-6 have been recorded in both the groups. Moreover, a significant decrease in the transcript levels of *SMC2* has been recorded in the group without treatment with LPS as compare to cell lines treated with LPS after exposure of BRM270 (Figure 3.7).

3.4. IL-6 augmented neoplasia chemotherapeutic drug resistance ameliorated via co-suppression of p65 and Cdk6 by BRM270 in SLCICs: as a mechanistic approach.

The relationships between the level of IL-6 with the expressions of Cdk6, NF- κ B and Casp-8 in CD133 expressing Cal72 SLCICs have been investigated (Figure 3.8) to understand the role of IL-6 in crosstalk between NF- κ B signaling cascades in SLCICs mediated cancer progression and MDR. On comparison of the transcriptional levels of candidate genes after BRM270 treatment with respect to NC, the Cdk6 has shown significantly higher transcript levels in Cal72 SLCICs than in BRM270 treated group (Figure 3.8). Similarly, NF- κ B also over

expressed in non-BRM270 treated SLCICs while after treatment it was suppressed simultaneously with Cdk6 (Figure 3.8).

Further, we targeted to investigate the effect of BRM270 on IL-6 induced NF- κ B activation pathway. IL-6 is reported to enhance the stemness of the oncogenic cells which were demonstrating the MDR to Dox. An attempt has been made to find the efficacy of BRM270 on SLCICs in dose dependent manner (Figure 3.1). Although, it recruits the Cdk-6 to catalyze the cyclin-D which up-regulates cell cycle in G0/G1 phase (Figure 3.5) in cancer stem cell. It has been observed that CD133⁺ SLCICs induces tumorigenesis via NF- κ B signaling where Cdk6 is co-localized with p65 (Figure 3.9). Moreover, qPCR analysis has demonstrated the efficacy of BRM270 which suppress the expression of p65 and Cdk6 significantly ($P < 0.05$) *in-vitro* (Figure 3.9). It further arrests the cell cycle at G1 phase and transit to G2/M phase (Figure 3.5). In the LPS treated group IL-6 has over expressed the stemness property of CD133⁺ SLCICs. It also exerted the MDR under *in-vitro* conditions (Figure 3.2). On the other hand, non-LPS treated group demonstrated higher cytotoxicity, which in turn led to decrease in the size of the tumor in Dox and BRM270 treated groups. Significantly higher blot expressions of I κ B α , p65 and IL-6 targeted towards the enhanced tumorigenicity under *in-vivo* conditions (Figure 3.7, 3.9). On treatment with BRM270 in the nude mouse under *in-vitro* conditions a dramatically down-regulated expression of NF- κ B was observed. Findings from qPCR and Western Blot also supported the concept of co-suppression of Cdk6 and p65 (Figure 3.9).

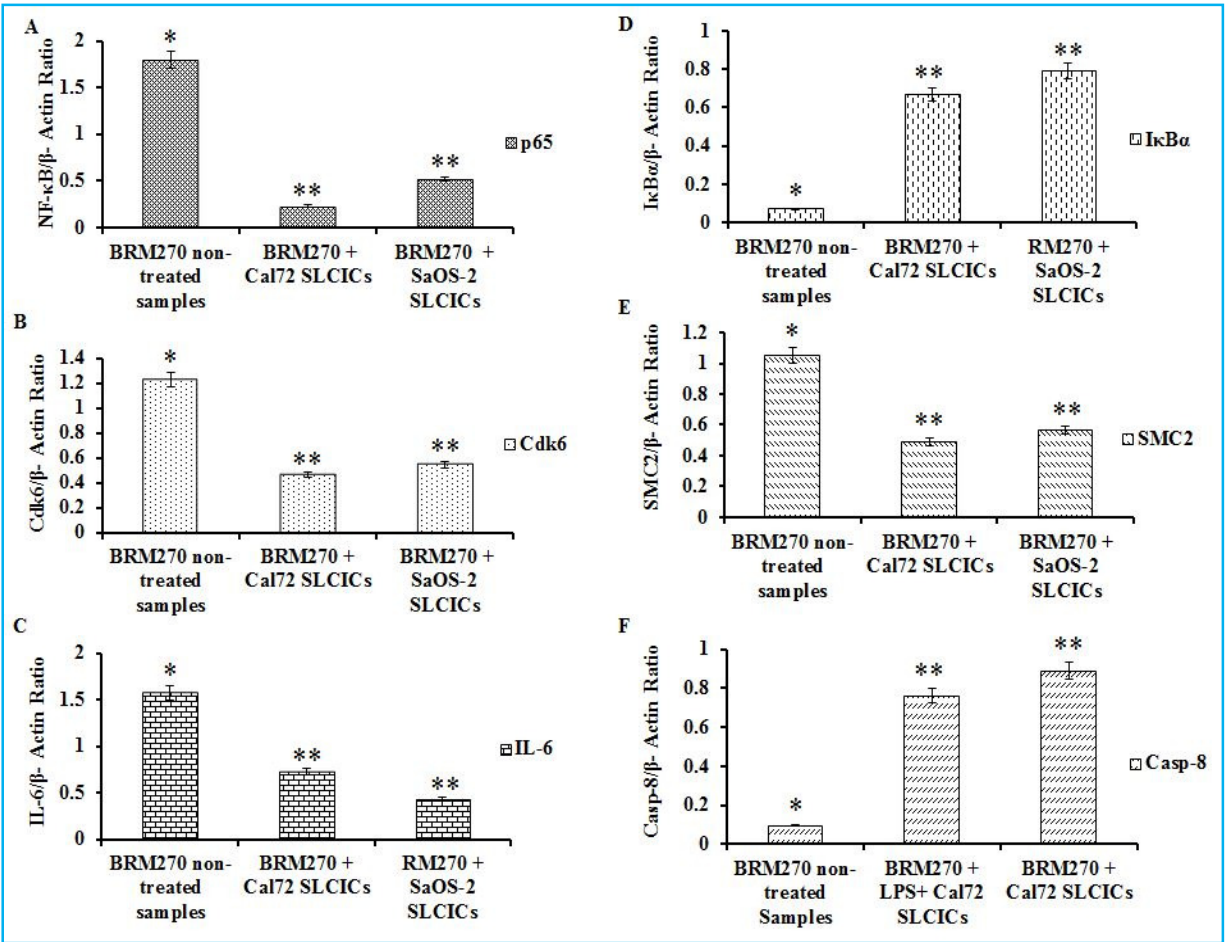


Figure 3.7. IL-6 augmented neoplasia chemotherapeutic drug resistance ameliorated via co-suppression of p65 and Cdk6 by BRM270 in SLCICs. Quantitative transcripts of Cal72 SLCICs with LPS and without LPS after treatment with BRM270. (A) Relative transcript levels of NF-κB-related genes in Cal72 SLCICs. (B) Relative expression of Cdk6 in Cal72 SLCICs. (C) Expression of pro-inflammatory cytokine-related genes; IL-6 in Cal72 SLCICs. (D) Quantitative expression of IκBα in Cal72 SLCICs. (E) Expression of SMC2 in Cal72 SLCICs. (F) Expression of Casp-8 in Cal72 SLCICs. The data are mean±S.E.M. (**P*<0.05).

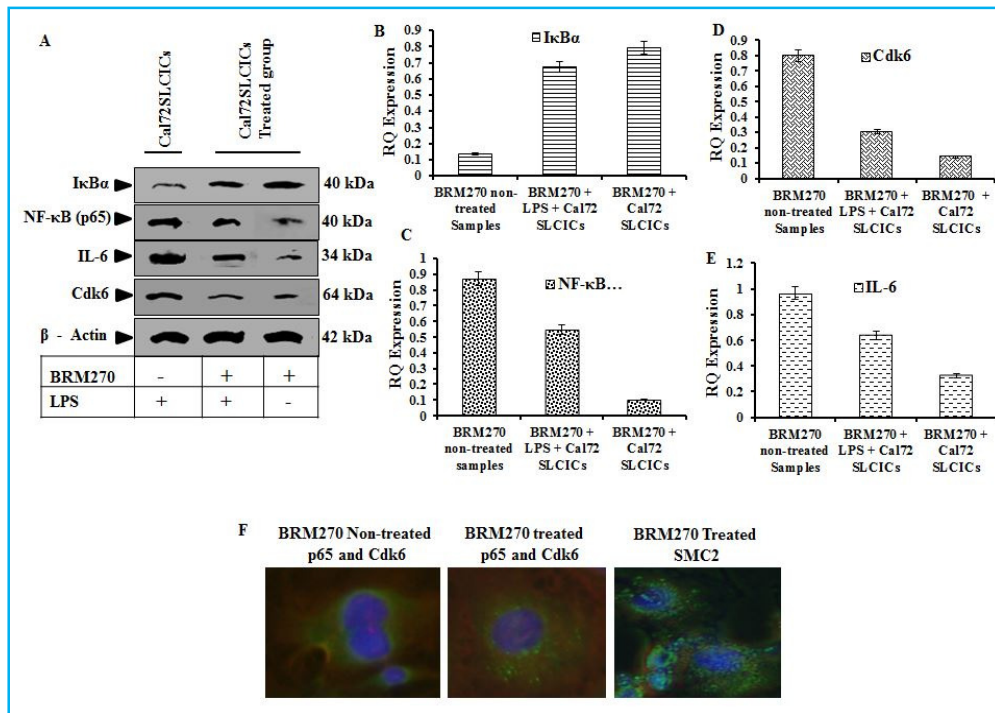


Figure 3.8. De-phosphorylation of NF-κB by CDK6/cyclin complexes by BRM270 in dose dependent manner. (A) Relative blot expressions of p65, Cdk6, IκBα and IL-6 after their normalization with blot expressions of β-actin under the influence of BRM270. (B) Relative quantitative expression of IκBα observed in Cal72 SLCICs. (C) Relative quantitative expression of p65 observed in Cal72 SLCICs. (D) Relative quantitative expression of Cdk6 observed in Cal72 SLCICs. (E) Relative quantitatively expression of IL-6 observed in Cal72 SLCICs. (F) Co-localization of p65 (NF-κB) with Cdk6 and SMC2 in Cal72 SLCICs in BRM270 non-treated and treated with LPS and without LPS. The data are mean±S.E.M. (* $P < 0.05$).

4. DISCUSSION AND CONCLUSION

Understanding the biological underpinnings of SLCICs induced tumor progression such as subcutaneous osteosarcoma and hepatocarcinoma are keys for advances in therapy. Aberrant expression of IL-6, NF- κ B with Cdk6 is found in many cancers (Iliopoulos *et al.*, 2009; Handschick *et al.*, 2006). Studies of the functional role of BRM270 as tumor suppressor can identify new pathways in cancers (CPC, 2010; Cao *et al.*, 2013; Cao *et al.*, 2013). It provides insight for the development of new or adjuvant therapies. First, we conducted a sphere-forming assay to confirm whether CD133 expressing Cal72 SLCICs have the stem-ness characteristic of CSCs or not (Figure 3.1). The Cancer stem cell hypothesis suggests that SLCICs are tumorigenic cells which contain intra-tumoral heterogeneity (Chen *et al.*, 2013; Prince *et al.*, 2007). The observation that systemic metastasis and treatment failure are often associated with the survival of a small number of cancer cells (Schober *et al.*, 2011; Prince *et al.*, 2007). To define the wide range of efficacy of BRM270 as a noble inhibitor of NF- κ B signaling cascade, its effective role in two cancer stem cell lines expressing CD133⁺ i.e. Cal72 and SaOS-2 SLCICs were studied. Furthermore, the cytotoxicity effect of BRM270 in normal hBMC line also has been studied. First of all, the SLCICs are enriched with CD133 protein on the cell surface which gets attached with anti-human CD133 magnetic MicroBeads, during their separation in the higher magnetic field (separator) (Soufizomorrod *et al.*, 2013). To have better understanding of SLCICs and their role in the cancer progression, an increased population of CD133 SLCICs induced primary tumor in a prospectively collected series of osteosarcoma cancer bearing nude mouse samples were analyzed in the current study (Figure 3.2). Similarly, Bertolini *et al* (2009) and Peickert *et al* (2012) reported that CD133⁺ subpopulation is efficient to tumorigenic in nude mouse with

respect to CD133⁻ SLCICs. The immunocytochemistry have been elucidated to confirm the expression of CD133 *in-vitro* which demonstrated the overexpression. Shmelkov *et al* (2008) reported that both CD133⁺ and CD133⁻ metastatic tumor subpopulations formed colony spheres in *in-vitro* cultures and were capable of long-term tumorigenesis in a NOD/SCID mouse. Similarly, our findings by immunocytochemistry (ICC) have revealed that the CD133 overexpressing SLCICs are capable to induce tumor sphere formation *in- vitro* and tumorigenesis in xenograft model (Figure 3.1). On the other hand, FACS analysis showed that the CD133 rich subpopulations have been observed in Cal72 SLCICs (2.05% and 16.12%) and tumor sample (18.31% and 48.48%). Furthermore, Soufizomorrod *et al* (2013) and Bertolini *et al* (2009) also found the subpopulation of CD133⁺ cells in A459 (Adeno lung carcinoma) and umbilical cord blood derived hematopoietic stem cells. CD133 expressed Cal72 SLCICs induced high grade tumor which was analyzed by a near infrared 2- DG optical imaging system on the basis of their intensity in nude mouse (Figure 3.1) which is parallel to the findings of Kovar *et al* (2009). In the present study, quantitative transcript levels in cancer stem cells showed the CD133 expression in *in-vitro* Cal72 and SaOS-2 SLCICs (Figure 3.3). Importantly, Shmelkov *et al* (2008) reported quantitative expression of CD133^{+/-} in human metastatic colon cancer through xenograft model in nude mouse.

MCD as a major phenomenon is observed in number of malignancies during abnormal mitosis checkpoints and apoptosis (Blank *et al.*, 2006; Castedo *et al.*, 2006). To determine the mitotic catastrophe and cell death, SLCICs were treated with Dox and phyto-drug such as BRM270, which later were stained with Hoechst 33342 to measure the shape of nuclear DNA. The stained cells, confirmed cell shrinkage, apoptosis and cell death (Figure 3.4) which has been supported by Blank *et al* (2006). Castedo *et al* (2004) and Kerr *et al* (1972) also reported that

DNA damage and multi-nucleation due to mitotic catastrophe and apoptosis in oncogenesis. While examining the mechanism of action of BRM270 in a SLCICs model of tumorigenesis, it was observed that treatment of BRM270 results in rapid and extensive apoptosis (Figure 3.4, 3.6). These results suggest a novel NF- κ B-inhibition-induced cell death response in SLCICs. Phyto-drugs including BRM270, play a novel anti-proliferative role in many cancers ((CPC, 2010; Cao et al., 2013; Cao et al., 2013; Zhang et al., 2012)). BRM270 also effective against Dox resistant cancer cells induces cell cycle arrest at G2/M phase in the CD133⁺ expressing SLCICs Cal72. BRM-270 has shown significant efficacy in Dox resistant cancer cells. The regulation of cell cycle in CSC is the one of the most effective antitumor mechanisms by inhibition of uncontrolled cell growth. The G2/M transition is a crucial step in the cell cycle for controlling cell proliferation (Luk *et al.*, 2005; Xue *et al.*, 2012). The G2/M checkpoint has been reported to block the entry into mitosis when DNA is damaged by natural products (Luk et al., 2005). BRM270 also caused DNA damage and cell cycle transition from G0-G1 phase to G2/M phase (15.49% and 27.06%) in the CD133⁺ expressing Cal72 and SaOS-2 SLCICs (Figure 3.5). Furthermore, UCC is a morphological hallmark of premature mitosis that is typical of cells with a defective G2/M checkpoint (Blank et al., 2006; Roninson et al., 2001). Our results demonstrate a clear distinction between the mechanisms that drive neoplasia due to over-expression of stemness oncogenic candidate genes which can markedly be mitigated by noble NF- κ B inhibitor BRM270.

The current study represents an attempt to demonstrate the mechanism of NF- κ B signaling cascade by induction via LPS. LPS induced overexpression of IL-6 enhanced the Cdk6 and p65 nuclear translocation in Cal72 SLCICs in the current study (Figure 3.9). Our finding about LPS induced overexpression of IL-6 and its effective role in NF- κ B signaling is also

supported by Urashima *et al* (1997) and Szczepanski *et al* (2009) where they have reported LPS binding with TLR4 on tumor cells enhance proliferation via induced NF- κ B translocation and production ($p < 0.05$). Importantly, the distinct morphology of apoptosis was observed after exposure of BRM270 in both Cal72 and SaOS-2 SLCICs (Figure 3.4). In this study, it has been revealed that BRM270 triggered the apoptosis and down-regulated the chromatin SMC2 in NF- κ B pathway of tumorigenesis (Figure 3.6). Similarly, Caspases are interleukin-1 β converting enzyme family that initiates apoptosis in mammalian cells (Kallenberger *et al.*, 2014). The increased protein levels of cleaved Casp-8 at 24 h after BRM270 treatment (Figure 3.6) confirmed the apoptotic activity and Kallenberger *et al* (2014) while working with Casp-8, also supported our findings. In the present study, LPS induced over-expression of cytokine IL-6 is inhibited by BRM270 (Figure 3.7). Further it induced apoptosis and significantly suppressed the expression of chromatin structure maintaining gene SMC2 (Condensin2) in the both BRM270 with LPS and BRM270 treated Cal72 SLCICs (Figure 3.6). Although, Hennessy *et al* (Hennessy *et al.*, 2011) demonstrated the LPS mediated lethal shock induced by over secretion of IL-6 *in vivo* mice-model which was reduced in CDK6-deficient mice. In addition, LPS stimulation results in an increase in NF- κ B production via IL-6 over secretion and subsequent pro-inflammatory response (Chanchevalap *et al.*, 2006). This result indicated that LPS can stimulate IL-6 production via regulation of Cdk6 and NF- κ B regulation. The validation of novel mechanism of IL-6 mediated activation of NF- κ B signaling cascade was confirmed by the exposure of Cal72 with LPS. Later it led to phosphorylation and activation of the kinase complex composed of IKK α , IKK β and STAT3 (De Simone *et al.*, 2014). BRM270 inhibits the significant expression of Cdk6 and IL-6 with signaling of NF- κ B. Conclusively, taken together, our study indicates that BRM270 is an effective apoptotic augmenter and novel anti-cancerous phyto-drug.

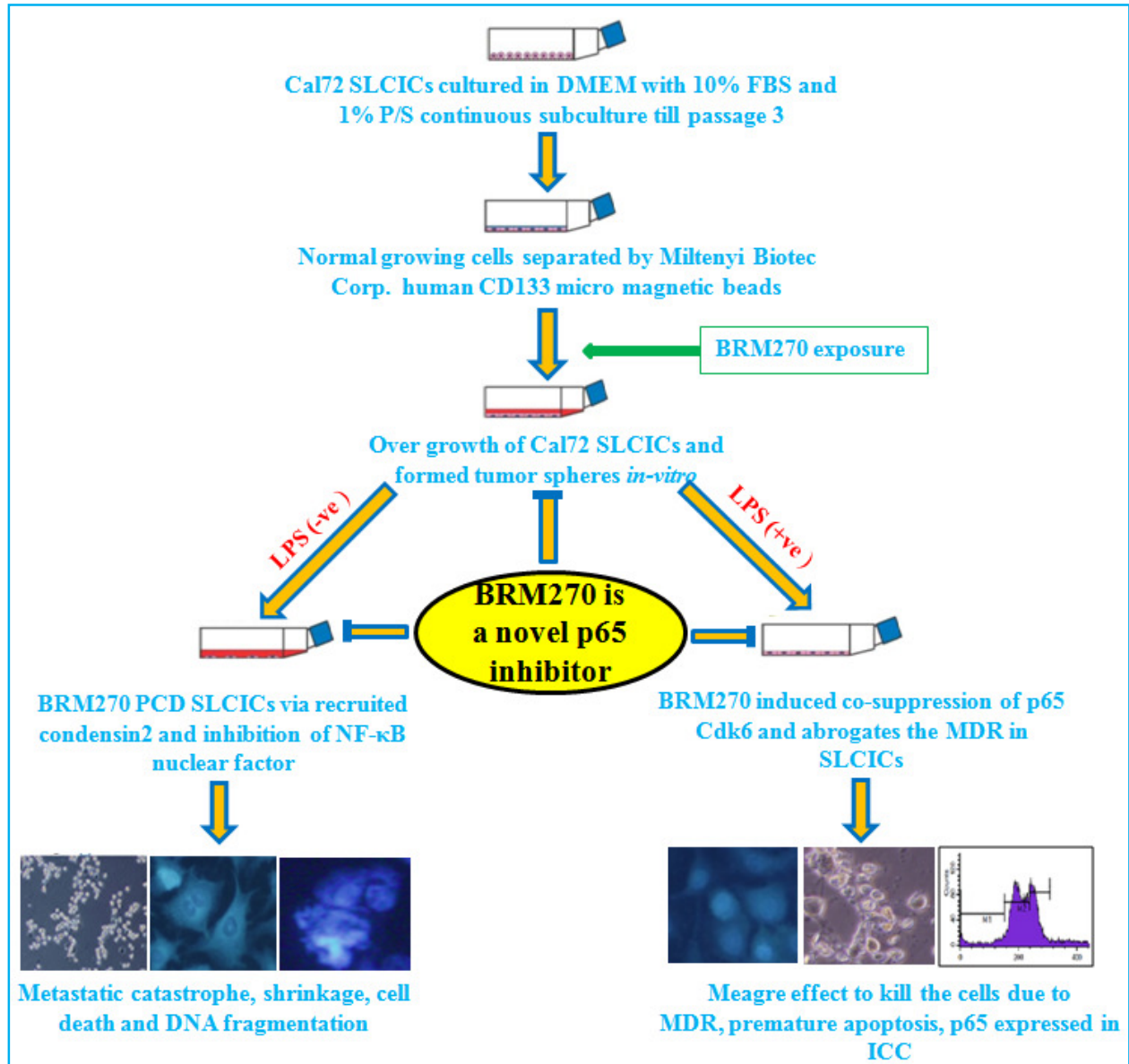


Figure 3.9. Diagrammatic representation of BRM270 as a novel inhibitor. Representation of NF-κB signaling cascade, regulation and amelioration of cancer progression by targeting the Cdk6 and p65 under the influence of BRM270.

In this study, we have provided evidence that IL-6 induces the activation of NF- κ B, an important proinflammatory pathway in cancer progression and tumorigenesis (Sansone *et al.*, 2012; De Simone *et al.*, 2014). Significantly increased expressions of CDK6 and NF- κ B in untreated group are complimented by Handschick *et al* (2014) (Figure 3.8). Meanwhile, CDK6 interacts and co-localizes with NF- κ B because it is a chromatin-bound cofactor for NF- κ B-dependent gene expression (Handschick *et al.*, 2014). A significant increase of IL-6 with NF- κ B observed in the CD133-overexpressing Cal72 SLCICs during the current study compliment the earlier reports (Figure 3.8). Similarly, a significant increase in phosphatase activity observed in the IL-6-overexpressing Cal72 and SaOS-2 SLCICs compared with control versus BRM270 treated (Figure 3.8, 3.9) is parallel with the findings of Handschick *et al* (2014) and Chanchevalap *et al* (Chanchevalap *et al.*, 2006). In the current study, BRM270 has been reported as a noble inhibitor of the IL-6-induced phospho-Rel family pathway. It is reported to abolish the activation of the NF- κ B pathway by targeting IL-6 and Cdk6 in dose dependent manner. Furthermore, efficacy of BRM270 exerts the high cell cytotoxicity in MDR-CD133⁺ cell surface bearing potent SLCICs (Figure 3.4). These data suggest that strategies aimed at the co-targeting of Cdk6/NF- κ B activation and interaction between them might represent an attractive and novel approach to combat neoplasia. Although, this drug resistance in CD133⁺ expressing SLCICs may be attributable to the persistence of a subpopulation of CSCs that exhibit MDR in lung cancer (Shmelkov *et al.*, 2008; Sarvi *et al.*, 2014). In the present study, it has been observed that CD133⁺ rich populations of SLCICs are tumor inducing cells (Figure 3.1) which overexpress the nuclear factor- κ B signal trafficking genes NF- κ B and Cdk6 along with stem-ness containing marker proteins CD133 and Oct3/4 (Figure 3.1, 3.4). Notably, these cells exerted drug resistance under *in-vitro* conditions against the Dox while BRM270 has revealed more cytotoxicity (Figure

3.4). Our findings demonstrate that BRM270 down regulates the over expression of IL-6 which induced Cdk6 to activate the apoptotic protein Casp-8 in both SaOS-2 and Cal72 SLCICs (Figure 3.7). Similarly, immunoblotting activity revealed the significant increased level in non-treated group with respect to treated samples of both SaOS-2 and Cal72 SLCICs (Figure 3.8). Notably, in our results BRM270 significantly up regulates the I κ B α in SLCICs (Figure 3.7, 3.8). It further, down-regulates the NF- κ B protein and blocks the translocation of NF- κ B into the nucleus and suppresses the expression of IL-6 (Figure 3.6-3.8). This finding is in line with the results from Yan *et al* (Yan *et al.*, 2014). It is interesting to note that once activated, JAKs phosphorylate, activate I κ B α and Rel family protein, promoting its dimerization and translocation to the nucleus (Lee *et al.*, 2014). Moreover, over expressed IL-6 triggers STAT3 this simultaneously regulates I κ B α during its dormant state in the cytoplasm (Lee *et al.*, 2014; McFarland *et al.*, 2013). Furthermore, LPS-mediated lethal shock, which is largely due to rapid release of inflammatory cytokines and chemokines including IL-6, was reduced in CDK6-deficient mice (Chanchevalap *et al.*, 2006). We also found that LPS induced activated p65 overexpressing SLCICs causes a significant increase in Cal72 SLCICs proliferation while enhancing their pluripotent phenotype (Figure 3.1, 3.9) and resistance to drug by blot analysis (Figure 3.4, 3.8). The combined efficacy of BRM270 phyto-drug on SLCICs with LPS and without distinctly indicated that it can be markedly inhibited the NF- κ B induction and suppressed the Cdk6 to arrest the cell cycle in G1 phase and transit to G2/M checkpoint (Figure 3.5). Similarly, Chinese MST press (2010) and Cao *et al* (2013) have revealed the more clear potentiality of BRM270 phyto-drug in different inflammatory conditions and cancers. Notably, we have shown that the co-overexpression of NF- κ B and Cdk6 in Cal72 SLCICs aggravates MDR complimented by Handschick *et al* (2014). Further, BRM270 has significantly suppressed, fragmented DNA and caused programmed cell

death (Figure 3.4, 3.8). Furthermore, our work shows that NF- κ B, in association with Cdk6 and IL-6, plays an important role in regulation and gene expression. Similarly, CDK6 regulates NF- κ B-dependent target gene expression in most of chronic inflammation and neoplasia (Buss *et al.*, 2012). Since blocking of the activity of NF- κ B has become a primary target for drug therapy in a number of different diseases. It is important to understand what kind of effects it may have on genes which are negatively regulated by NF- κ B and on the efficacy of the therapy itself.

This current study demonstrates the compelling evidence to down regulate the master regulator NF- κ B with Cdk6 by BRM270 as a noble inhibitor. To define the wide range of efficacy of BRM270, we have studied in SaOS-2 and Cal72 SLCICs while to effect on normal cells we also did analysis in hBMCs. Our findings aids in the identification of direct targets of molecular diatomous mechanism of carcinogenesis in CD133 expressing SLCICs. It can be significantly clinically relevant and will act as a base for the development of new therapeutic strategies.

CHAPTER 4

EPIGENETIC INDUCTION OF EPITHELIAL TO MESENCHYMAL TRANSITION BY *LCN2* MEDIATES METASTASIS AND TUMORIGENESIS, WHICH IS ABROGATED BY NF- κ B INHIBITOR BRM270 IN A XENOGRAFT MODEL OF LUNG ADENOCARCINOMA

ABSTRACT

Tumor initiating cancer stem like cells (TICSCs) have recently become the object of intensive study. Human-Lipocalin-2 (h*LCN2*) acts as a biomarker for cancers. The aim of the current study was to explore new insights regarding the potential role of *LCN2* in inducing epithelial to mesenchymal transition (EMT) by transfecting *LCN2* into CD133⁺-A549-TICSCs and its cross talk with the NF- κ B signaling pathway in adeno-carcinoma of lung. Further EMT was confirmed by transcriptomic analysis, immuno-blotting and immunocyto/histochemical analyses. Tumorigenesis and metastasis were further confirmed by molecular therapeutics tracer 2DG infrared optical probe in BALB/cSIC-nude mice. It was observed that the CD133⁺-expressing-*LCN2*-A549 TICSCs population increased in adeno-carcinoma of lung than in the normal lung tissue. The expressions of genes involved in stemness, adhesion, motility and drug efflux were higher in these cells than in their non-*LCN2* expressing counterparts. The current study revealed that elevated expression of *LCN2* significantly induced metastasis via EMT. Over-expression of *LCN2* has significantly increased stemness and tumor metastasis by modulating NF- κ B cellular signaling. BRM270, a novel inhibitor of NF- κ B plays a significant

role in the EMT reversal. BRM270, a naturaceutical induces cell shrinkage, karyorrhexis and programmed cell death (PCD) which were observed by Hoechst 33342 staining while flowcytometry analysis showed significant ($P<0.05$) decrease in cell population from G0-G1 phases. Also, 2DG guided *in vivo* model revealed that BRM270 significantly ($P<0.0003$) reduced tumor metastasis and increased percent survival in real time with complete resection. An elaborated work on the novel concept with respect to linking of naturaceuticals as selective and potential anticancer agent that eliminates the elevated *LCN2* induced EMT and tumor dissemination through cooperation with the NF- κ B signaling as the baseline data for the planning of new therapeutic strategies has been conducted for the first time. Our results also illustrate a molecular mechanistic approach for 2DG-guided molecular imaging based cancer therapy using BRM270 as a novel cancer therapeutic drug to enhance the effect of Doxorubicin (Dox) resistant *LCN2* induced metastasis of solid tumors in nude mice.

Key words: naturaceuticals, 2DG optical probe, tumor initiating cancer stem like cells, karyorrhexis, Lipocalin-2, epithelial to mesenchymal transition

1. INTRODUCTION

Stem cell research is a promising arena for the therapeutic advancement in oncology, clinical-genetics and degenerative disorders (Jordan *et al.*, 2006; Kitamura *et al.*, 2009; Wang *et al.*, 2013). Focus of cancer research is on the properties and mechanisms of formation of cancer stem cells (CSCs) or tumor initiating cancer stem like cells (TICSCs) (Jordan *et al.*, 2006; Kitamura *et al.*, 2009). However, the mechanisms governing the conversion of malignant cells into CSCs are poorly understood for majority of cancers (Wang *et al.*, 2013; Bertolini *et al.*, 2009). Most soft and solid neoplasms contain specific TICSCs expressing cell surface glycoprotein markers that are different from normal cells (Bertolini *et al.*, 2009; Akururu *et al.*, 2012). These putative surface markers have enabled the identification and characterization of TICSCs. Furthermore, TICSCs exist distinctly in epithelial-mesenchymal-transition (EMT) and mesenchymal-epithelial-transition (MET) states (Tsai and Yang, 2013). Notably, EMT induced TICSCs are efficient in inducing tumor formation and metastasis (Li *et al.*, 2012). CD133⁺ (transmembrane glycoprotein cell surface marker)-TICSCs have shown phenotypical reversion from the epithelial to mesenchymal state in lung cancer stem cells (Bertolini *et al.*, 2009; Akunuru *et al.*, 2012).

An activation of EMT in carcinogenic cells gives rise to cells that are stem-like in nature (Tsai *et al.*, 2013). The EMT plays an important role in embryogenic differentiation and biological processes associated with cancer progression (Akunuru *et al.*, 2012; Tsai *et al.*, 2013; Li *et al.*, 2012). During EMT, the expression of epithelial maintaining genes (E-cadherin, and TJP-1) is reported to be antagonized and mesenchymal candidate marker genes (vimentin, Twist-1 and SNAI2) are augmented (Casas *et al.*, 2011; Nagai *et al.*, 2012). During oncogenesis, EMT is associated with several signaling cascade including the NF- κ B pathway (Li *et al.*, 2012).

Overexpression of p65 (NF- κ B) induces transcriptional upregulation of Twist-1 along with EMT in mammary epithelial cells.

Human Lipocalin-2 (*LCN2*) is a biomarker for many inflammatory-based diseases and cancers including lung carcinoma (Huber *et al.*, 2004; Zhai *et al.*, 2012; Shi *et al.*, 2008). Furthermore, *LCN2* has been reported to promote resistance to drug-induced apoptosis, enhance invasion through its physical association with matrix metalloproteinase-9 and to promote *in vivo* tumor growth with poor prognosis (Lin *et al.*, 2012). *LCN2* is also reported to promote various cancers by inducing EMT via signaling (Zhai *et al.*, 2012; Shi *et al.*, 2008; Lin *et al.*, 2012; Candido *et al.*, 2014; Yang *et al.*, 2009; Zhao *et al.*, 2014; Rodvold *et al.*, 2012; Nakamura *et al.*, 2014; Leung *et al.*, 2012; Krysan *et al.*, 2013). Furthermore, *LCN2* promotes EMT that facilitates an invasive tumor phenotype and metastasis. Therefore, *LCN2* can be considered as a potential diagnostic/prognostic marker for cancer progression.

Lung cancer is an aggressive disease with very high mortality rates (Torre *et al.*, 2015). Refined studies on the mechanisms of tumorigenesis and chemoresistance of lung cancer are needed to improve the survival rate. Adeno-carcinoma of lung exhibits a very low survival rate especially in *LCN2*-A549 lung cancer (Shi *et al.*, 2008). Therefore, selective inhibitors with no cytotoxic effects on normal cells need to be developed for the treatment of lung cancer. Phyto-drug-based approaches provide avenues to ameliorate therapeutic strategies for effective cancer treatment (Chen *et al.*, 2012; Mongre *et al.*, 2015). BRM270 is a promising anticancer medicinal plant extract that is widely distributed in Northeast Asia, mainly in China, Korea and Japan (Mongre *et al.*, 2015). Apart from that TICSCs in general, relative to normal cells, demonstrate elevated glucose metabolism but the mechanism for this is unknown. The clinical utility of these biomarkers to detect tumor localization and targeting using image-guided therapy has been

limited to the use of 2-[F-18]-fluoro-2-deoxy-D-glucose (FDG or 2DG) and positron emission tomography (PET) to identify cancerous tissues (Kover *et al.*, 2009). The current study hypothesis, the extent to which elevated *LCN2* mediated tumorigenesis and metastasis increase their uptake and metabolism of glucose is predictive of cancer cell susceptibility to 2DG-induced radio-/chemo-sensitization and oxidative stress in adenocarcinoma of Lung. The goal of this work is to provide a novel mechanism based biochemical rationale for the use of glucose metabolic differences and functional imaging to develop biologically guided combined modality therapies to treat oncogenes (such as *LCN2*) induced carcinogenesis based on tumor specific sensitivity to metabolic oxidative stress.

In the present study, we aimed to explore the potential role of *LCN2* in inducing EMT and its cross talk with the NF- κ B signaling pathway. Secondly, the role of *LCN2* in EMT mediated tumorigenesis and adeno-carcinoma of lung in xenograft models was investigated by 2DG optical probe as image-guided therapeutics strategy. In addition, we also sought to establish the novel paradigm of EMT *in vitro* systems and implemented *in vivo* models. Further, tumorigenic ability of CD133⁺-*LCN2*-A549 TICSCs has also been compared with CD133⁺-A549-TICSCs. The current study potentially targeted on the establishment of a novel therapeutic strategy linking 2DG to *LCN2* induced EMT and growth promotion of lung cancer cells through cooperation with the NF- κ B signaling with zero cytotoxicity to normal tissue against adeno-carcinoma of lung through the use of BRM270 as a novel anticancer naturaceutics with 2DG optical probe.

2. MATERIALS AND METHODS

2. 1. *Animal model of EMT induced metastasis*

Nude 6 week old male BALB/cSlc nu/nu mice were purchased from Japan SLC, Inc. They were housed under uniform environmental and nutritional conditions. Mice were sacrificed at 10, 11, and 12 week age according to the standard protocols of Jeju National University. The research proposal and the relevant experimental procedures were approved by the institutional review board of the Department of Animal Biotechnology, Jeju National University, Jeju Special Self-Governing Province, Republic of Korea, 690-756. All animal studies were conducted to induce tumor. Tumorigenesis induction was performed in 34 nude mice. To study the tumorigenesis and metastasis, all the mice were grouped into six groups. Six mice each were used as positive control of EMT (non-*LCN2* transfected A549 TICSCs induced tumor group), the test group of EMT and metastasis (*LCN2*-A549 TICSCs induced mouse group). Also, the 6 mice each were incorporated as a treatment group of EMT (*LCN2*-A549 TICSCs BRM270-treated group) and positive control (Dox-treated group). Four mice were used in a negative control group in which hBMCs were injected. To analyze the tumorigenic efficiency of CD133⁺ A549 TICSCs and *LCN2*-A549 TICSCs, we have injected 5×10^6 cells/mL concentrations of cells into lower right flanks of nude mouse by micro needle syringe (29 gauge x 1/2" 12.7 mm needle, Ultra-Thin Plus™ Korea).

2. 2. *Optical probe guided molecular imaging of tumor metastasis*

For pre-and intraoperative tumor localization in real-time resection, we conducted *in vivo* tumor localization assay using IRDye® 800CW 2-DG (2-deoxy-D-glucose) optical probe which is purchased from LICOR, Biosciences, USA (926-08946). To evaluate and establish metastatic

potential of A549 vs *LCN2*-A549 TICSCs, characterized cells were inoculated subcutaneously to nude mice. After 7 days experimental metastasis was observed followed by observation of distinct "spontaneous metastasis", where the tumor cells were first allowed to form a primary tumor at the site of injection and then escaped into lymphatic or blood circulation. Probe was dissolved in phosphate buffer saline (1X PBS) and was injected into the tail vein of the tumor bearing nude mice then mice were observed after they were anesthetized with Zoletil50 (Virbac, Carros, France) 1 mL/kg intraperitoneally and all surgical procedures were performed under general anesthesia at different time intervals. Metastasis is detected using optical molecular imaging, in particular near-infrared fluorescence (NIRF) range.

2. 3. *Cell lines propagation and reagents*

The human lung adenocarcinoma A549 cell line was purchased from Korean Cell Bank, South Korea (KCBL No. 10185). Cells were propagated in Dulbecco Minimum Eagle's Medium (DMEM) with 10% Fetal Bovine Serum (FBS) (Hyclone, UT, USA), 1% antibiotic-antimycotic (Gibco, CA, USA) at 37°C and 5% CO₂ under humidified atmosphere. The cells were sub-cultured after attaining confluency level of 80%. For the current experimental study, the cells in passage 3 were used. The hBMCs procured from a 59 years old Caucasian male were purchased from Korean Cell Line Bank, Seoul South Korea (KCLB No. 10246) and then were separated by Ficoll-paque density gradient centrifugation (GE Healthcare, USA). The potential hBMCs were further cultured in RPMI1640 supplied with 20% FBS, 1% antibiotic-antimycotic and 10 nM epithelial growth factor (E9644-Sigma,USA). To test the properties of A549 cells as TICSCs, they were characterized with human anti-CD133 micro magnetic beads (25). Later, after

characterization, cells from the pure colonies were injected subcutaneously on the right lower flank of nude mouse. Seven days of post injection, palpable tumors were observable.

2. 4. Cloning and gene transfer of *LCN2* into lung adenocarcinoma A549 Cell line

Primers for the cloning of *LCN2* coding sequence were designed on the basis of the homologous regions of Humans (Gene Bank accession No. NC_000009). Primers were designed using primer 3.0 tool for 5'-RACE (rapid amplification of cDNA ends) and 3'RACE to obtain the C-terminal coding region of the *LCN2* gene (F- ATGTCACCTCCGTCCTGTTT, R- GTCAGCTCCTTGGTTCTCC). The polymerase chain reaction (PCR) was performed using cDNA from human A549 cells using Prime Taq Premix (2X), (GenetBio, S. Korea) in a total volume of 20 µl mixture. The amplified DNA fragments were subsequently cloned into pUC57. Purified PCR products of *LCN2* was sequenced and compared by “Cosmo genetech”, South Korea.

For the cloning of *LCN2*, the plasmid vector PiggyBac was procured (Clontech, USA). For the propagation of plasmid and as a maintenance host, *E. coli* Oneshot[®] Top10 (Invitrogen, USA) competent cells were used. HindIII restriction enzyme was used to linearize the vector and later, the respective target gene of human lung carcinoma from A549 cells was picked by PCR. Sub-cloning was performed with cloning primers having restriction enzyme sites for EcoRI and Hind III incorporated in forward and reverse primers respectively. PCR products were separated on 1.2% agarose gel and were extracted by Expin Gel (GeneAll Biotech, South Korea) extraction kit by following the user guidelines.

2. 5. *Cell proliferation (EZ-CyTox) assay*

Suspended cells (100 μ l) at density of 5,000 cells/well were seeded in 96-well plate (Nunc™, Wiesbaden, Germany). After 24 h of recovery the cells were incubated in humid atmosphere at 37°C and 5% CO₂ and treated with BRM270. The BRM270 was procured from the Biological Response Modifier International Heath Town Corp., Korea. The cells were treated with varying concentrations of BRM270 such as 15.6-125 μ g/mL and Doxorubicin (Dox) 10 μ M/mL in cell cytotoxicity assay while 125 μ g/mL BRM270 in rest of the experiments were incubated for 24 h. The enhanced cell viability assay was conducted with EZ-CyTox kit (Daeil Lab Service Co. Korea) to measure the viable cells. EZ-CyTox solution (10 μ l) was added to each well and then cells were incubated for 4 h at 37°C and 5% CO₂. The light absorbance was determined at 450 nm by the Model 680 microplate-reader (Bio-Rad, Berkeley, USA).

2. 6. *DNA fragmentation assay*

CD133⁺ A549 and *LCN2* transfected A549 TICSCs (1X10⁶ cells) were seeded in 6-well microtitre plate (NuncNunclon™ Delta, USA). Then the cells were treated with the 125 μ g/mL concentrations of BRM270 for 24 h for analysis of genomic DNA fragmentation, shrinkage as our previous study (25). Later, the cells were washed with 1X phosphate-buffered saline (Gibco, Life Technologies™, USA) and were fixed with 4% paraformaldehyde for 10 min followed by incubation with 50 μ M Hoechst 33258 staining solution for 5 min. After three washes with cold PBS, the cells were viewed under a fluorescence microscope (IX-70-Olympus, Japan). Then, genomic DNA was extracted by AccuPrep® Genomic DNA Extraction kit (Bioneer). DNA (5 μ g) was separated on a 1.2% agarose gel. DNA in the gel was stained with ethidium bromide (EtBr) and was visualized under UV light.

2. 7. Flow cytometry and cell cycle analysis

The analysis of cell cycle was detected by PI staining and analysis was performed by flow cytometry using a fluorescence-activated cell sorting (FACS) caliber (Becton-Dickinson). Subsequent to the treatment with 100 $\mu\text{g}/\text{mL}$ and 10 $\mu\text{M}/\text{mL}$ concentrations of BRM270 and Dox for 24 h, CD133⁺ expressing A549 and LCN2-A549 TICSCs were harvested at concentration of 1×10^6 cells/mL. The cells were fixed in 70% ethanol and incubated at 4°C overnight. The fixed cells were washed twice with cold PBS and then incubated for 30 min with Ribonuclease A (#R-5125, Sigma, 8 $\mu\text{g}/\text{mL}$) and PI (10 $\mu\text{g}/\text{mL}$). Then the cell samples were transferred to meshed blue capped tubes (BD Falcon™ Tubes #352235). Later, the fluorescent signals were detected through the FL2 channel and the proportion of DNA that was present in the various phases was analyzed using ModfitLT Version 3.0 (Verity Software House, ME, USA).

2. 8. Analysis of EMT induced metastasis by immunocyto/histochemistry (ICC)

Cultured CD133⁺LCN2-A549 and A549 TICSCs were washed and fixed in 4% phosphate buffered paraformaldehyde for 25 min at room temperature (RT) then washed three times with cold 1X PBS and permeabilized with 1% Triton X-100 in PBS for 15 min at RT. Incubation with primary antibodies in 1% BSA overnight at 4°C. The cells were then washed with 0.2% Tween-20 (Sigma) in PBS before addition of appropriate FITC-conjugated secondary antibody reagents for 1 h at RT in the dark. Cells were then washed with cold PBS and were counterstained with 4', 6-diamidino-2-phenylindole (DAPI, Invitrogen, USA). After incubation for 5 min again washed with cold 1X PBS and added 1 mL mounting media and cells were observed under the

fluorescence microscope (Olympus, Milan, Italy) with adaptable filter consistent with Alexa Flour 488, Alexa Flour 546, GFP (green fluorescence protein) and phycoerythrin (PE).

2. 9. RNA Isolation and quantitative real time PCR (qPCR)

Cells were seeded at a density of 2×10^6 cells/T25-mm flask (NuncThermo Scientific, Korea) and were continuously sub cultured till passage three (P-3) in T75 mm³ flask. At 70 % confluency after incubation for 24 h, the culture medium was replaced with RPMI1640 containing 2% FBS. The cells were detached by Trypsin-EDTA 0.5% (Gibco, USA) and total RNA was extracted by easyBlue (Intron Biotech, South Korea). The purified RNA which was quantified by using Photometer (Biorad, *Hercules*, USA). 1 μ g of purified RNA was subjected to first strand c-DNA synthesis using Superscript-III first-strand c-DNA synthesis kit and OligodT primer (Invitrogen, USA). The c-DNA was subjected to qRT-PCR for the quantification of the relative transcript levels of, h*LCN2*, E-cadherin, Vimentin, Twist1, TJP-1, SNAI2, p65, and c-Myc using the specific primers which were procured from Cosmo genetech Korea.

2. 10. Quantitative western blot

The cells were plated in 60-mm plates and allowed to grow overnight. The cells were then placed in low serum medium (1% FBS) for 16 h, after which the medium was replaced with low serum medium containing either in 10% FBS with G418 or only in DMEM with 10%. While to mitigate the tumorigenesis in *LCN2*-A549 and A549 injected in mice, BRM270 treatment was given to the nude mouse at the rate of 5 mg/mL/day for 2-4 weeks. Total proteins were isolated by ice-cold radioimmunoprecipitation assay (RIPA) buffer supplied phenyl-methane-sulfonyl-fluoride (PMSF) (Sigma-Alrich, USA) and ready to use protein inhibitor cocktails (Thermo

Scientific, USA). Protein concentrations were calculated by using Pierce® BCA Protein Assay Kit (Thermo Scientific, IL USA) following the manufacturer's instruction. Forty micrograms of proteins were then loaded per well. Proteins were separated on 12% polyacrylamide gel and transferred to polyvinyl-denedi-fluoride membranes (PVDF; Sigma-Alrich Corp., USA) in the Bio-rad western blot system (Bio-rad, California, USA). The membrane was incubated with the primary antibodies (NF-κB, *Lipocalin-2*, E-cadherin, Vimentin, SNAI2, Twist1, MMP-9, TJP-1 and SMC2 rabbit polyclonal) with control β-actin for overnight and then incubated for one hour with secondary antibodies. All antibodies were procured from Santa Cruz Biotechnology, Inc. CA USA. The proteins of interest were detected by an enhanced chemiluminescence detection kit following manufacturer's instructions using LAS400 machine (GE Healthcare, NJ, USA).

2. 11. Statistical Analyses

The relative quantitative expressions of the genes by real-time qPCR and western blotting were analyzed by the analysis of variance (ANOVA). Kaplan-Meier curves of overall survival of mice were analysed Log-rank (Mantel-Cox), and Gehan-Breslow-Wilcoxon test using GraphPad Prism 6 software (CA, USA). The tumor was measured with Vernier's calipers and the volume of the tumor (mm³) was calculated by the following formula:

$$Volume = (width)^2 \left(\frac{length}{2} \right)$$

Further, the size and the extent of metastasis of tumor under *in vivo* conditions was detected using 2DG-infrared-guided imaging by LI-COR pearl small animal image analyzer (LI-COR Biosciences, USA). All the mice were sacrificed for the collection of tumor samples. The significant differences between the mean expressions of different genes at $P < 0.05$ and $P < 0.001$ were analyzed by Tukey's b-test. The values have been expressed as mean±SEM.

3. RESULTS

3.1. Over-expression of LCN2 is directly associated with CD133 expression and induces an EMT like morphology leading to metastasis in A549-TICSCs

To systematically identify candidate differentially expressed genes (DEGs) in EMT, the EMT-inducing *LCN2* expressing CD133⁺-A549-TICSCs were established using the Nucleofector™-Amaxa Lonza System. Compared to control cells transfected with p^{maxGFP}, over-expression of *LCN2* changed the cell morphology in DMEM/F12 supplemented with 10% FBS (Figure 4.1). The *LCN2* over-expression leads to the secretion of multiple soluble factors that markedly transform cancer cells into EMT-induced TICSCs. It causes a phenotypic switch leading to an elongated mesenchymal morphology (Figure 4.1B). Further, *LCN2* was transfected into CD133⁺-A549-TICSCs and analyzed both *LCN2*-A549 cells and un-transfected A549 cells. Immunocytochemistry (ICC) confirmed the expression of *LCN2* in the transfected CD133⁺-A549-TICSCs. Compared to non-transfected cells, significant changes were observed in the epithelial cell morphology to mesenchymal morphology (Figure 4.1B). As expected, the results revealed higher expression of *LCN2* in *LCN2*-A549-TICSCs than in non-transfected A549 cells (Figure 4.1C). qPCR and blot expression also demonstrated a significant ($P<0.05$) increased mRNA and proteins levels for *LCN2*-A549-TICSCs compared to normal A549-TICSCs and BRM270 treated *LCN2*-A549-TICSCs (Figure 4.1D and E). CD133⁺-A549-TICSCs efficiently induced tumors in male nude mice that detected using 2DG infrared optical probe by LICOR image analyzer (Figure 4.1F). Moreover, CD133⁺-A549 and *LCN2* A549-TICSCs were tumorigenic in nature, but *LCN2*-A549 induced long term growth of solid primary tumors, metastasis initiation and poor prognosis in response to Dox treatment.

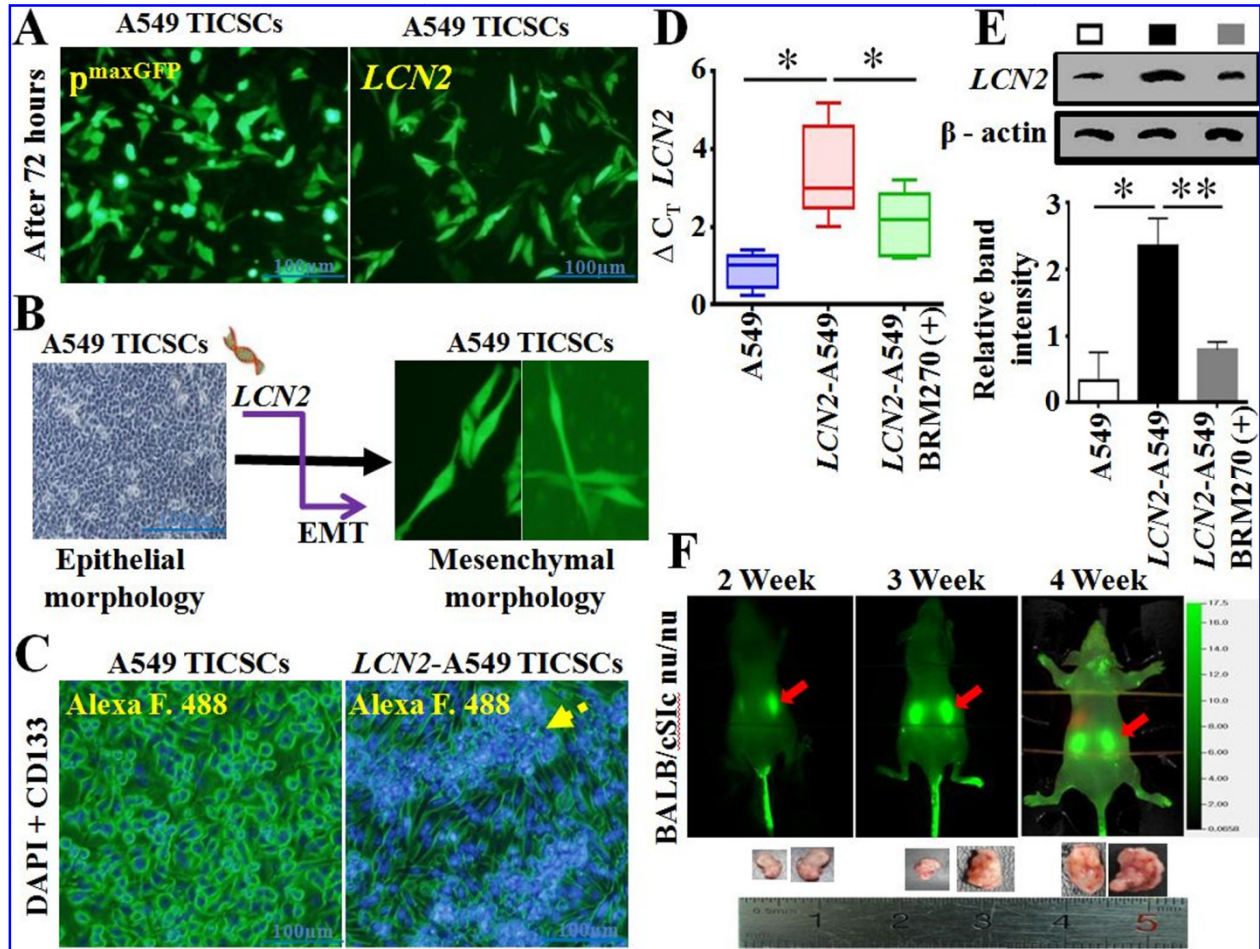


Figure 4.1. LCN2 modulates epigenetic switching in CD133⁺-A549-TICSCs induce tumorigenesis. A. The transfection efficiencies of *LCN2* and $p^{\max GFP}$ in A549 cells were detected by fluorescence microscope (100X). B. Genetic transformation of A549-TICS epithelial-to-mesenchymal under the influence of *LCN2*. C. ICC analysis of CSC marker CD133⁺ in the transfected A549-TICSCs to show enhanced metastatic cells (yellow arrow). D. Whisker and Box plot representing mRNA levels of *LCN2* in CD133⁺-TICSCs. E. Quantitatively blot expression and relative band intensity of *LCN2*. F. Detection of tumors in BALB/cSic-(nu/nu) nude mice using IRDye-800CW-2DG optical probe (LICOR, pearl image system).

3.2. The novel NF- κ B inhibitor BRM270 mitigates LCN2 induced metastatic proliferation by down regulation of CD133⁺-CyclinD1 mediated premature apoptosis and DNA catastrophe

Mitotic catastrophe and programmed cell death in cancer are the most important mechanisms for eradication of TICSCs. It was observed that over-expression of *LCN2* induced stemness in *LCN2*-A549-TICSCs.

Specifically, FACS analysis showed that CD133 expression was considerably increased in *LCN2*-A549-TICSCs (4.23%) compared to non *LCN2* expressing A549-TICSCs (0.79%) (Figure 4.2A). Similarly, qPCR showed that transcript levels of CD133 were significantly higher in *LCN2*-A549 TICSCs than A549 and BRM270 treated (Figure 4.2B). Furthermore, a reduced ability to form tumor spheres was observed in A549-TICSCs compared to *LCN2*-A549-TICSCs, indicating that *LCN2* drives tumor formation in A549-TICSCs (Figure 4.2C). Efficacy of BRM270 exerts anti-cancerous activity. To elucidate the cell shrinkage, morphological DNA fragmentation and programmed to cell death by BRM270, we conducted a dose dependent BRM270 treatment with compared to Dox. The CD133⁺-A549 and *LCN2*-A549 TICSCs treated with BRM270 for 24 and 48 h, were stained with Hoechst 33258 and ICC to analyze the extent of genomic DNA fragmentation and cleavage of chromosomal DNA at inter-nucleosomal sites, interruption of microtubule cytoskeletal formation in Dox resistant TICSCs, as well as formed chromosomal condensation (pyknosis) and multinucleated fragmentation (karyorrhexis) (Figure 4.2D and E, red-yellow-arrows).

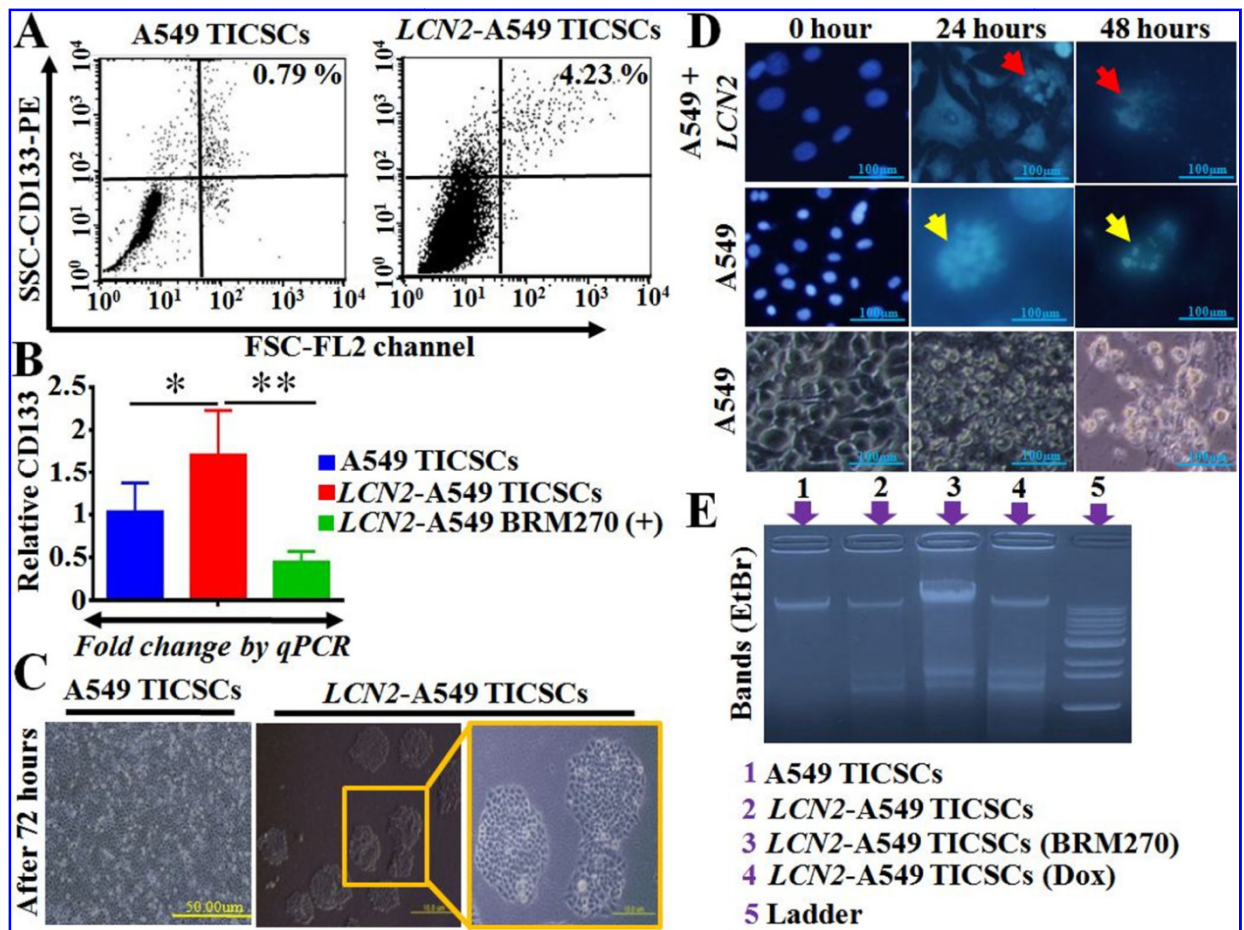


Figure 4.2. NF- κ B novel inhibitor BRM270 abrogates metastatic TICSCs via DNA fragmentation and cell shrinkage. **A.** Characterization of CD133⁺-A549-TICSCs stained with CD133-PE by flowcytometry. **B.** qPCR analysis of CD133⁺ in both TICSCs with or without BRM270. **C.** Tumor sphere forming and colonogenicity efficiency of CD133⁺-LCN2 transfected A549-TICSCs. **D.** DNA fragmentation after condensation and shrinkage of cells with Hoechst 33342 staining (blue). The untreated TICSCs looking flat oval-shaped nuclei uniformly blue; the nuclei of early apoptotic cells lobular or fragmented blue bodies as Karyorrhexis (red-yellow-arrows). **E.** Genomic DNA fragmentation of A549 and LCN2-A549 TICSCs exposed to BRM270 with different concentration for 24 h exposure. DNA laddering formation was viewed on ethidium bromide-stained gel (1.2%).

Specially, in dose dependent viability assay showed, BRM270 caused significantly more cytotoxicity which was mediated by DNA cleavage and cell death (Figure 4.2E and 4.3A-B). An EZ-WST-Cytox cell proliferation assay (ECPA) in a time dependent manner showed decreased viability of *LCN2*-A549-TICSCs and confirmed the potential of BRM270 as an anti-cancer inhibitor. At a concentration of 100 $\mu\text{g}/\text{mL}$ for 12, 24, 48 and 72 h cell viability relative to control A549-TICSCs was calculated as 32.10%, 10.46%, 3.12%, and -11%, respectively. Similarly, 10 μM exposure of Dox for the same duration resulted in 34.10%, 26.22%, 12.21% and 9.21% viable *LCN2*-A549-TICSCs respectively. The cell viability assay of hBMCs, confirmed lesser cytotoxic effect of BRM270 with higher percentage of viable cells i.e. 98.21%, 96.25%, 97.01% and 96.12% respectively as compared to control. Dox treatment of hBMCs under the similar conditions demonstrated 93.12%, 92.32%, 95.01%, and 94.13% cell viability respectively. It further confirmed significantly ($P<0.05$) higher toxicity by Dox than BRM270. In addition, elevated *LCN2* mediated induced stemness of A549 TICSCs was also significantly abrogated by BRM270 via activation of condensation and catastrophe by suppression of CD133 and recruitment of Condensin-I (SMC2) complex (Figure 4.3C and D). To address the potential role of BRM270 in regulation of cell cycle progression, cell cycle analysis was performed by FACS. The cell cycle progression is highly regulated at several checkpoints; BRM270 selectively inhibits cell proliferation via CyclinD1 (CCND1) targeted cell cycle arrest and induces G2/M transition (Figure 4.4A and B). It significantly ($P<0.05$) showed decreased CyclinD1 via recruitment of proapoptotic Casp-3 in transcriptomic analysis (Figure 4.4C and D).

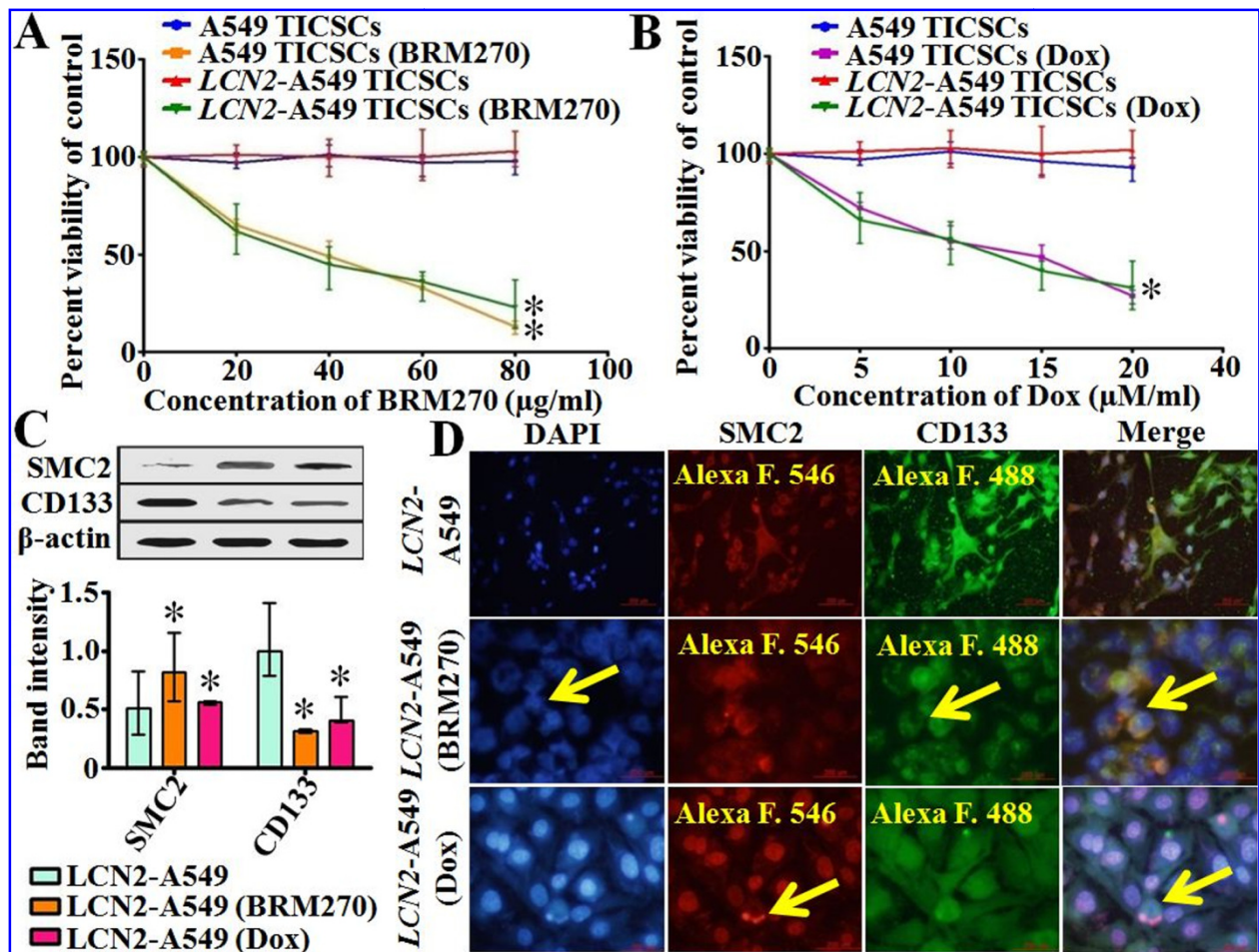


Figure 4.3. Novel NF- κ B inhibitor BRM270 inhibits cell proliferation via targeting of Condensin (SMC2)-I complex in CD133+ over-expressing LCN2-A549 TICSCs by dose dependent manner. **A & B.** The percent viability of TICSCs by EZ-CyTox cells proliferation test. **C.** Total lysates were immune blotted for SMC2-mediated cell shrinkage and catastrophe in TICSCs. **D.** Protein-protein interaction and localization by ICC that showed DNA fragmentation and PCD counter stained with DAPI (blue DNA).

3.3. BRM270 abrogates LCN2 induced EMT and down-regulates Twist-1 expression, there by affecting NF- κ B trafficking in lung adenocarcinoma

EMT plays a pivotal role in promoting metastasis in epithelium-derived carcinomas such as adeno-carcinoma of lung via multistep developmental programs. To study the *in vitro* and *in vivo* induction of EMT in adeno-carcinoma of lung, CD133⁺ expressing A549-TICSCs for EMT markers were examined by ICC. Over-expression of *LCN2* was strongly associated with epithelial-derived-mesenchymal solid tumors.

Significantly higher *LCN2* expression in transfected A549-TICSCs induced mesenchymal phenotypic induction (Figure 4.1B-F and 4.5A). E-cadherin and tight junction protein-1 (TJP-1) also have shown lesser expression in transfected cells (Figure 4.5A). Consequently, the loss of both epithelial maintaining proteins led to the phenotypic reversion of *LCN2* transfected A549-TICSCs to a mesenchymal morphology (Figure 4.1B and 4.5A-C). However, over-expression of *LCN2* stimulated the expression of the oncoprotein Twist-1 and Vimentin in *LCN2*-A549-TICSCs (Figure 4.5A). A critical role for SNAI2 and Twist-1 in mediating the oncogenic functions of *LCN2*, as well as the molecular changes related to EMT markers has been highlighted in the current study. Targeted induction of SNAI2 and Twist-1 efficiently reduced the expression of epithelial marker proteins, which could play a role in promoting *LCN2* induced EMT in A549-TICSCs (Figure 4.5A). The transcript levels of EMT related genes SNAI2 (F- CCTGGTTGCTTCAAGGACAC, R- AGCAGCCAGATTCCTCATGT), Twist1 (F- TCCTCACACCTCTGCATTCT, R- ATGGTTTTGCAGGCCAGTTT) ($P < 0.05$), involved in maintaining the mesenchymal phenotype were significantly ($P < 0.001$) higher in *LCN2*-A549-TICSCs than in A549-TICSCs (Figure 4.5B). On the contrary a significant reduction in the transcript levels of E-cadherin (F-

GCTGGAGATTAATCCGGACA, R- ACCTGAGGCTTTGGATTCCT) and TJP-1 was detected in *LCN2*-A549-TICSCs compared to A549-TICSCs (Figure 4.5A and B).

It was observed that after 24 h, BRM270 (100 $\mu\text{g}/\text{mL}$) dramatically ($P < 0.001$) down regulated the expression of mesenchymal biomarkers as compared to Dox (Figure 4.5B). The essential diatomous phenomenon of EMT induced by *LCN2* has been investigated. Further, it has been observed that *LCN2* induces a biochemical hallmark of EMT, which is loss of expression of epithelial markers with a concurrent increase in the expression of mesenchymal markers (Figure 4.5C). Western blot analysis demonstrated that BRM270 significantly down-regulated ($P < 0.001$) the tumorigenic EMT induced protein Vimentin and increased E-cadherin in both TICSCs compared to untreated cells (Figure 4.5D). Moreover, blot analysis of proteins also demonstrated that BRM270 significantly suppressed ($P < 0.05$) the expression of oncogenic proteins as compared to untreated cells (Figure 4.5C and D). Collectively, our findings suggest that *LCN2* induces EMT in A549-TICSCs and exhibits *in vitro* as well as *in vivo* capacity to induce metastasis via the appropriate signaling cascade.

3.4. BRM270 abrogates LCN2 mediated invasion and metastasis in a molecular imaging in vivo model of adenocarcinoma of lung

The expression of *LCN2* is up-regulated in cancer and it enhances formation, progression, and metastasis of adeno-carcinoma of lung. To evaluate whether *LCN2* augments tumor growth and metastasis *in vitro* and *in vivo*, the cell culture of CD133⁺ both TICSCs were optimized to generate cells to induce high-grade solid tumors in nude mice. Both cell lines were injected subcutaneously, ortho-topically into the lower right flank of male nude mice (Figure 4.6A).

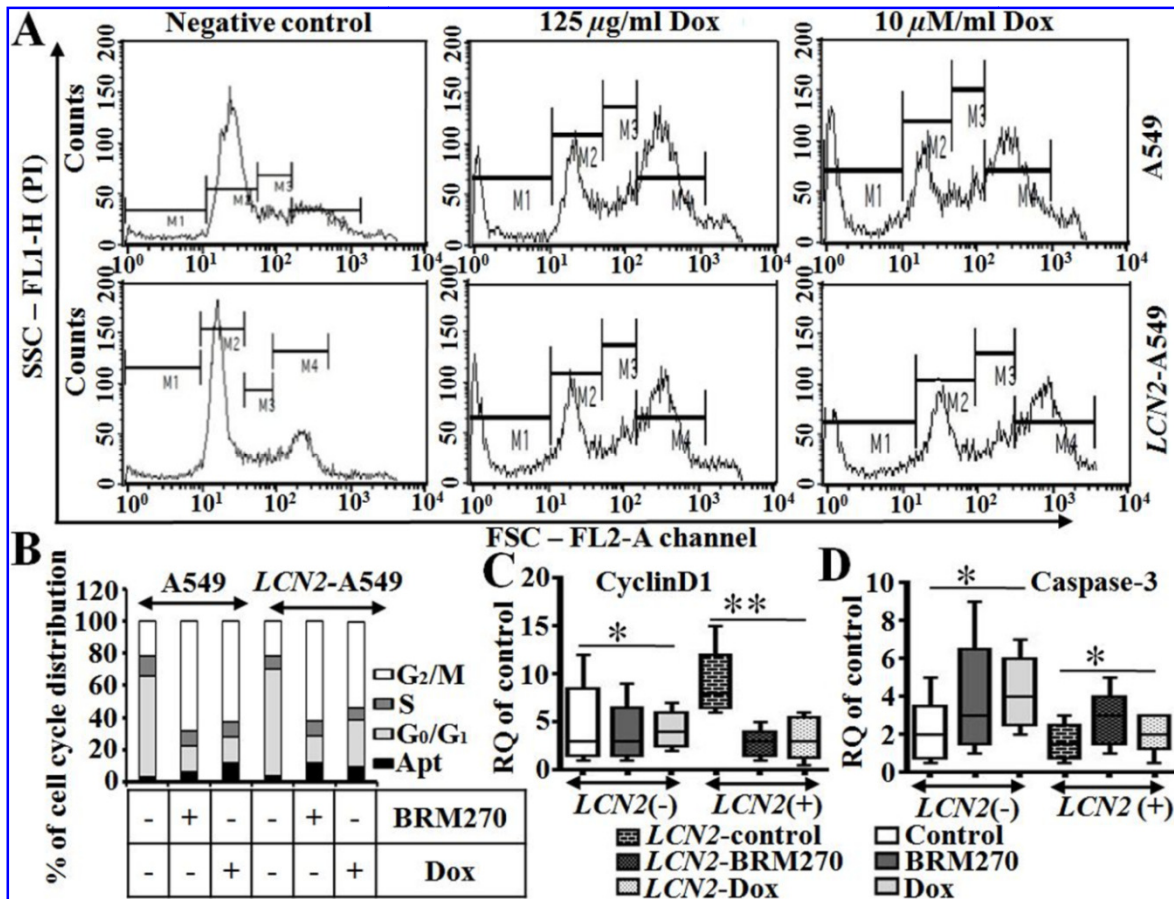


Figure 4.4. Influence of BRM270 on cell cycle progression and apoptosis in TICSCs. **A.** Cell cycle analysis of CD133⁺-A549 and LCN2-A549-TICSCs after being cultured with BRM270 for 24 h showing an increase in G₂/M phase cells (%). **B.** Percent of cell cycle distribution in different checkpoints: flowcytometry analysis showing G₀-G₁ arrest and transition to G₂M checkpoints. **C&D.** mRNA folds change of CyclinD1 and procaspase-3 with or without BRM270 compared to Dox.

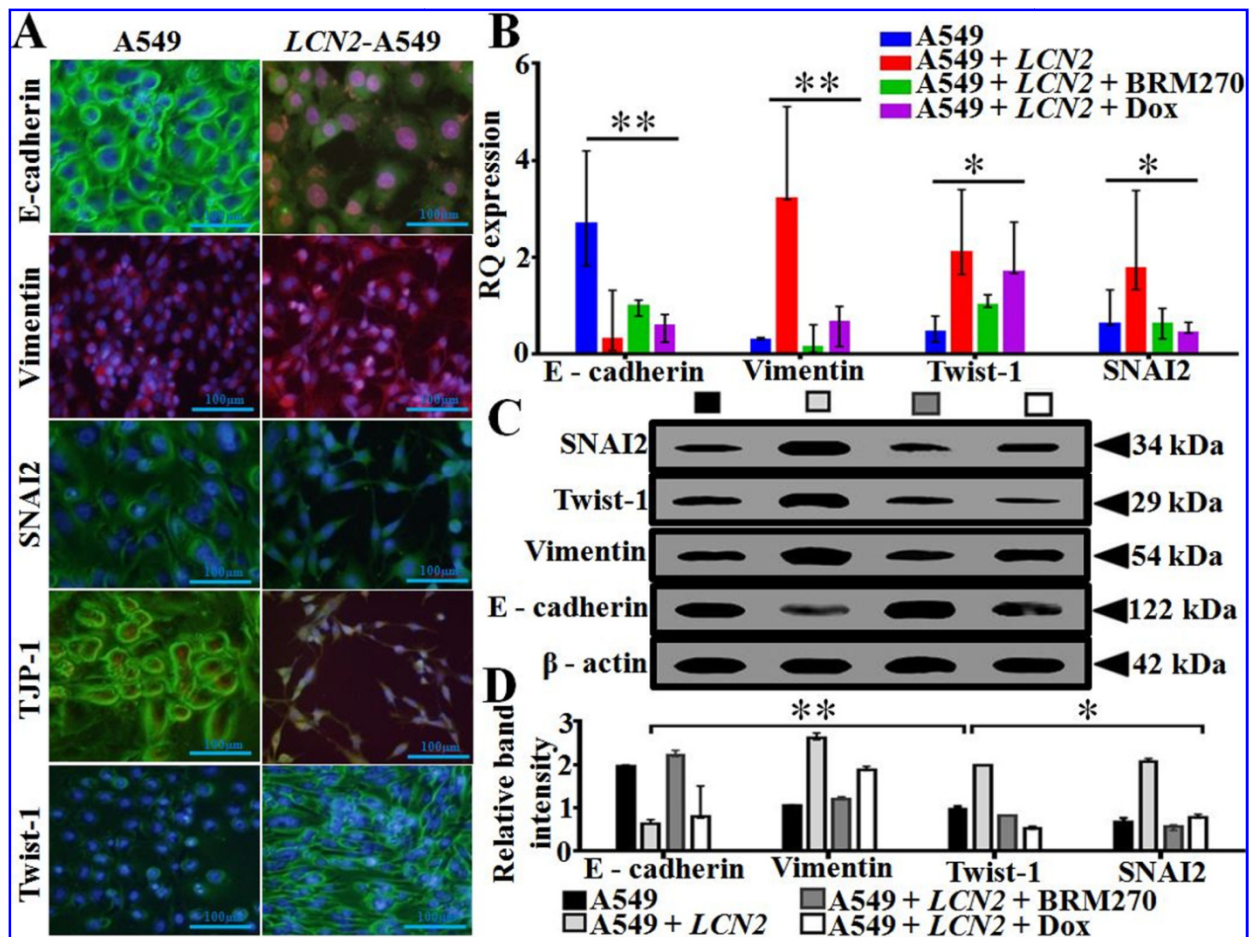


Figure 4.5. LCN2 augments SNAI2/Twist1 mediated EMT and phenotypic reversion in lung adenocarcinoma. **A.** ICC for EMT inducing proteins with DAPI counterstaining for DNA (blue, 200X). **B.** Summary of gene expression switches with qPCR showing mean fold change in mRNA abundance. **C.** Total lysates were immune blotted for EMT markers in TICSCs and BRM270 treated with positive control Dox. **D.** The image densitometry analysis by image J.

Tumor formation and metastasis were confirmed *in vivo* using a small animal image analyzer system. CD133⁺-LCN2-A549-TICSCs efficiently induced tumor and metastasized to other organs, while A549-TICSCs induced only localized tumor and did not metastasize (Figure 4.6B). Infra-red (IR) dye-800CW-2-deoxy-D-glucose (2DG) wavelength based images were taken at different time intervals (2, 3 and 4 week) to monitor tumor progression (Figure 4.6B). 2DG has been used as a tracer for identification of tumors and their metastases because the rate of glycolysis is elevated in highly proliferative tumors and metastasized organs. The tumors were detectable at day 7 after the implantation of both TICSCs in nude mice. The tumor signal intensity was significantly ($P>0.05$) higher in LCN2-A549 tumors than A549 tumors at third and fourth weeks respectively, indicating that LCN2-A549 tumors were larger (Figure 4.6B). To ascertain that LCN2 mediates tumor cell proliferation and metastasis, tumor growth patterns were analyzed in both implanted group. The results of *in vivo* experiment confirmed that BRM270 significantly ($P<0.05$) inhibited tumor progression in a dose and time dependent manner.

It also had a positive impact on disease prognosis compared to Dox treated mice (Figure 6B). Further, CD133⁺-LCN2-A549-TICSCs tumor bearing mice displayed a significantly ($P<0.0003$) lower relapse free survival rate (11.4286%) than A549-TICSCs tumor bearing mice (30.2098%) (Figure 6C). BRM270 significantly ($P<0.0005$) increased the prognosis value and enhanced the survival rate of LCN2-A549-TICSCs tumor bearing mice from around 40% to 65.625% compared to Dox treated mice (57.2727%) in 2DG guided *in vivo* model (Figure 6C). To support our findings, we compared the weights of tumors in both groups. It was observed that LCN2-A549-TICSCs were more invasive and metastatic in nature because the tumor weight increased significantly ($P<0.05$) between the second and fourth week ($P<0.001$).

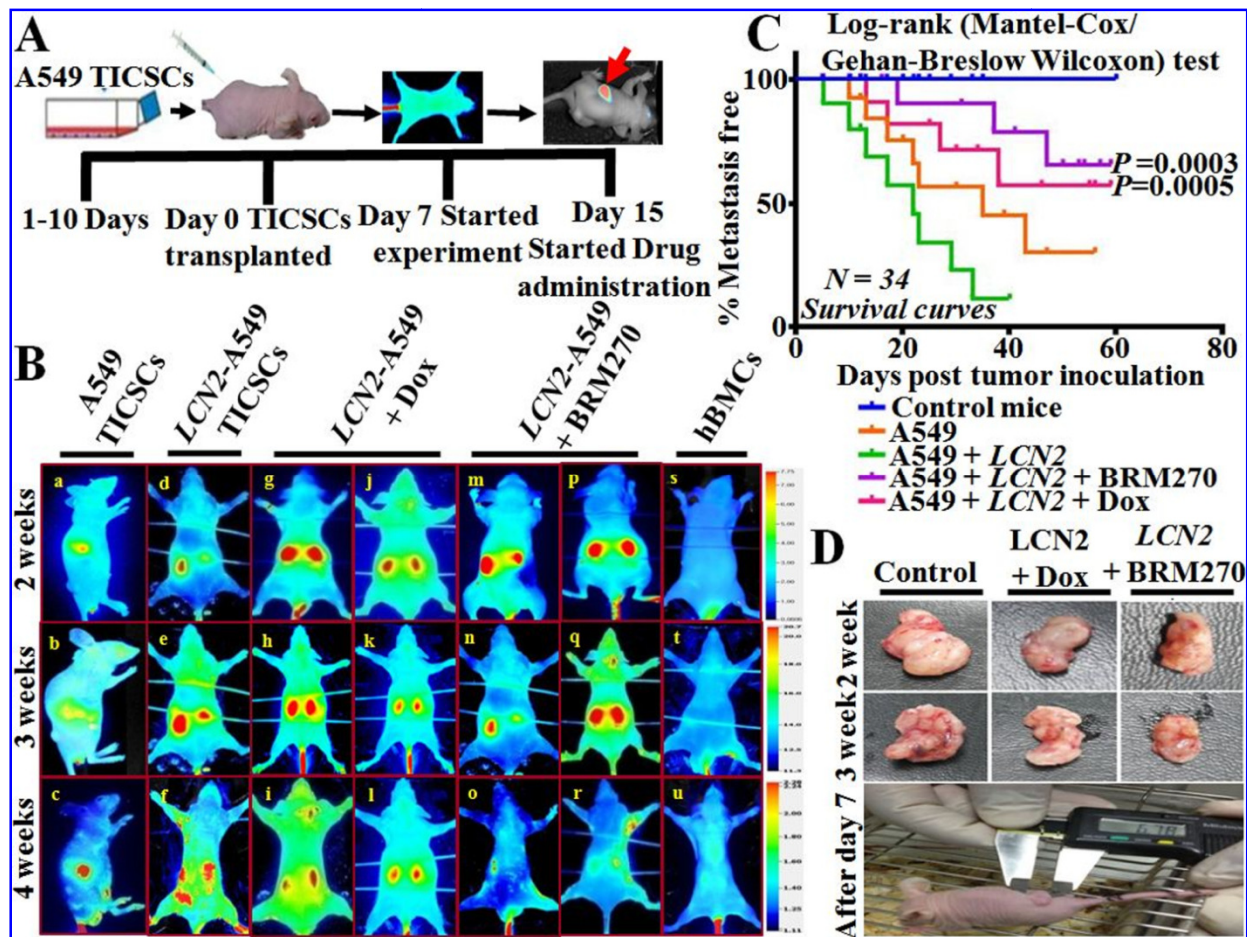


Figure 4.6. 2DG-guided molecular imaging based in vivo model of adeno-carcinoma of lung. **A.** Establishment, characterization of metastatic TICSCs and their subcutaneous inoculation into nude mice. **B.** Analysis of CD133⁺-TICSCs induced palpable solid tumors and metastasis in male BALB/cSlc-(nu/nu) nude mice, under *in vivo* conditions using LI-COR image analyzer. **C.** Progression-free-survival curve was calculated with the Kaplan-Meier method and compared by using the log-rank test. *** $P < 0.0003$ and 0.0005 considered as extremely significant of control and treated group. **D.** *In vivo* and *ex vivo* measurement of the volume of tumors.

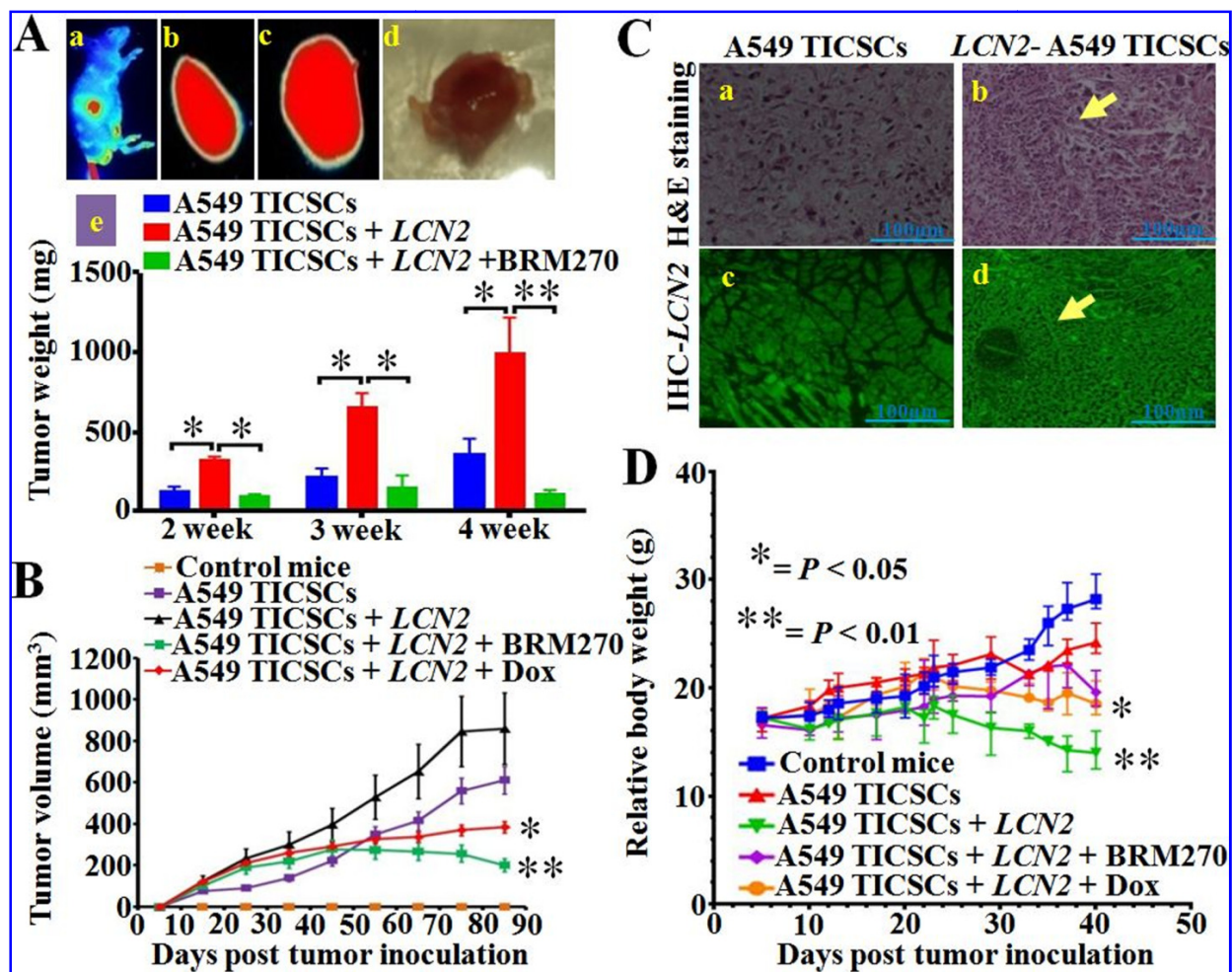


Figure 4.7. BRM270 reduced tumor extent in dose and time dependent manner. **A.** Diagrammatic presentation of relative weight of solid tumors. **B.** Representation of tumor volumes over the different time intervals. **C.** IHC and H&E staining of LCN2-A549 and A549 induced adeno-carcinoma of tumor sections-(20X). **D.** Relative body growth curves of tumor groups. Data was analyzed using GraphPad prism6.

However, BRM270 significantly reduced the volume of tumor over time as compared to untreated mice (Figure 4.6D and 7Aa-Ae). Significantly ($P<0.001$) enhanced reduction in tumor weight was observed with BRM270 at a dose rate of 10 mg/kg/day twice a week (Figure 4.7Ae). The mean tumor volume of A549 and *LCN2*-A549-TICSCs tumors was measured (Figure 4.7B). Post inoculation on day 7, a marked difference in tumor volume and onset of metastasis was observed. Surprisingly, day 9 of post appearance of palpable tumors A549-TICSCs tumors grew at a significantly slower ($P<0.05$) rate than *LCN2*-A549-TICSCs tumors (Figure 4.7B). A significantly lower average volume of metastatic tumors was observed in both BRM270 treated A549 and *LCN2*-A549 tumor bearing mice (Figure 4.7B). Histological analysis of metastatic tumor samples demonstrated significantly higher proliferation rate of *LCN2*-A549-TICSCs than A549-TICSCs (Figure 4.7C). The correlation of the relative body weight with tumor metastasis and amelioration by BRM270 showed a significant reduction in body weight in high grade metastasized tumor bearing mice (Figure 4.7D). It was also confirmed that while acting as novel anticancer phyto-drug, BRM270 does not significantly affect relative body weight of mice compared to Dox. Taken together results revealed that *LCN2* over-expression correlates with tumor malignancy, metastasis and mediates adeno-carcinoma of lung.

3.5. The *LCN2*-*Twist-1*/*MMP-9* interaction mediated EMT cross talk with the *NF-κB* signaling cascade

It was targeted that *LCN2* regulates cell-cell adhesion, EMT induced metastasis, followed by cross talk with the *NF-κB* signaling pathway (Figure 8A and B). To define the molecular mechanism of *LCN2* mediated EMT, a cancer-associated protein-protein interaction network was constructed using STRING bioinformatics approach (Figure 4.8A).

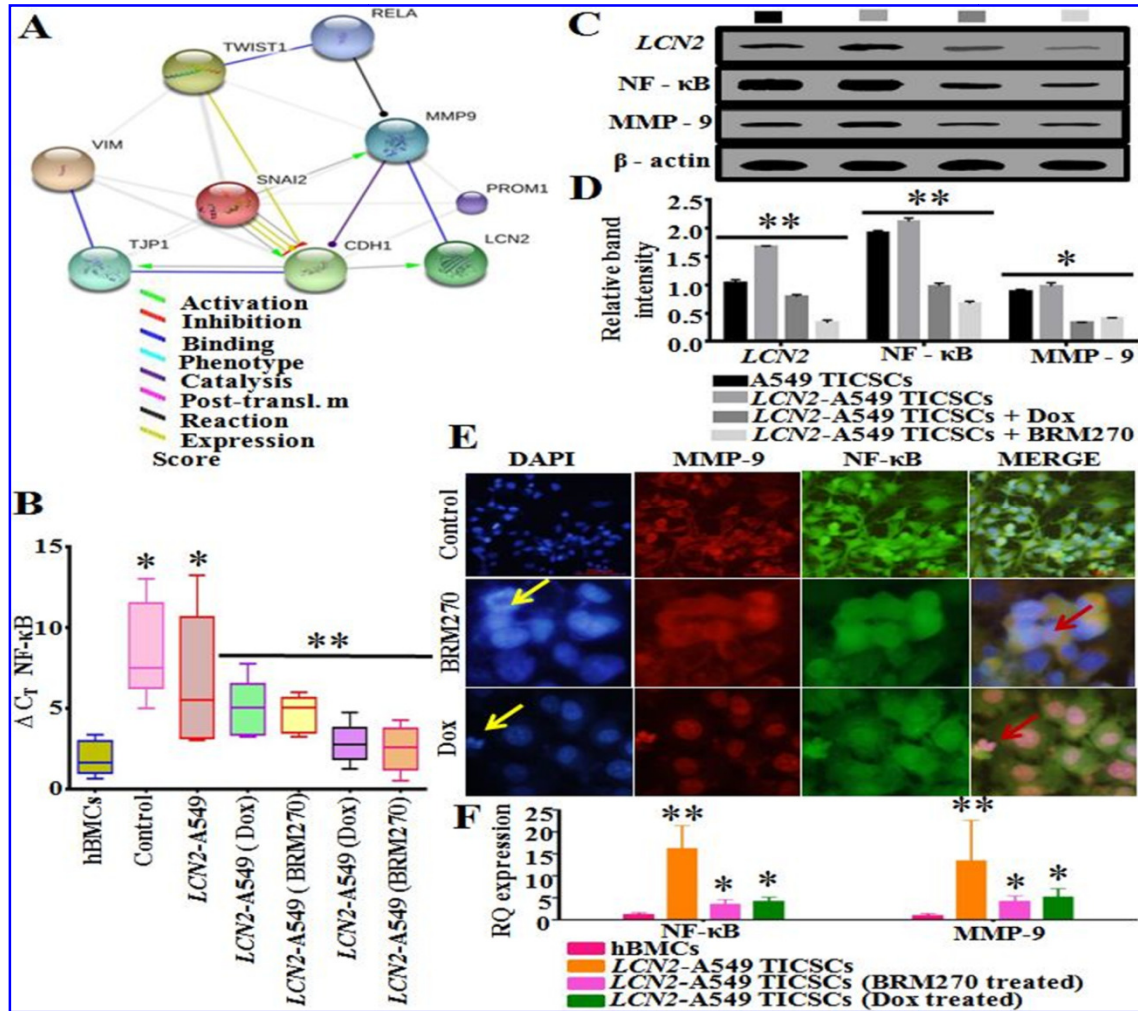


Figure 4.8. LCN2 enhances EMT and cross talk with the NF- κ B signaling cascade. **A.** Cancer-associated protein-protein interactions network was constructed using a bioinformatics STRING. **B.** Whisker and Box plot for NF- κ B activity using Data Assist of qPCR analysis. **C.** Protein lysates were analyzed by western blot for NF- κ B cross talk with EMT and their interaction in *LCN2* induced metastatic tumor. **D.** Quantification of band intensities using Image-J. **E.** ICC revealed novel inhibitor BRM270 abrogates the protein-protein interaction and cross talk with NF- κ B. **F.** qPCR showed the relative significant suppression of both MMP-9 and NF- κ B mRNA levels by BRM270. * $P < 0.05$, ** $P < 0.001$ have been opted as significant differences.

The results showed that *LCN2* binds to MMP-9 that is activated by SNAI2 and is involved in Twist-1 activated EMT. Over-expression of *LCN2* directly increased MMP-9 expression, and it was also activated by the mesenchymal EMT markers (Figure 4.8A). The results were further confirmed by western blot and subsequent densitometry quantification of protein expressions. We found that *LCN2* induction negatively regulates E-cadherin both protein interaction and mRNA fold change levels (Figure 4.5A-C and 4.8A). In agreement with the role of NF- κ B signaling cascade in mediating MMP-9 interaction, immunoblot and transcriptomic analysis revealed that ΔC_T levels of NF- κ B (F- CTGAACCAGGGCATAACCTGT, R-GAGAAGTCCATGTCCGCAAT) and MMP-9 simultaneously with *LCN2* were significantly ($P < 0.001$) down-regulated with BRM270 treatment compared to Dox (Figure 4.8B-D). ICC and qPCR also showed that protein expression and mRNA levels of MMP-9 and NF- κ B in both group samples were significantly reduced after 24 h exposure with naturaceutics BRM270 (Figure 4.8E and F).

It was observed that *LCN2* induced the expression of MMP-9 and Twist-1 and elevated protein interaction in high-grade tumors, indicating that co-expression of NF- κ B and Twist-1 enhances the aggressive and metastatic mesenchymal phenotype of A549-TICSCs (Figure 4.1B, 4.5B and 4.8F). Collectively, these results suggest that *LCN2* induced EMT via NF- κ B-MMP-9 interaction in A549-TICSCs induced lung carcinoma. Novel naturaceutics BRM270 anticancer activity elucidated that over-expression of *LCN2* induced adeno-carcinoma of lung and metastasis of high-grade solid tumors can be eradicated using novel naturaceutics.

4. DISCUSSION AND CONCLUSION

Stem cell research is a promising arena for the therapeutic advancement in oncology including lung cancer (Jordan *et al.*, 2006; Kitamura *et al.*, 2009; Wang *et al.*, 2013). EMT, an essential normal physiological process for embryonic development, tissue remodeling and wound healing, has recently been implicated in cancer progression (Tsai *et al.*, 2013; Li *et al.*, 2012; Casas *et al.*, 2011). Epithelium-derived tumors switch to a mesenchymal phenotype that facilitates migration and invasion potential resulting in increased tumor aggressiveness, recurrence and overall poor prognosis (Rich and Bao, 2007; Casas *et al.*, 2011). We hypothesized that EMT was the likely mechanism by which *LCN2* increased cell migration and invasion as well as tumorigenesis in adeno-carcinoma of lung *in vitro* and in 2DG guided *in vivo* model (Figure 4.5A and 4.6B). Epigenetic induction of EMT in TICSCs is positively correlated with poor prognosis, metastasis, motility and multiple-drug chemotherapeutic resistance (Rich and Bao, 2007; Leung *et al.*, 2012; Krysan *et al.*, 2012). The present study was designed to define the potential of *LCN2* in the switching of EMT in adeno-carcinoma of lung with 2DG infrared optical probe as an *in vivo* molecular tumor tracer. The current study showed that, ectopic over-expression of *LCN2* resulted in morphological reversion from the epithelial to the mesenchymal phenotype in A549-TICSCs (Figure 4.1A and B). *LCN2* is also known to promote breast cancer progression via down regulation of epithelial markers and the acquisition of mesenchymal markers with TF in infrared optical probe based *in vivo*-models (Yang *et al.*, 2009; Choi *et al.*, 2015). In present study, the mRNA levels of *LCN2* were significantly ($P<0.05$) higher in *LCN2*-A549-TICSCs than in normal A549-TICSCs (Figure 4.1D). Over expression of *LCN2* in A549-TICSCs was confirmed by ICC in both *LCN2* transfected and non-transfected

cells (Figure 4.1C). Further, enhanced cell proliferation with its over-expression *in vitro* (Figure 4.1C and 4.2C) is supported by earlier literature (Candido *et al.*, 2014; Yang *et al.*, 2009). The putative CSC marker CD133 strongly expressed on the cell surface of A549-TICSCs (Figure 4.1C) as earlier reports and confirmed the tumor inducing ability (Bertolini *et al.*, 2009; Akunuru *et al.*, 2012). The higher metastasis and invasive rates in *LCN2*-A549-TICSCs with respect to A549-TICSCs (Figure 4.6B) during the current study are supported by the findings of a pancreatic ductal adeno-carcinoma xenograft model (Leung *et al.*, 2012). Further, enhanced stemness, MDR and tumorigenicity under *in vitro* and *in vivo* by *LCN2* has been supported by the earlier findings for many cancers especially lung cancer and ductal adeno-carcinoma (Yang *et al.*, 2009; Leung *et al.*, 2012; Choi *et al.*, 2015).

Mitotic catastrophe can induce programmed cell death that often occurs in conjunction with apoptosis. In our previous study, we demonstrated that BRM270 is a potential and selective anticancer phyto-drug that induces programmed cell death and mitotic cell death (MCD) due to unrepaired DNA damage during premature apoptosis (Mongre *et al.*, 2015; Mantena *et al.*, 2006). Further, the efficacy of BRM270 is related to its ability to subdue the mRNA expression of *LCN2* and consequently CD133⁺ stemness and tumorigenicity of A549 TICSCs (Figure 4.2B-C and 4.6B). The efficiency of BRM270 to significantly abrogate ($P < 0.001$) the increased CD133⁺ expression in A549 and *LCN2*-A549-TICSCs compared to Dox treatment, in time and dose dependent manner, is in line with our previous study (Mongre *et al.*, 2015). DNA catastrophe and MCD are prominent mechanisms in carcinogenesis (Mongre *et al.*, 2015; Choi *et al.*, 2015), during chemotherapy or cancer progression by premature mitosis and uneven chromatin condensation and BRM270 has significantly facilitated such activities in the current study (Figure 4.2D and 4.3D). In addition, BRM270 is also known to regulate cell cycle arrest

and transit from G0-G1 to G2/M checkpoints by Casp-3 via down-regulation of CyclinD1. This is a causal hallmark of premature apoptosis, cells with defective G2/M phase by induction of Casp-3 dependent pro-apoptosis (Choi *et al.*, 2015; Mantena *et al.*, 2006).

Current study elucidates a pivotal role for *LCN2* in EMT. It also confirmed in line with the earlier studies that over-expression of *LCN2* significantly ($P<0.05$) antagonizes the expression of epithelial markers, upregulates mesenchymal markers (Figure 4.5A-D and 4.8A) and drives EMT via E-cadherin, SNAI2, Twist-1, NF- κ B and MMP-9-dependent and independent mechanisms (Tsai *et al.*, 2013; Yang *et al.*, 2009; Rodvold *et al.*, 2012). As expected, the up-regulation of NF- κ B induced stemness, tumor sphere formation and metastasis (Figure 4.1F, 4.2C, 4.6B and 4.8C). Several earlier studies also indicated that the versatile role of *LCN2* in the early stage of tumor development and its higher expression in ovarian, thyroid, liver, colon, kidney, and pancreas (Zhai *et al.*, 2012; Candido *et al.*, 2014; Yang *et al.*, 2009; Iannetti *et al.*, 2008; Tung *et al.*, 2013; Ruiz-Morals *et al.*, 2014). Further it has been observed that elevated transcript levels induced degradation of I κ B proteins and resulted in the liberation of NF- κ B. It allowed nuclear translocation and binding to cognate DNA motifs that induce transcription of EMT promoting proteins and augment tumor sphere formation in *in vitro* and metastasis *in vivo*. Consequently, transcription of EMT related genes involved in EMT and cross talk to NF- κ B occurs (Figure 4.5A-D and 4.8A). The present study demonstrates a functional role for *LCN2* and several known EMT mediators, showing that induction of EMT in adenocarcinoma of lung proceeds via activation of NF- κ B signaling and activation of Twist-1 and SNAI2. Thus it provides new insights into the mechanism of EMT induction in lung carcinoma. Moreover, it shows that BRM270 functions as a novel inhibitor that blocks EMT mediated

oncogenesis. Taken together, these results suggest that *LCN2* triggers EMT, which is associated with increased potential for metastasis and invasion.

One of the important and clinically relevant aspects of cancer stem cell tumorigenicity is the degree of cancer spread beyond the primary tumor in various cancers including adenocarcinoma of lung. The current study suggests that *LCN2* transformed A549 TICSCs induced metastatic tumors in nude mice (Figure 4.6A and B). Similarly, *LCN2* decreases differentiation and increases breast tumor local invasion, lymph node metastasis and primary tumor growth *in vivo* (Yang and Moses, 2009). Our findings also confirmed that *LCN2* regulates a variety of cellular functions in carcinogenesis that could either induce or suppress cancer metastasis and invasiveness (Ruiz-Morals *et al.*, 2014; Kaur *et al.*, 2014; Shiiba *et al.*, 2013; Mannelqvist *et al.*, 2012; Bolignano *et al.*, 2010). Further, a significant difference in the baseline tumor volume between the two groups confirmed significantly ($P < 0.05$) faster growth rate by *LCN2*-A549-TICSCs than A549 TICSCs (Figure 7B). This result suggests that *LCN2* has significant oncogenic activity, which is supported by the earlier reports (Shiiba *et al.*, 2013; Bolignano *et al.*, 2010). Findings of Mannelqvist *et al.* that 51% survival in tumors with no *LCN2*, 46% in medium *LCN2* expression and 3% in endometrial cancer tumors that strongly express *LCN2* strongly supported our results (Mannelqvist *et al.*, 2012). This suggests that *LCN2* expression leads to poor tumor prognosis and can serve as a biomarker for treatment. *LCN2* causes tumor progression in bladder, colorectal, liver, ovarian and pancreatic carcinoma (Candido *et al.*, 2014; Bolignano *et al.*, 2010), which supports our result of *LCN2* in adenocarcinoma of lung by 2DG infrared optical probe guided molecular imaging based *in vivo* model.

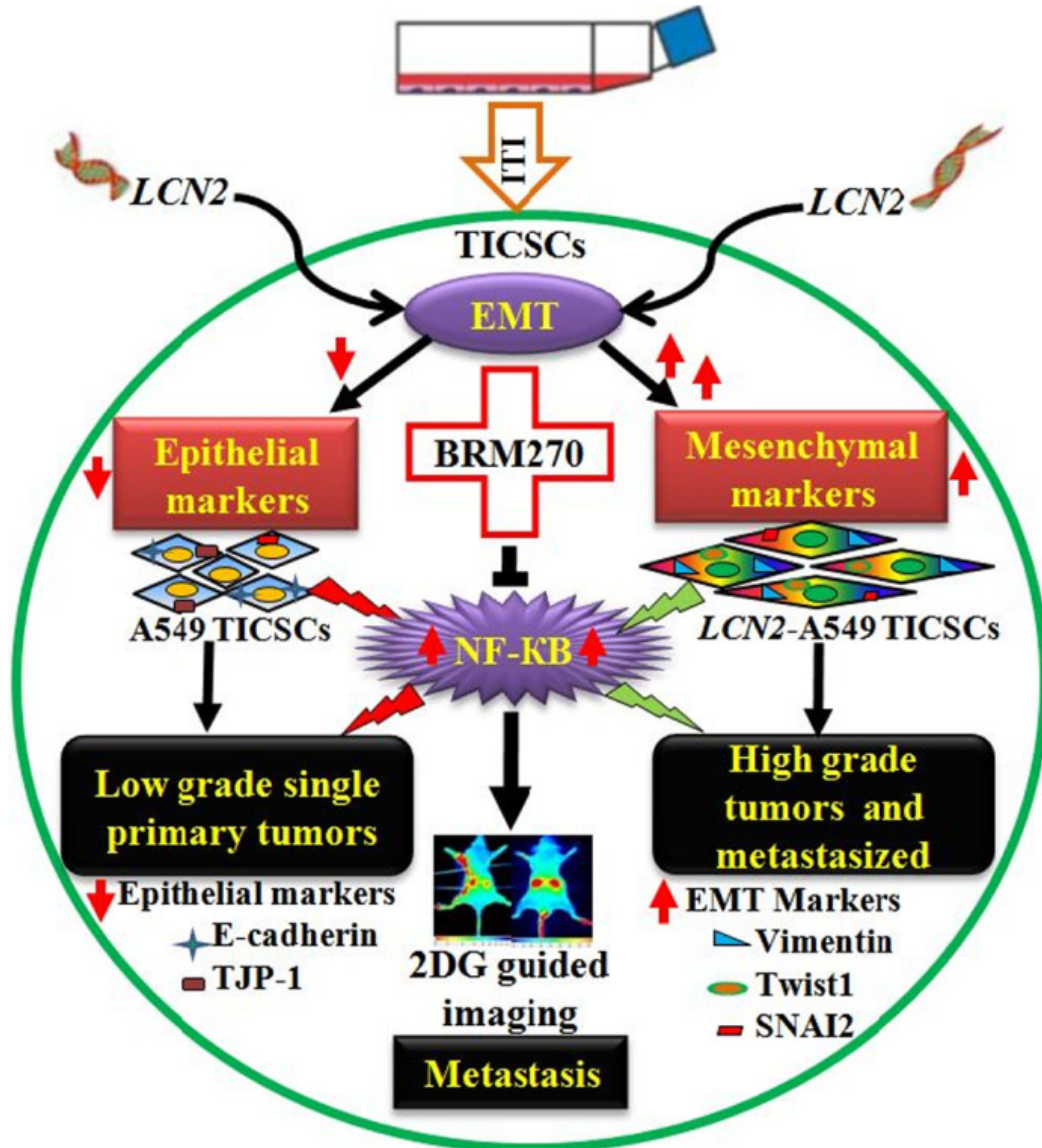


Figure 4.9. Schematic representation of epigenetic induction of EMT and their cross talk with NF- κ B signaling cascade in lung adenocarcinoma. Representation of BRM270 as a novel inhibitor, amelioration of EMT mediated cancer progression and metastasis by targeting the Twist-1 and NF- κ B using 2DG for pre-and intraoperative tumor localization in real-time resection.

The novel infrared probe 2DG is a potential molecular navigation therapeutics tracer that detects tumors in real time intra-operatively in contrasting pseudo-colors, which allows more complete tumor resection (Kover et al., 2009). Therefore, *in vivo* targeting experiments indicated the 2DG-based complex had great potential for image-guided cancer therapy. This study suggests that *LCN2* have potential as a non-invasive biomarker for metastasized advance cancer progression and 2DG is a novel optical probe to target the tumor recurrence and metastasis.

LCN2 enhances EMT mediated cancer progression by activation of Twist-1/SNAI2 and cross talk with the NF- κ B signaling cascade a novel paradigm in most cancers (Huber et al., 2004; Rodvold et al., 2012; Ruiz-Morals et al., 2014; Kaur et al., 2014). The current study provides evidence for a novel cellular signaling mechanism regarding *LCN2* induced EMT and cross talk with NF- κ B in lung carcinoma (Figure 4.9). Similarly, Shrivastava et al. demonstrated cancer-associated expression of MMP-9 and c-FOS with *LCN2* protein network interaction and signaling using the same STRING bioinformatics strategy used in this study (Shrivastava et al., 2015). In addition, they also demonstrated that the activator protein-1 (AP-1) complex formed by the association of c-Fos and c-Jun has recently implicated in the maintenance of colon cancer stem cells, which correlates with our findings of the CDH1 and MMP-9 complex with NF- κ B (Figure 8A-F).

This study provides compelling evidence of epigenetic switching of *LCN2* mediated EMT and cross talk with NF- κ B. Also, it proposes a wide range of strategies by which BRM270 mitigates the progression and metastasis of A549 and *LCN2*-A549-TICSCs induced adenocarcinoma of lung *in vitro* and 2DG infrared optical probe guided *in vivo* model (Figure 9). Our findings can aid in the identification of molecular mechanisms of carcinogenesis in CD133⁺-*LCN2* transfected A549-TICSCs induced carcinoma by optical probe guided molecular imaging

based therapeutic strategies in *know-in* experiments. This information is a novel clinically relevant and can act as the baseline data for the development of new naturaceuticals with direct target to resection of tumor and metastasis by image-guided therapeutic strategies. Conclusively, current study provide a molecular mechanistic and photodynamic based approach for using BRM270 as a novel cancer therapeutic drug to enhance the effect of Dox resistant *LCN2* induced metastasis of solid tumors in nude mice.

CHAPTER 5

CHEMOPREVENTIVE AND ANTICANCER POTENTIAL OF NOVEL NATURACEUTICAL BRM270 IN METASTATIC STEM LIKE CANCER INITIATING CELLS OF HEPATOCELLULAR CARCINOMA

ABSTRACT

Hepatocellular carcinoma (HCC) is a major threat to human health worldwide and development of novel antineoplastic drug is urgently needed. BRM270, a natural plant product, is a proprietary combination of different phytochemical extracts, has been shown to be effective against a wide range of tumors. In this study, the antitumor effect of BRM270 on human hepatoma cell line, CD133⁺ expressing stem-like cancer-initiating cells (MSCICs) HepG-2 and SNU-398, and the mechanism involved have been investigated. Multistep intervention models including EZ-CyTox-WST assay, cell cycle regulation and apoptosis were analyzed using Hoechst 33342 staining and flow-cytometric Annexin-VI/PI double staining method. Gene expression profiling by qPCR and specific cellular protein expressions were measured using immunocytochemistry and western blot analysis. *In vivo* imaging in mice model using 2DG-(2-Deoxy-D-Glucose) optical-probe was performed to delineate the size and extent of metastasized tumor. Cellular and molecular traits revealed a typical CyclinD1-dependent DNA-fragmentation, cell cycle arrest and Casp-3-mediated apoptosis after treatment with BRM270. Moreover, qPCR/blot analysis and *in-vivo* imaging study revealed significant attenuation ($P<0.05$) of c-Myc, Bcl2 and c-Jun involved in HCC metastasis. The present study indicates that BRM270 can

effectively inhibit proliferation and induce apoptosis in hepatoma HepG-2 and SNU -398 cells and the apoptosis induction is related with down-regulation of CyclinD1 mediated c-Jun-JNK apoptotic pathway.

***Keywords:* Metastatic stem like cancer initiating cells, Karyorrhexis, BRM270, naturaceuticals, 2DG**

1. INTRODUCTION

Hepatocellular carcinoma (HCC) is the sixth most prevalent cancer and the third leading cause of deaths related to cancer (Venook *et al.*, 2010). Each year HCC neoplasm is diagnosed in more than half a million people worldwide with 748,000 new cases each year (Venook *et al.*, 2010; El-Serag, 2011). In addition, HCC rarely occurs before the age of 40 years and reaches a peak at approximately 70 years of age (El-Serag, 2011). Major risk factors for HCC include infection with Hepatitis C Virus (HBV), alcoholic liver disease, metabolic diseases and most probably fatty liver disease (El-Serag, 2011; Shibata *et al.*, 2014). Most of these risk factors lead to the formation and progression of cirrhosis, which is present in 80 to 90% of patients with HCC. Although the epidemiologic risk factors for HCC are well known, but still the molecular mechanisms underlying hepatocarcinogenesis are not well characterized. The need to understand the molecular pathogenesis of HCC and to develop more effective targeted therapies remains urgent. In this study, we utilized 2-deoxy-D-glucose (2DG) guided *in vivo* model to reveal the regulatory and inhibitory phenomenon of CD133⁺ expressing hepatocellular stem like cancer cells induced HCC and metastasis via negatively attenuation of CyclinD1 mediated c-Jun-JNK apoptotic pathway in CRJORI: CD-1-5WM nu/nu male mice.

The incidence of liver cancer requires several functional cell signal transductions and an interaction between proto-oncogenic proteins, legends and many stimulus agents (Shibata *et al.*, 2014). Interestingly, alterations in tumor stroma microenvironments may also facilitate the development of tumor cell heterogeneity through the extrinsic activation of certain tumor cell signaling pathways (Yamashita *et al.*, 2013). Uncontrolled cell proliferation is the hallmark of cancer, and tumor cells have unregulated expression of certain genes that directly regulate the

check points of cell cycle. G1 is the only phase of the cell cycle that is strictly dependent on extra or intracellular mitogens (Vermeulen *et al.*, 2003). In addition, Cyclin D1 is a member of the G1 cyclin family and is involved in regulating the transition through the G1 phase of the cell cycle (Joo *et al.*, 2001). The elevated association of CyclinD1 and c-Jun with Myc has been implicated in cancer development (Joo *et al.*, 2001; Vermeulen *et al.*, 2003; Wang *et al.*, 2007). The caspase-3 belongs to a member of the cysteine-aspartic acid protease family and gets activated in both extrinsic as well as intrinsic pathways of cell apoptosis (Chang *et al.*, 2000). Caspase-3 impart crucial role in the execution phase of apoptosis activated by various stimuli. Among all caspases, caspase-3 is the best implicated in several apoptotic pathways. Zhang and his colleagues proposed that phyto-extract ursolic acid modulates phosphorylation of Bcl2 and activation of Caspase-3 via c-Jun N-terminal kinase pathway in DU145 apoptotic cancer cells (Zhang *et al.*, 2009). In the current study, BRM270 induced Caspase-3 dependent induced programmed cell death by dephosphorylation of Bcl2 and suppression of c-Myc in CD133⁺ expressing HepG-2 and SNU-398 MSCICs induced liver neoplasm.

The stem cell theory of cancer proposes that among all cancerous cells, few of them act as stem cells that reproduce themselves and sustain the cancer. Nevertheless, some cell surface glycoproteins such as Prominin1 (CD133⁺) are potential biomarkers for stemness with maintenance of self-renewal and tumorigenicity via multiple signals cross talk (Hou *et al.*, 2012). Although the existence of cancer stem cells (CSCs) or MSCICs were first proposed 40 years ago, nevertheless MSCICs have been objects of intensive study. Previous studies also characterized CD133 to mark a specific CSC subset in HCC via activated JNK pathway (Hou *et al.*, 2012; Yoon *et al.*, 2012; Tong *et al.*, 2015; Shmelkov *et al.*, 2008). CD133 expression in cancer cells

may indicate a transformation of primary CD133⁺ cancer into more aggressive in metastatic HCC tumors (Shmelkov *et al.*, 2008).

Current development in targeting cancer stem cell include several regimens to encounter MSCICs induced cancers such as surgery, chemotherapy, radiation therapy, hormonal therapy and gene targeted therapy in different ways (Kitanaka *et al.*, 2013; Park *et al.*, 2009). However, multiple drug resistance (MDR), side-effects, hemorrhage and genetic manipulations are the major consequences of these approaches. Therefore, the utmost requirement is to design novel natural drug with zero xeno-footprint/non-toxic for normal cells and possess anti-proliferative potential against MSCICs induced hepatic carcinoma. BRM270 is a one of the promising anticancer medicinal super cocktail phyto-extract which is a proprietary combination of *Saururus chinensis*, *Arnebia euchroma* (Royle) Johnst, *Scutellaria baicalensis*, *Citrus unshiu markovich*, *Portulaca oleracea*, *P. vulgaris* var. *lilacina* and *Aloe vera* which are widely distributed in Northeast Asia mainly China, South Korea and Japan (Mongre *et al.*, 2015; Kowalczyk *et al.*, 2006; CPC, 2010; Zhang *et al.*, 2012; Lee *et al.*, 2015; Hwang *et al.*, 2013; Zhao *et al.*, 2013; Xiong *et al.*, 2009; Yonehara *et al.*, 2015). Component of BRM270 are well-known traditional Chinese natural medicines, which is used to treat a variety of diseases including cancers (Lee *et al.*, 2015; Hwang *et al.*, 2013; Zhao *et al.*, 2013; Xiong *et al.*, 2009; Yonehara *et al.*, 2015). Specially, *Saururus chinensis*, *Arnebia euchroma* (Royle) Johnst, *Scutellaria baicalensis*, *Citrus unshiu markovich*, *Portulaca oleracea*, *P. vulgaris* var. *lilacina* demonstrated *in vitro* and *in vivo* anti tumor activity against cervical, lung, liver, stomach, and breast carcinoma as well as prostate cancer (Zhang *et al.*, 2012; Lee *et al.*, 2015; Hwang *et al.*, 2013; Zhao *et al.*, 2013; Xiong *et al.*, 2009). Yonehara *et al.* (2015) during their *in vitro* experiment proposed the efficacy of *Aloe vera* against neuroblastoma. Earlier studies by our group reported that BRM270 is a novel NF-

κ B inhibitor and negatively attenuates stem like cancer initiating cells (SLCICs) *in vitro* as well as *in vivo* (Mongre *et al.*, 2016). While Cao *et al.*, (2013) revealed the BRM270 efficacy in inhibiting the cyclin-D1 dependent cell proliferation and caused programmed cell death by cell cycle arrest at G1 checkpoint. In this study we investigated in detail the effect of BRM270 on Myc mediated activation of multidrug resistance (MDR) and c-Jun induced JNK signaling cascade. To the best of our knowledge this is one of the pioneer studies where efficacy of BRM270 as an anticancer product under *in vitro* and *in vivo* conditions has been studied for HCC. Collectively, in current study our findings proposed novel molecular mechanisms of carcinogenesis in CD133⁺- expressing HepG-2 and SNU398 liver MSCICs induced extra-migratory metastasis in CJORI-CD nu/nu mice using 2DG infrared based optical probe guided molecular *in vivo* imaging model and anti-tumor potential of BRM270 via regulation of CyclinD1 mediated c-Jun-JNK apoptotic pathway.

2. MATERIALS AND METHODS

2.1. Animal model of hepatocellular carcinoma

6 week old CRJORI: CD-1-5WM male mice were purchased from KS HI-TEC, Inc Korea. Mice were housed in similar environmental and nutritional conditions. Mice were sacrificed at 10, 11 and 12 weeks of age according to the standard protocols of Jeju National University. The research proposal and the relevant experimental procedures were approved by the institutional review board of the Department of Animal Biotechnology, Jeju National University, Republic of Korea, 690-756. All animal studies were conducted to induce tumor and to evaluate the anti-cancer potential of BRM270. In order to design tumorigenesis and metastasis induction experiment, 36 male mice were distributed into six groups. Group one was designated as positive control of HepG-2-HCC (n = 6, treated with Dox 5mg/kg/day). Second group used as test group of HepG-2-HCC (n = 6, treated with BRM270 5mg/kg/day). Another third group opted as positive control for SNU-398-HCC (n = 6, treated with Dox 5mg/kg/day) and fourth group was chosen to be a test group for SNU-398-HCC (n = 6, treated with BRM270 5mg/kg/day). Fifth group, which was comprised of mice with non-treated tumor was designated as negative control group (n = 6). The sixth group included normal mice (n = 6). These doses were selected based on our previous study (28). In the treatment group, administration of BRM270 in drinking water (2 mg/ml, at a daily dose of 5mg/kg/day) was started from next day of transplantation of hepatocellular cancer cells. In the positive control group, administration of Dox through peritoneal injection (at the daily dose of 5mg/kg/day) was started from next day after inoculation of hepatocellular cancer cells. In the control group, drinking water without BRM270 was supplied.

2.2. Materials and reagents

Standard drug Doxorubicin was purchased from Sigma Aldrich, EZ-CyTox kit from Daeil Lab Service Co., Seoul, Korea, RPMI1640 from Gibco, EMEM from ATCC, and all antibodies were obtained from Santa Cruz Biotechnology, USA. BRM270 is a highly popular and promising anti-cancerous medicinal plant among North-East Asian countries. Its super cocktail product was procured from the Biological Response Modifier (BRM) International Health Town Corp., Republic of Korea. As per the manufacturer's details, it is a proprietary combination of *Saururus chinensis*, *Arnebia euchroma* (Royle) Johnst, *Scutellaria baicalensis*, *Citrus unshiu markovich*, *Portulaca oleracea*, *P. vulgaris* var. *lilacina* and *Aloe vera* (widely distributed in Northeast Asia mainly China, South Korea and Japan). Aqueous extract was prepared by boiling the dried roots, stem and leaves of the plant followed by spray-drying. Super cocktail is prepared by mixing equal proportion of above constituents to the total amount of 10 mg and dissolved in 20 ml of water. For experiments, the product mixture was filtered through ordinary filter paper and the filtrate was evaporated using rotary vacuum evaporator at 40–45°C. The 10 mg of the dried extract was suspended in cell culture medium, filter sterilized and used at the concentration of 10-200 µg/ml in cell cytotoxicity assay and Doxorubicin hydrochloride (5 µM/ml) for cell viability assay and 125 µg/ml for the rest of experiments. For consistency, the same lot was used throughout the entire study.

2.3. Cell culture and propagation

The cell line HepG-2 used in the study was purchased from the American Type Culture Collection (Manassas, USA). SNU-398 human hepatocellular carcinoma cell line was procured from Korean Cell Line Bank (KCLB-00398.1) and propagated in RPMI1640 complete media

with 10% FBS and 1% antimycotic and antibiotics. No cross-contamination of other human cells was observed. HepG-2 cells were grown in ATCC-formulated Eagle's Minimum Essential Medium (EMEM, Catalog No. 30-2003) supplemented with 10% FBS (v/v) and 1% non-essential amino acids (v/v), at 37°C, 5% CO₂. The human bone marrow cells (hBMCs) procured from the old Caucasian male (59 years) were purchased from Korean Cell Line Bank, Seoul, South Korea (KCLB No. 10246). The potential hBMCs were further cultured in DMEM high glucose supplied with 10% FBS, 1% antibiotic-antimycotic and 10 nM epithelial growth factor (E9644-Sigma, USA).

2.4. Establishment of CD133⁺ metastatic hepatocellular stem like cancer initiating cells

The population of CD133⁺ expressing HepG-2 and SNU398 cells was isolated by anti-human CD133 MicroBead kit (MiltenyiBiotec Corp., Auburn, CA, USA) using MidiMACS separator (MiltenyiBiotec Corp.) by following the user instruction manual. The HepG-2 and hBMCs from 3rd and 4th passage were confirmed as normal control cells against the efficacy of BRM270. To confirm CD133⁺ expressing the stem like cancer initiating cell, immunocytochemistry analysis was performed. Later, to investigate its tumorigenic efficiency, we performed *in vitro* tumor sphere forming assay and 2DG guided xenograft model to resect the tumor localization *in vivo*.

2.5. EZ-CyTox cell proliferation assay

Cells were seeded 24 h prior to drug treatment at 2500 cells/well in 96-well plate (Nunc™, Wiesbaden, Germany). After 24 h of recovery the cells were incubated in humid atmosphere at 37°C and 5% CO₂. The cells were treated with varying concentrations of BRM270

such as 10µg/ml - 200µg/ml and Doxorubicin (Dox) 10 µM/ml for 24 h. Later, 125µg/ml BRM270 also treated in rest of the experiments were incubated for 24 h. The enhanced cell viability assay was conducted with EZ-CyTox kit (Daeil Lab Service Co., Seoul, Korea) to measure the viable cells. EZ-CyTox solution (10µl) was added to each well and then cells were incubated for 2 h at 37°C and 5% CO₂. The light absorbance was determined at 450 nm by the microplate-reader (Model 680, Bio-Rad, Berkeley, USA).

2.6. Immunofluorescence staining

Suspended cells in 200µl media at density of 50 cells/well were seeded in four chambered slide (Nunc™, Wiesbaden, Germany). Localization and interaction of both CyclinD1 and Casp-3 proteins were carried out by indirect immunofluorescence staining. Cells were fixed in 4% formaldehyde in 1X PBS for 25 min, washed in cold PBS and permeabilized with 0.1% Triton X-100 in 1% BSA at room temperature for 15 min. Cells were then incubated at 4°C for overnight with both respective primary polyclonal antibodies i.e. rabbit IgG (Santa cruz Biotechnology). Next day, followed the staining with Alaxa flour 488/546 and GFP conjugated anti-rabbit IgG (secondary antibodies). Then, cells were washed twice with cold PBS and were counterstained with 4', 6-diamidino-2-phenylindole (DAPI, Invitrogen, USA). After incubation for 5 min again washed with cold 1X PBS and added 1 ml mounting media and cells were observed under the fluorescence microscope (Olympus, Italy) with adaptable filter consistent with Alexa Flour 488, Alexa Flour 546, and GFP.

2.7. Analysis of cell cycle distribution by flow cytometry (FACS)

The effect of BRM270 treatment on the progression of cell cycle was determined by flow cytometry following staining with Propidium Iodide as described previously (19). In brief, desired cells (1×10^6) were treated with BRM270, Dox or DMSO and both floating and attached cells were collected. The cells were fixed in 70% ethanol overnight at 4°C. Next day, the cells were centrifuged at 1200 rpm for 5 minutes, pellet washed twice with cold PBS, suspended in 500 μ l 1x PBS, and incubated with 5 μ l RNase (20 μ g/ml final concentration) for 30 minutes. The cells were then stained with Propidium Iodide (50 μ g/ml final concentration), and the cell cycle distribution was determined using a BD FACS Calibur flow cytometer.

2.8. DNA fragmentation assay by Hoechst 33342 staining

Fragmented DNA or condensed chromatin Cells were seeded on sterile cover glasses placed in the four chambered slide. When they grew to approximately 70% confluence, cells were treated with BRM270 @ 125 μ g/ml and were incubated for 24 h. Next day, cells were washed twice in ice-cold PBS (pH 7.4). After washing, the cells were fixed with 4% Paraformaldehyde in PBS for 30 minutes at 4°C, washed twice with PBS and stained with Hoechst 33342 (Thermo Fisher Scientific) at a final concentration of 10 μ g/ml at room temperature for 5 min. Nuclear morphology was then examined using a fluorescent microscope (Olympus).

2.9. Pre and late apoptosis by Annexin-V-FITC/PI double staining method

Apoptosis and programmed cell death was assessed by addition of 0.5 μ g/ml Propidium Iodide (PI, Sigma) and 1.0 μ g/ml Annexin-V-FITC (BD, Biosciences) in culture medium.

Images were taken after 24 h of exposure of BRM270 (125 $\mu\text{g/ml}$) with respect to Dox (10 $\mu\text{M/ml}$) through a 20X objective of phase contrast microscope. Further, we also conducted the flowcytometry (FACS) analysis for pre and late apoptosis as our previous study (19). In FACS, excitation was at 488 nm for PI and fluorescein. PI fluorescence was collected through a 560nm long-pass filter and FITC from a 505-530 nm band pass filter. The samples were analyzed on a BD FACS Calibur flow cytometer. A minimum of 10,000 events were assayed for each sample.

2.10. Real Time-qPCR (qPCR) and primers

The cellular RNA was purified using Qiagen RNeasy mini kit according to the manufacturer's instructions. The purified RNA was quantified by using Photometer (BioRad, *Hercules*, USA). Later, 1 μg of purified RNA was subjected to first strand cDNA synthesis using Superscript III first-strand cDNA synthesis kit and OligodT primer (Invitrogen, USA). The cDNA was subjected to qRT-PCR for the quantification of the relative transcript levels of using SYBR Green PCR master mix according to the manufacturer's instructions. A StepOne™ Real-time PCR System (Life Technologies) was used to perform real time qPCR. The primer sequences enlisted in table 5.1. were used for the current study.

Table 5.1. Primer Sequence Used in Quantitative Real-Time PCR (qPCR)

S. No.	Gene	Sequence	T _M °C	Accession number
1.	B - Actin	F- GGACTTCGAGCAAGAGATGG R- AGCACTGTGTTGGCGTACAG	57.50	NM_001101
2.	Bcl-2	F- AGGACATTTGTTGGAGGGGT R- AAACGGAGCTGCACTTTGAG	60.20	NM_000633
3.	c-Jun	F- TTTCAGGAGGCTGGAGGAAG R- CTGCCACCAATTCCTGCTTT	56.45	NM_002228
4.	CD133	F- GCCAGCCTCAGACAGAAAAC R- CCAAGCCTTAGGAGCATCTG	57.50	NM_001145848
5.	c-Myc	F- AACACACAACGTCTTGGAGC R- GCACAAGAGTTCCGTAGCTG	63.10	NM_002467

2.11. Western blot and protein interaction

Total protein lysates were extracted with a lysis buffer (50 mM TrisHCl, pH 7.5, 1 mM EDTA, 1 mM EGTA, 1% (v/v) Triton X-100, 50 mM NaF, 5 mM sodium pyrophosphate, 10 mM sodium-glycerophosphate, 0.1 mM PMSF, 1/100 protease inhibitor mixture, and 1/100 phosphatase inhibitor mixture). After 1h at 4°C on a rotating wheel shaker, the lysates were centrifuged at 10,000 g for 15 min at 4°C and total protein concentration was measured with BCA assay in the supernatant. 40 µg of proteins were resolved by SDS-PAGE (10% gels) and transferred onto nitrocellulose membrane. The membranes were blocked with 5% nonfat dry skimmed milk in TBS-T (10 mM Tris-HCl, pH 8, 100 mM NaCl, 1% (v/v) Tween-20) and incubated with appropriate primary antibody (rabbit poly. β-actin, Casp-3, c-Myc, Cyclin D1, Bcl-2 and c-Jun purchased from Santa Cruz Biotechnology, USA) for overnight at 4°C, followed by incubation with horse radish peroxidase-conjugated and anti-rabbit secondary antibody for 1 hour at room temperature (RT). Super Signal West Dura Extended Duration Chemiluminescent

Substrate was used for the ECL reaction and the signal was detected and quantified using the LAS4000 imaging system (Japan).

2.12. Optical probe guided molecular imaging of tumor localization and metastasis

For pre-and intra operative tumor localization in real-time resection, we conducted *in vivo* tumor localization assay using IRDye® 800CW 2-DG(2-deoxy-D-glucose) optical probe which purchased from LICOR, Biosciences, USA (926-08946). To evaluate and establish metastatic potential of both HepG-2 and SNU-398 MSCICs inoculated subcutaneously to nude mice. After day 7 of inoculation, “experimental metastasis” was observed distinct from “spontaneous metastasis”, where the tumor cells are first allowed to form a primary tumor in the site of injection and then escape into lymphatics or blood circulation. Probe was injected through tail vein to tumor bearing male mice and then mice were observed after anesthetizing with Zoletil 50 (Virbac, Carros, France) 1 ml/kg intra-peritoneal and all surgical procedures were performed under general anesthesia at different time intervals. Metastasis is detected using optical imaging, in particular near-infrared fluorescence (NIRF) range.

2.13. Statistical analyses

The relative quantitative expressions of the genes and proteins were analyzed by the analysis of variance (ANOVA). Kaplan-Meier curve of overall survival of mice was plotted and analysed by GraphPad Prism 6 software (Graphpad software, La Jolla,CA, USA). Further, to study the *in vivo* xenograft tumorigenesis, after day 7 of inoculation of metastatic cells, tumors were measured with digital Vernier’s calipers and the volume of each tumor (mm³) was calculated by the following formula:

$$Volume = (width)^2 \left(\frac{length}{2}\right)$$

Further, the size and the extent of metastasis of tumor under *in vivo* conditions was detected using 2DG infrared optical probe based imaging analyzer (Pearl impulse small animal *in vivo* analyzer, LI-COR Biosciences, USA). On the final day of experiment all the mice were sacrificed for the collection of tumor and their weights were analyzed using t-test. The significant differences between the mean expressions of different genes at $P < 0.05$ were analyzed by Tukey's b-test. The values have been expressed as mean \pm SEM.

3. RESULTS

3.1. CD133⁺ overexpressing heterogenic of liver cancer cells are highly tumorigenic under in vitro conditions and can be xenotransplanted in mice

To define stemness and tumorigenic invasiveness of CD133⁺ expressing metastatic HepG-2 and SNU-398 stem like cancer initiating cells, the glycoprotein cell surface ectopic expression analysis of MSCICs was carried out *in vitro*. We analyzed CD133 expression by immunocytochemistry (ICC) that showed significantly ($P < 0.05$) higher expression in HepG-2 and SNU-398 MSCICs compare to hBMCs (Figure 5.1A). It indicated the difference in expression levels between normal hBMCs and both the MSCICs. After characterization cells were cultured in appropriate growth medium and it was observed that HepG-2 MSTICs were efficiently transformed into colonies and sphere than hBMCs (Figure 5.1A, Phase contrast, lower panel). In addition, similar pattern of differences in both CD133 mRNA expression levels was observed between the non-cancerous hBM cell line and the both HepG-2 and SNU-398 MSCICs (Figure 5.1B and C). Based on this observation, we chose to use CD133 as stem cell marker to validate the stemness and tumorigenic property. Lastly, malignant potential of the CD133 positive MSCICs was investigated in an experimental animal model. To investigate metastatic and tumorigenic efficiency of both MSCICs, we designed xeno-transplantation tumor model. Specifically, CSCs characterized both MSCICs lines were harvested and inoculated at various concentrations such as 3×10^4 , 3×10^5 , 3×10^6 and 3×10^7 cells into right and left lower flank of CRJORI-CD nu/nu male mice. Comparatively, the inoculation dose of 3×10^7 MSCIC cells was efficient to induce palpable tumor at day seven of post inoculation (Figure 5.1D).

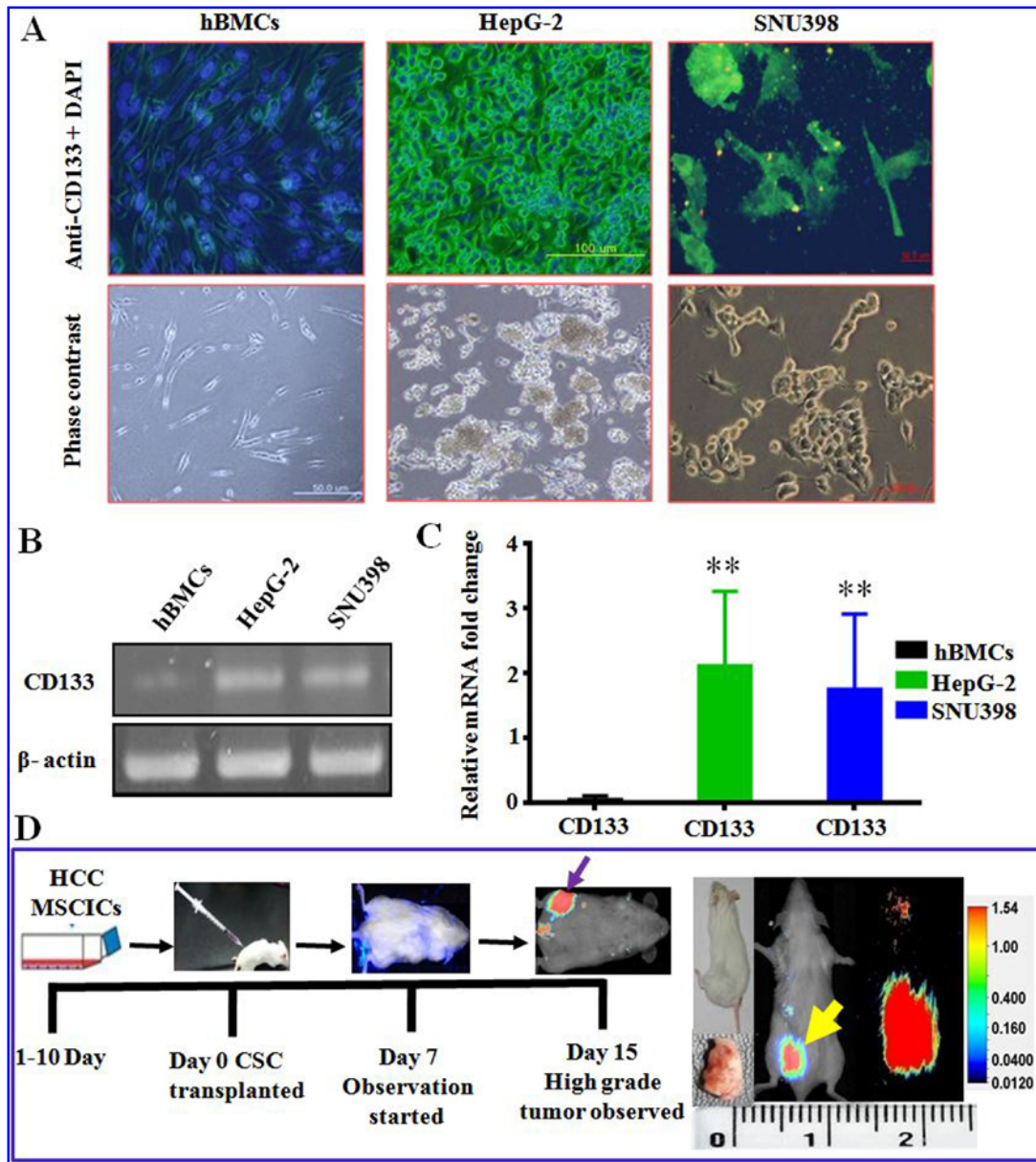


Figure 5.1. CD133⁺ overexpressing heterogeneity of liver HepG-2 and SNU-398 MSCICs are highly tumorigenic. **A.** Immunocytochemistry exerted overexpression of CD133⁺ (prominin1) in HepG-2 and SNU-398 MSCICs compared to hBMCs while lower panels showing tumorigenic phase contrast microscopic image of growing HepG-2 and SNU-398 cells. **B and C.** Relative expression of CD133 CSC markers using RT and qPCR. **D.** Cellular propagation of HepG-2 MSCICs and palpable xenograft experiment with mice.

On day eight of post inoculation, observation of palpable tumor metastasis and its recurrence was determined via infrared optical probe 2DG IRDye[®] 800CW non-radioactive (10 μ M/100 μ l dissolved in 1X PBS and injected through tail vein). Tumor localization and resection was detected by *Pearl Impulse* imaging system. It showed high grade tumor due to higher metabolic rate exemplified by an elevated rate of glycolysis under *in vivo* (Figure 5.1D). The result showed that CD133⁺ expressing MSCICs are more tumorigenic, more invasive and are able to form the palpable tumor by the day seven of post inoculation.

3.2. BRM270 inhibits proliferation of hepatocellular cancer cells

BRM270 has antiproliferative effect on HCC cell lines. It could inhibit the growth of CD133⁺ HepG-2 and SNU-398 cells *in vitro* in a dose-dependent manner. Dox and cell culture medium were used as positive and negative control respectively. As shown in Figure 5.2A, the morphological changes of HepG-2 and SNU-398 cells were observed with a microscope following treatment with 125 μ g dose of BRM270 and Dox (10 μ M) for 24 h. The results revealed that the BRM270 and Dox treated cells detached from the plates and floated as rounded structures due to morphological changes associated with the cell shrinkage and programmed cell death (Figure 5.2A). In this study, CD133⁺ HepG-2 and SNU-398 cells were treated with different doses of BRM270. EZ-CyTox-WST assay was used to examine the anti-proliferative effect of BRM270 on CD133⁺ HCC cell lines.

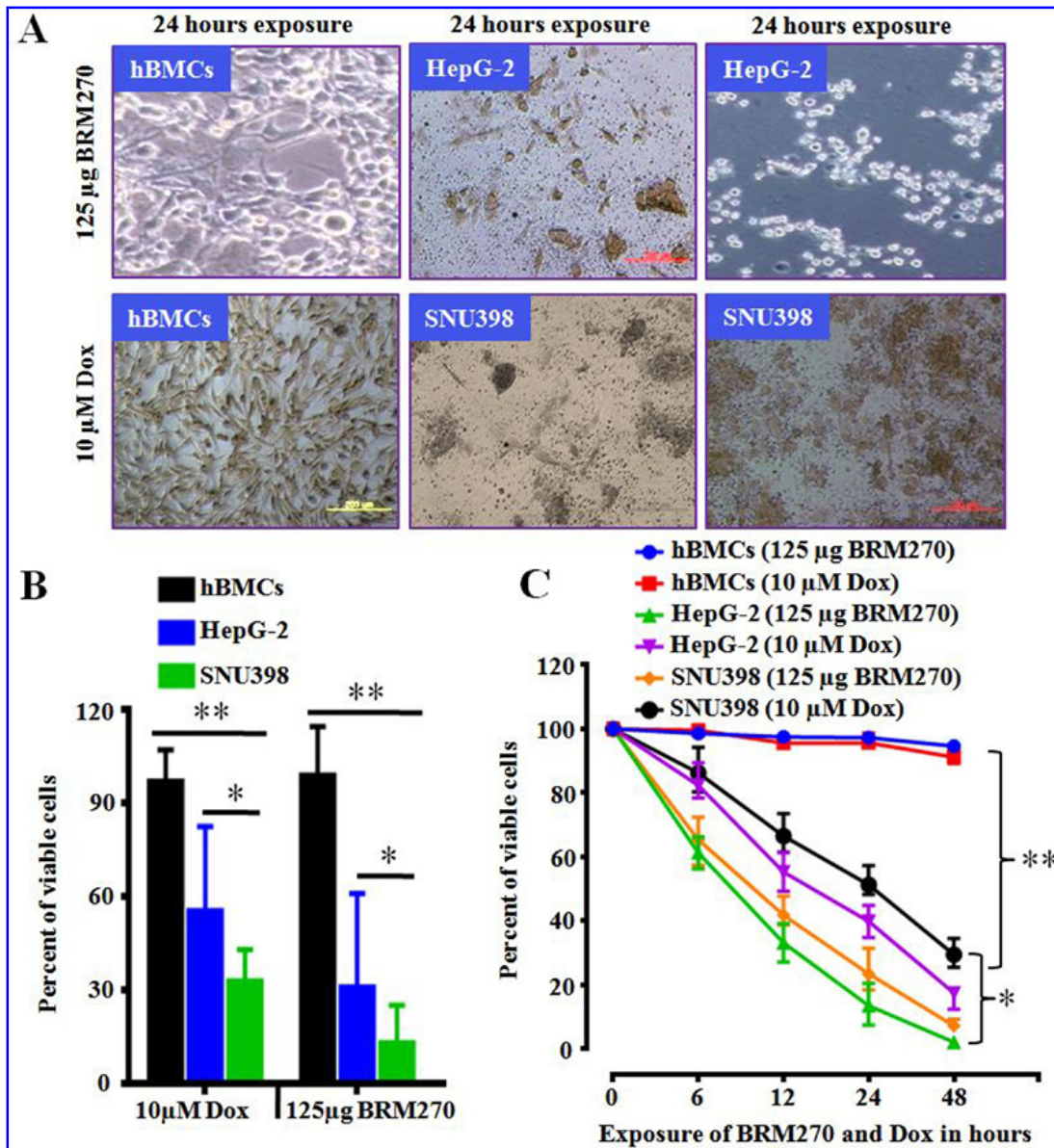


Figure 5.2. Natural drug BRM270 inhibits proliferation of Hepatocellular carcinoma stem like cancer cells. **A.** Phase contrast micrographs 24 h HepG-2 and SNU-398 cancer cells showed morphological cell death and cytotoxic effect exert by BRM270 (125µg) and Dox (10µM) against metastatic stem like cancer initiating cells (MSCICs). **B.** HepG-2 and SNU-398 cells were treated with 125µg concentrations of BRM270, Dox (10µM) and the percentage viability by EZ-CyTox kit at 24h. **C.** Time course studies of BRM270 with compared to Dox against both HepG-2 and SNU-398 cells up to 48 h.

Interestingly, BRM270 significantly ($P<0.01$) reduced the percentage of live hepatocarcinoma cells after exposure with 125 μ g/ml in 24 h as compared to 10 μ M Dox (Figure 2B). In addition, BRM270 exhibited higher cytotoxicity at 125 μ g/ml when compared to Dox (10 μ g/ml). The percentage of viable HepG-2 MSCICs after treatment with BRM270 decreased to 63.01%, 37.12%, 17.20% and 4.10% while Dox reduced viability by 85.41%, 58.22%, 44.25% and 26.04% in 6, 12, 24 and 48 hrs respectively (Figure 5.2C). Similarly, BRM270 exhibited higher cytotoxic activity against SNU-398 MSCICs when compared to Dox in time dependent manner and viability was decreased by 66.23%, 44.04%, 23.27% and 7.54% in 6, 12, 24 and 48 hrs respectively. Dox demonstrated 89.21%, 71.25%, 58.22% and 38.10% cell viability in the experiment (Figure 5.2C). Additionally, we also elucidated the side-effects of BRM270 on normal human hBMCs compared with Dox which was 98.01%, 98.25%, 98.2% and 97.25% while Dox affected cell viability by 98.32%, 96.32%, 97.02% and 96.01% in 6, 12, 24 and 48 hrs respectively (Figure 5.2C).

3.3. Effect of super cocktail BRM270 on G_1 DNA-damage checkpoint control

Anticancer agents avert cell division at various checkpoints of cell cycle and thereby, slow down growth and proliferation of cancerous cells including hepatocellular carcinoma. To assess whether BRM270 downregulates cell proliferation by arresting the cell cycle in HepG-2 and SNU-398 cells, a flow cytometric analysis was carried out. In this study both MSCIC cells were treated with BRM270 and Dox for 24 h at 125 μ g and 10 μ M concentration. Result of this study indicated that BRM270 significantly ($P<0.01$) modulated G_1 cell cycle and its transition to G_2/M phase when compared to untreated cells (Figure 5.3 and table 5.2).

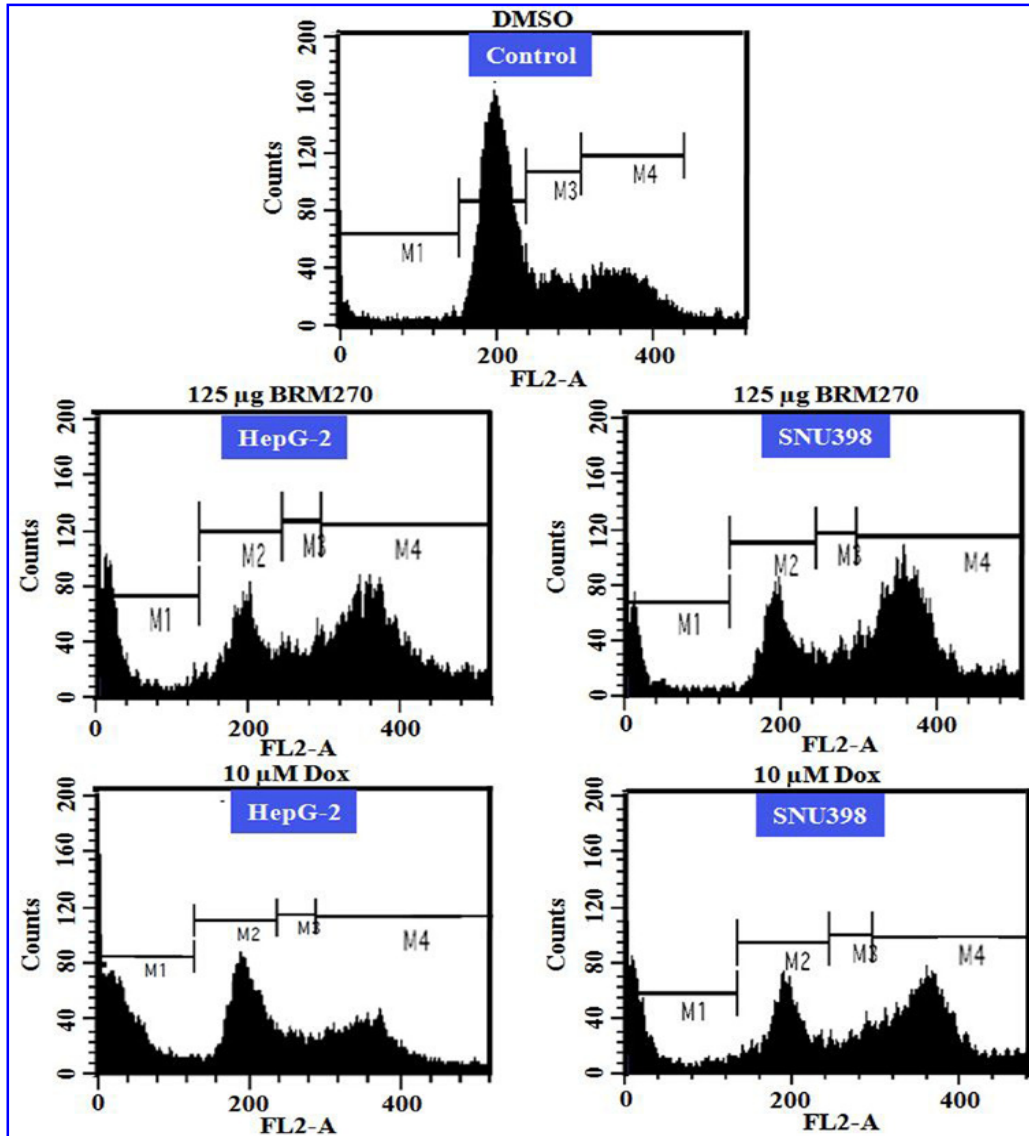


Figure 5.3. Cell Influence of BRM270 on cell cycle progression/distribution in HCC MSCICs. Effect of BRM270 and Doxorubicin on cell cycle progression in HepG-2 and SNU-398 cells incubated for 24 h at 125 μ g and 10 μ M concentrations respectively.

Table 5.2. Influences of BRM270 and Doxorubicin on cell cycle progression in liver HepG-2 and SNU-398 cells

Group	Conc.	% of cells at indicated checkpoints of cell cycle			
		M1 = G0	M2 = G1	M3 = S	M4 = G2/M
Control	0 μ M	6.2	63.71	12.34	17.75
Dox treated HepG-2	10 μ M	24.34	30.48	7.63	37.55*
Dox treated SNU-398	10 μ M	18.65	28.17	8.26	44.92**
BRM270 treated HepG-2	125 μ g	19.87	31.26	9.73	39.14**
BRM270 treated SNU-398	125 μ g	14.20	29.95	9.17	46.68**

The percentage of distributed cells in different cell cycle checkpoints are presented as mean \pm SD (n = 3).

* $p < 0.05$ versus the percentage of apoptotic cells of the control; ** $p < 0.01$ versus the percentage of apoptotic cells of the control

The percentage of cells in the BRM270 treated groups significantly decreased at the S phase and G0/G1 phase, simultaneous increase at the G2/M phase of both HepG-2 and SNU-398 cells was also recorded. These results indicated that BRM270 can induce cell cycle arrest at the G2/M phase in HepG-2 and SNU-398 cells. After treatment of BRM270 at 125 μ g concentration, the percentage of HepG-2 and SNU-398 cells accumulated in G2/M phase was 39.14% and 46.68% (approximately 61 %) while 17.75% untreated cells in G2/M phase were there (Figure 5.3, table 5.2). Similarly, after treatment of Dox at 10 μ M concentration, the percentage of HepG-2 and SNU-398 cells accumulated in G2/M phase was 37.55% and 44.92% (approximately 82%). This study reveals that BRM270 notably arrests MSCIC cells at G2/M checkpoint and blocks transition to next phase of cell cycle as compared to Dox at 10 μ M concentration.

3.4. *BRM270 treatment induces DNA fragmentation, nuclear condensation and apoptosis*

To investigate the apoptotic and DNA fragmentation activity induced by BRM270, first of all HepG-2 and SNU-398 MSCICs were stained with Hoechst 33342 and observed under a fluorescence microscope (Olympus). Interestingly, it was observed that the condensed chromatin of apoptotic cells was stained more brightly than chromatin of normal cells. The morphological changes because of cell apoptosis included condensation of chromatin as well as nuclear fragmentation via pyknosis and karyorrhexis and such changes were observed in the BRM270 treated groups (Figure 5.4A, yellow arrow), while a few in the apoptotic cells of positive control group. Again, to better understand the mechanisms of essential BRM270 augmented apoptosis, we conducted biparametric cytofluorimetric analysis, using Propidium Iodide (PI) and Annexin-V FITC double staining method in HepG-2 and SNU-398 cells. Indeed, the number of Annexin-V-FITC positive cells was increased significantly when HCC MSCICs cells were treated with BRM270 and it was found better than Dox (10 μ M) as shown in Figure 5.4B and table 5.3. Findings of current study highlighted that after 24h of exposure BRM270 (125 μ g) resulted in 21.33% and 52.93% apoptosis and while Dox (10 μ M) displayed 6.52% and 32.74% apoptosis in HepG-2 and SNU-398 cells, respectively. The lower and upper right quadrant in Figure 5.4B indicates early and late apoptotic cells.

Whether BRM270 can enhance the activation of caspases-3 were also examined and result were verified with immunocytochemistry as well as western blot analysis. Our findings showed that BRM270 significantly enhanced expression of Casp-3 via suppression of cyclinD1 (Figure 5.5A upper panel compared to lower panel negative control). Specifically, CyclinD1 was more significantly ($P<0.05$) down-regulated following BRM270 exposure for 24 h and reciprocally proapoptotic Casp-3 protein level was upregulated in immunoblot study (Figure 5.5B-E).

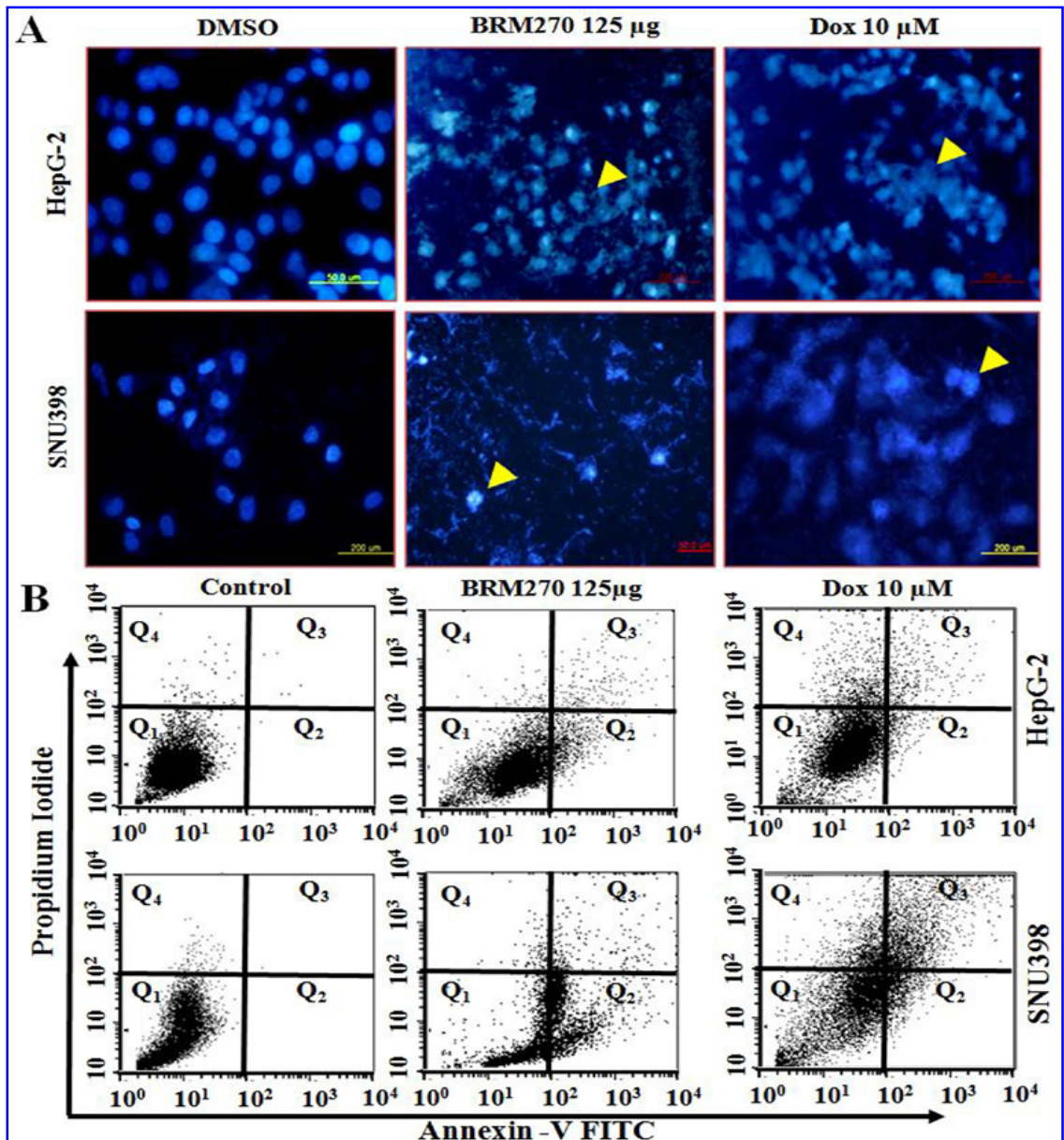


Figure 5.4. Novel nutraceuticals BRM270 induces nuclear condensation, fragmentation and apoptosis on hepatocellular carcinoma cells. **A.** Fluorescent images of Hoechst staining displaying BRM270 and Dox induced cell death after 24 h treatment at 125µg and 10 µM concentrations. **B.** Flow cytometric quadrant dot plot of apoptotic HepG-2 and SNU-398 cells after 24 h treatment with BRM270 and Doxorubicin.

Table 5.3. Quantitative apoptosis assay of hepatocellular carcinoma MSCICs using Annexin-V/PI dual staining method by FACS

Group	Conc.	Viable cells (Q1 %)	Early apoptosis cells (Q2 %)	Late apoptosis cells (Q3 %)	Necrotic cells (Q4 %)	Apoptotic cells (Q2+Q3)
Control-HepG-2	0 μ M	98.63	0.001	0.004	1.13	0.005
Control-SNU-398	0 μ M	98.89	0.0	0.001	1.10	0.001
Dox treated HepG-2	10 μ M	83.72	2.31	4.21	9.76	6.52**
Dox treated SNU-398	10 μ M	50.72	12.96	16.78	16.54	32.74***
BRM270 treated HepG-2	125 μ g	77.47	18.31	3.02	1.20	21.33**
BRM270 treated SNU	125 μ g	45.35	47.04	5.89	1.72	52.93***

The percentage of viable cells, early apoptotic cells, late apoptotic cells, and necrotic cells are presented as mean \pm SD (n = 3).

* $p < 0.05$ versus the percentage of apoptotic cells of the control; ** $p < 0.01$ versus the percentage of apoptotic cells of the control; *** $p < 0.001$ versus the percentage of apoptotic cells of the control.

An involvement of group II caspases (which includes caspase-3) was demonstrated by the abrogation of CyclinD1 after 24 h exposure to BRM270 (Figure 5.5A-E). Collectively these data demonstrates that novel phyto-drug BRM270 efficiently abrogates the metastatic liver stem like cancer initiating cells via Casp-3 dependent early and late apoptosis.

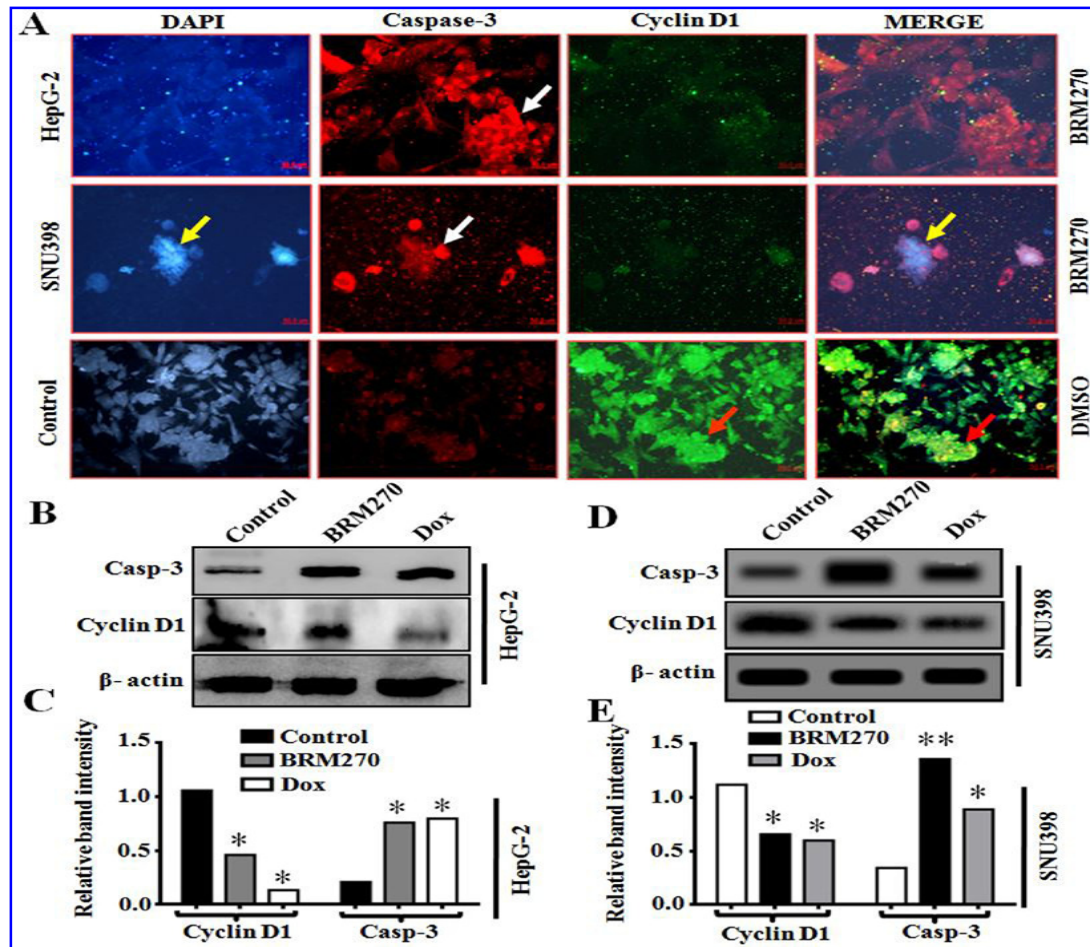


Figure 5.5. BRM270 recruits Casp-3 to negatively attenuate cell proliferation by Cyclin-D1 mediated early and late apoptosis. **A.** Immunofluorescent staining of HepG-2 and SNU-398 cells showing effect of BRM270 on Caspase-3 and CyclinD1 expression. MSCICs cells were treated with BRM270 and Doxorubicin for 24 h then stained with mouse monoclonal caspase-3 and CyclinD1 antibodies and followed by incubation with FITC (Green) and Alexa flour 546 (red) conjugated goat anti-mouse IgG. The images were visualized under a fluorescence microscope. **B-E.** Whole cell lysates were subjected to SDS-PAGE and analyzed by Western blot analysis using anti-Casp-3 and CyclinD1 antibodies to detect their relative expression.

3.5. BRM270 is efficacious in controlling tumor growth and metastatic dissemination in a xenograft mice model of HCC

Based upon the efficacy of BRM270 against CD133⁺ over-expressing metastatic cancer cells *in vitro*, we carried out anti-cancerous activity of BRM270 in knock-in experiment in mice model. Meier Kaplan survival log rank test showed that BRM270 significantly ($P<0.05$) increased the prognosis value and enhanced the survival rate of MSCICs tumor bearing mice from around 32% to 73% as compare to Dox treated (5mg/kg/day) mice (60%) (Figure 5.6A and B). The CD133⁺ MSCICs tumor bearing mice displayed a significantly ($P<0.01$) lower relapse free survival rate on day 80 in non-treated (32.08%) than BRM270 administered (5mg/kg/day) tumor bearing mice (72.72%) (Figure 5.6A). Similarly, Dox also revealed significantly ($P<0.01$) free survival rate 60.12% than non-treated group 29.12% (Figure 5.6B). BRM270 significantly ($P<0.05$) increased the prognosis value and enhanced the survival rate of MSCICs tumor bearing mice from around 32% to 73% compared to Dox treated (5mg/kg/day) mice (60%) (Figure 5.6A and B). Both MSCICs induced high grade subcutaneous solid tumors in mice (Figure 5.6C). Mice were sacrificed after BRM270 and Dox treatment followed by the measurement of relative weight and volume of tumor using digital Vernier calipers. A significant ($P<0.01$) reduction in weight and tumor size was observed in BRM270 treated mice compared to untreated and Dox treated mice group (Figure 5.6D and E). Additionally, it was also determined whether BRM270 treatment is key factor to reduce cancer incidence as well as the size of the tumors in local and systemic metastasized tumor-bearing mice (Figure 5.7A). Uptake of 2-DG within subcutaneously inoculated MSCICs induced liver cancer tumor xenografts were imaged (using a small animal image analyzer system, LICOR, Biosciences, USA) before and after BRM270 treatment compared to Dox (Figure 5.7A and B).

Table 5.4. Dose response to BRM270 administered on hepatoma cell line induced carcinoma in CRJORI: CD-1-5WM mice.

Treatment groups	No. of mice with tumor	Tumor incidence (%)	Total tumor burden (g)	Inhibition %	Average tumor weight (g)	Inhibition %
Gp-1: DOX-HepG-2	5/6	84	16.72	24.75	3.32 ± 1.20	29.6
Gp-2: BRM270-HepG-2	4/6	66	9.67	56.45	2.10 ± 0.56	59.2*
Gp-3: DOX-SNU-398	4/6	66	13.62	38.65	3.72 ± 0.64	27.6
Gp-4: BRM270-SNU-398	3/6	34	2.68*	87.93	1.4 ± 0.35	76.73*
Gp-5: Negative control	5/6	84	22.2	-	5.14 ± 1.21	-

A significantly higher signal-to-background ratio (due to elevated levels of glycolysis *within* tumor proliferative cells) was observed in mice inoculated with MSCICs (metastatic group) compared to BRM270 treated group. The results of *in vivo* experiment confirmed that BRM270 significantly ($P<0.05$) inhibited tumor progression in a dose and time dependent manner (Figure 5.6E and Table 5.4).

Toxicity and side-effects of the BRM270 were assessed by monitoring the relative bodyweight, behavioral appearance, intake of water and food of the mice on daily basis. Analysis showed that there was no statistically significant difference in body weight between the BRM270 treatment groups and the control (normal mice) observed which suggesting that the treatments were not overtly toxic for the mice (Figure 5.7C). Collectively these data indicates that administration of BRM270 inhibits tumor growth *in vivo* and results are significantly ($P<0.05$) better when compared to Dox treatment.

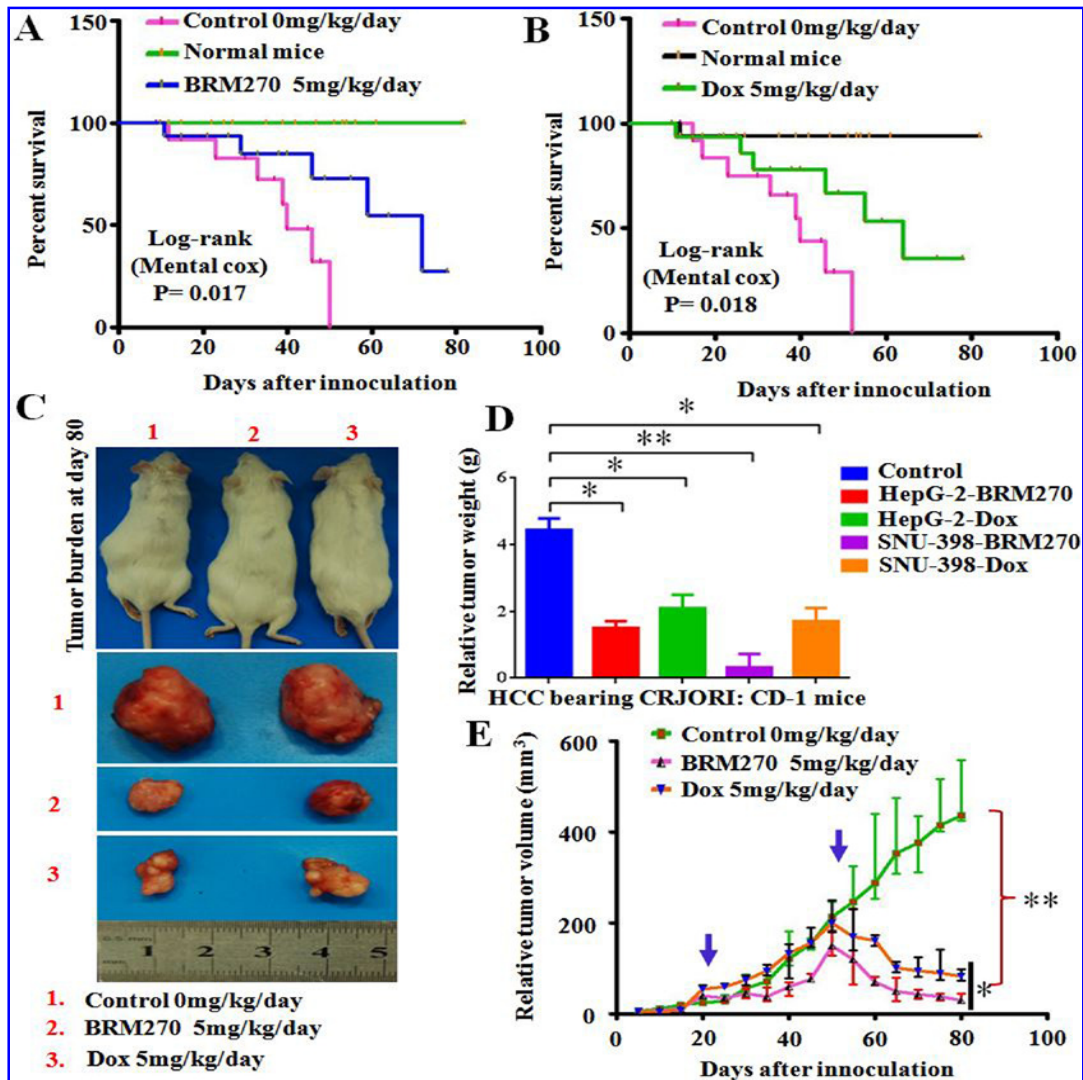


Figure 5.6. Phyto-drug BRM270 reduces metastatic dissemination to the lung in a CRJORI:CD-1-5WM mice. A-B. Progression-free-survival curve was calculated with the Kaplan-Meier method and compared by using the log-rank test. $***P < 0.018$ and 0.017 opted as an extremely statistically significant. **C.** HepG-2/SNU-398 induced high grade HCC solid tumor compared with Dox. **D.** Relative tumor weight in untreated animals, DOX (5mg/kg/day) treated animals and BRM270 (5mg/kg/day) treated animals. **E.** Tumor volume in untreated animals, DOX (5mg/kg/day) treated animals and BRM270 (5mg/kg/day) treated animals.

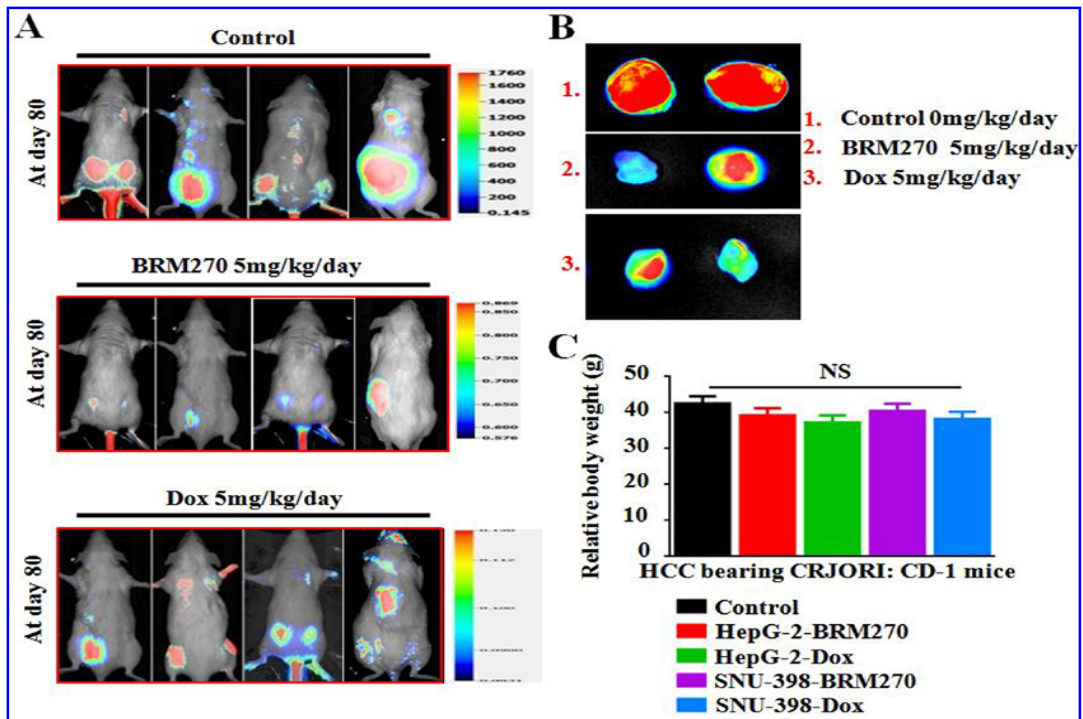


Figure 5.7. BRM270 reduces metastatic dissemination and mitigates tumor progression in IRDye®-2DG guided molecular imaging xenograft model. A. 2DG infrared optical probe guided analysis of CD133⁺-MSCICs induced palpable solid tumors and metastasis in male mice, under *in vivo* conditions using LI-COR image analyzer. **B.** Tumor resection and localization by LI-COR *Pearl* small animal imaging system. **C.** Relative body weight of various treated and non-treated mice in HepG-2/SNU-397 MSCICs induced HCC groups.

3.6. Super cocktail BRM270 reduces c-Myc and Bcl-2 associated metastasis, poor prognosis via suppression of c-JUN interaction

To investigate the correlation between the overexpression of c-Myc and Bcl-2 in metastasized HCC, the expression levels were compared between primary subcutaneous and their paired metastatic tumors. Tumor samples were randomly divided into groups and then mRNA fold inductions were analyzed using qPCR. Specially, c-Myc, anti-apoptotic Bcl-2 and c-Jun expression significantly ($P<0.05$) down regulated following exposure of BRM270 in both HepG-2 and SNU-398 inoculated tumors samples (Figure 5.8A). Similarly, significantly higher protein expression levels of c-Myc, Jun and Bcl-2 was observed under *in vivo* conditions in untreated group (Figure 5.8B). BRM270 treatment significantly reduced Bcl-2, Myc and c-Jun expression ($P<0.05$) in the mice model (Figure 5.8B). Collectively, these findings supported the concept of co-suppression of Myc, CyclinD1 and c-Jun interacted proteins by novel phyto-drug BRM270 in HepG-2 and SNU-398 MSCICs (Figure 5.8B).

To define the molecular mechanism of CyclinD1-c-Jun mediated tumorigenesis, a cancer-associated protein-protein interaction network at translational level was constructed using a bioinformatics STRING approach (Figure 5.8C). Collectively, significant suppression of Jun activity by BRM270 hints toward its participation in c-Jun N-terminal kinase apoptosis pathway for induction of apoptosis as well as reducing tumors size and metastasis *in vivo* studies.

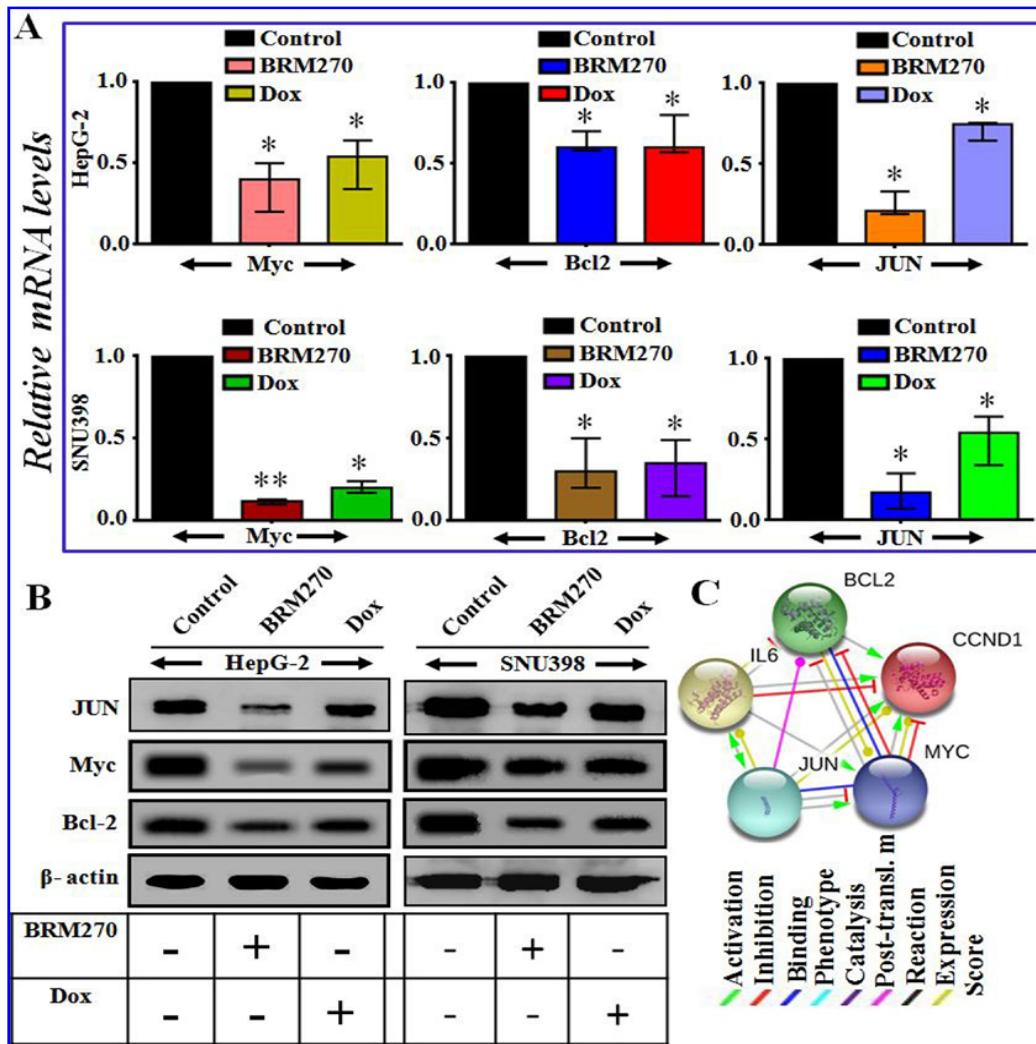


Figure 5.8. Overexpression of c-Myc and Bcl-2 associated with metastasis and poor prognosis, which abrogated by BRM270 via suppression of JUN interaction. A. qPCR relative expression of candidate genes their mRNA levels changes observed in HepG-2 and SNU-398 tumor samples. **B.** Total lysates were immune blotted for oncogenic proteins and its densitometric bar graphs in non-treated and BRM270 treated with positive control Dox. **C.** Cancer-associated protein-protein interactions network was constructed using a bioinformatics approach-STRING. * $P < 0.05$, ** $P < 0.001$ have been opted as significant differences.

4. DISCUSSION AND CONCLUSION

Liver cancer is an aggressive disease with a poor prognosis (Venook *et al.*, 2010). Present study including earlier research suggests that HCC is very likely to be originated from progenitor stem (MSCICs) like cells (Venook *et al.*, 2010; Yamashita *et al.*, 2013). These cells are responsible for tumor relapse, metastasis and chemoresistance. MSCICs have been characterized based on the expression of specific cell surface biomarkers, such as CD133. CD133 is a trans-membrane glycoprotein involved in cell adhesion, migration and drug resistance (Yamashita *et al.*, 2013; Chang *et al.*, 2000). To test for *in vitro* expression of metastatic markers, ICC and qPCR were performed. It revealed significantly ($P<0.05$) higher co-expression of CD133 in both MSCICs than hBMCs (Figure 5.1A-C) which is parallel to the previous study (Hou *et al.*, 2012). Next, to examine the tumorigenic ability of CD133⁺ MSTICs, both cell lines were inoculated subcutaneously, ortho-topically into the lower right flank of male CJORI-CD mice (Figure 5.1D). It was observed that these CD133 positive subpopulations of MSCICs can efficiently induce invasive tumor recurrence and metastasis in 2DG 800CW (IR) optical probe guided molecular imaging model of HCC and results were parallel to findings of earlier studies (Cao *et al.*, 2013; Chow *et al.*, 2013).

The “mitotic catastrophe, DNA fragmentation and condensation” induced PCD is a major phenomenon in arresting of the cell cycle arrest and apoptosis (Mongre *et al.*, 2016). Cytotoxicity and apoptotic studies revealed significant reduction in MSCICs cell proliferation following BRM270 treatment.

We observed that the cell and nucleus were enlarged and halted cell cycle progression after BRM270 treatment. Though both MSCICs cells were arrested in the G2/M phase by BRM270, there was no increase in the mitotic index in the BRM270-treated cells compared with

the untreated cells (Figure 5.3). This illustrates that both the HepG-2 and SNU-398 cells are mostly arrested in the G2 phase and do not reach the M phase. Therefore, it can be concluded the transition of the MSCIC cells from the G2 to the M phase is blocked (Figure 5.3). The current observation matched with our earlier study where BRM270 induced G2/M transition and arrest in A549 lung cancer cell line (Mongre *et al.*, 2015).

Apoptosis is a major pathway by which most of the anticancer including natural drugs kill tumor cells (Kovar *et al.*, 2009). The stimulation of apoptosis has been considered as a essential and novel approach in anticancer therapy (Kovar *et al.*, 2009; Elmore *et al.*, 2007). Therefore apoptotic effect of BRM270 was evaluated by Hoechst 33342 staining and biparametric cytofluorimetric analysis, using Propidium Iodide (PI) and Annexin-V FITC double staining method as well qPCR and western blot in both HepG-2 and SNU-398 cells. Our findings (Figure 5.4B) revealed that BRM270 caused early + late (21.33% and 52.93 %) while Dox induced early + late (6.52% and 32.74%) apoptosis respectively in HepG-2 and SNU-398 cells and results are supported by the findings of an earlier study by Mongre *et al* (2015). Later, immunoblotting studies also revealed similar findings after exposure with novel naturaceutics BRM270 in CD133⁺ MSCICs.

The caspase-3 belongs to a member of the cysteine-aspartic acid protease family and gets activated in both extrinsic as well as intrinsic pathways of cell apoptosis (Chang *et al.*, 2000; Zhang *et al.*, 2009). An elevated level of Casp-3 has been observed in BRM270 treated both MSCICs compared to non-treated cells (Figure 5.5A-D). Because pro-apoptotic Casp-3 seems to work as an augmenter for PCD that binds CyclinD1 than inducing its degradation and up-regulation of Casp-3 target protein serves as a necessary readout of CyclinD1 inhibition (Zhang *et al.*, 2009). Collectively, current study suggesting that phyto-drug BRM270 induced Casp-3

mediated apoptosis through Cyclin D1 dependent modulation of G1/S cell cycle checkpoints in the MSCICs cell response to programmed cell death in prevention of liver carcinogenesis.

The major limitation to the success of chemotherapy in HCC is the development of multidrug resistance (MDR) and cancer recurrence (El-Serag, 2011). Answers to all such queries might come from the knock-in experiments in which the combined approach of phyto-drug with animal model is put into use. Our earlier findings also suggests that novel inhibitor BRM270 significantly ($P<0.05$) reduced the metastatic proliferation of CD133⁺ SLCICs under *in vitro* conditions (Mongre *et al.*, 2015). As we expected, it significantly ($P<0.05$) increased the percent survival than Dox administered tumor bearing CRJORI-CD mice (Figure 5.6A and B). Similarly, an earlier study reported that natural drug (amarogentin) prevented liver carcinogenesis and increased percent survival of tumor bearing mice through modulation of G1/S cell cycle checkpoint and induction of apoptosis (Chen *et al.*, 1998). Specifically, this treatment resulted in reduced tumor size and presented effects comparable to those of Dox (Figure 5.6D and E). Parallel to these finding, BRM270 significantly reduced the extent, size and volume of metastatic tumors (Mongre *et al.*, 2016). Collectively, this suggests that liver MSCICs inoculated carcinogenic expression leads to poor tumor prognosis and can serve as a biomarker for treatment which can be significantly reduced by natural inhibitor BRM270.

Activation of the JNK pathway has been shown to be a common phenomenon in apoptotic induced programmed to cell death (Chen *et al.*, 2012). Novel anti-cancer naturaceutics like BRM270 can induce programmed cell death via Casp-3 attenuated early and late apoptosis (Mongre *et al.*, 2015). To understand the mechanism regulating the inhibition of proliferation, activation of JNK pathway status along with expression analysis of different genes associated with G1/S phase of cell cycle checkpoint were analyzed. It has been noted that there is an inverse

correlation of cellular proliferation and apoptosis during liver carcinogenesis. BRM270 administration could reduce rate of proliferation and simultaneously induce apoptosis in the liver lesions particularly from 3rd week onwards thereby preventing progress of carcinogenesis. The induction of apoptosis might be due to the increased Bcl-2 resulting in activation of caspase-3 (Figure 5.5A-D and 5.8A-C). Similarly, previous studies by Cao *et al.* (2013) and Mongre *et al.* (2015) demonstrated BRM270 inhibits the CyclinD1 and caused early and late apoptosis induced programmed cell death by cell cycle arrest at G1 checkpoints. Apart from that, over expression of c-Myc and CyclinD1 has already been reported in carcinogenesis (Wang *et al.*, 2007; Elmore, 2007). However, significantly ($P<0.05$) down regulation in the expression pattern of cMyc, cyclinD1, Bcl-2, and c-Jun after exposure with anticancer phytochemical BRM270 was observed (Figure 5.8A and B). Next, before going to translational level of protein expression profiling, we performed protein-protein interaction network using STRING which exerts co-interaction and activation of c-Jun mediated JNK apoptosis pathway as similar to MMP-9 and c-FOS cancer-associated protein-protein interactions network bioinformatics approach by previous report (Pal *et al.*, 2012). Similarly, in the current study BRM270 negatively attenuates anti-apoptotic Bcl-2 induced JNK pathway via suppression of carcinogenic c-Myc in immunoblot study at significant level ($P<0.05$) (Figure 5.8B-C). Earlier studies have reported the similar mechanism that BRM270 significantly augments Casp-3 mediated Bcl-2 dependent apoptosis via suppression of c-Myc and IL-6 in NF- κ B and c-Jun N-terminal kinase pathways in other cancers (Zhang *et al.*, 2009; Chen *et al.*, 1998, 34). From the present observation it may be concluded that the cumulative alteration of both cellular proliferation and apoptosis, by BRM270 treatment, can prevent the progress of carcinogenesis in liver.

In conclusion, this study provides compelling evidence of epigenetic switching of MSCICs inoculated hepatocellular carcinoma in *in vivo* model and cross talk with N-terminal kinase JNK pathway. Several therapeutics regimens can prevent the progress of carcinogenesis in liver. However, MDR, side-effects and genetic aberration are the main consequences in cancer therapy including HCC. Therefore, it is need of hours to develop natural photochemical based zero-toxic/xeno-footprint to normal cells, but specific novel inhibitors regimen to MSCICs with significant therapeutic potential. The current study also proposes a wide range of strategies by which BRM270 mitigates the progression and metastasis of CD133⁺ HepG-2 and SNU-398 MSCICs induced HCC. The preventive action of BRM270 during carcinogenesis seems to be more effective as well as its therapeutic action. Further studies are required to throw more light on the mechanism of action of BRM270 like naturaceuticals, and will help to elucidate the best possible timing and extent of intervention with this compound for prevention of liver carcinogenesis. This study is clinically relevant and would act as the baseline data for the development of new therapeutic strategies.

CHAPTER 6

BRM270 INHIBITS TUMORIGENESIS BY UPREGULATION OF *LET-7* MICRORNA THROUGH ACTIVATION OF MITOCHONDRIAL INTRINSIC APOPTOTIC PATHWAY

ABSTRACT

MicroRNA (miRNA) is a post transcription modulator and its abnormal expression has been observed in various types of cancers. In the current study, we have shown that the *let-7* miRNA negatively regulates *LIN28*. Elevated level of *LIN28* simultaneously suppresses *let-7* and activates mitochondrial intrinsic apoptotic gene expression in a *let-7*-dependent manner. Both transcriptomic and translational analysis showed the efficacy of BRM270 as significant anticancer agents to augment apoptosis by up-regulation of *Let-7* mRNA while it simultaneously inverse the expression of *LIN-28*. Furthermore, proteome microarray also revealed that BRM270 significant induces expression of intrinsic apoptotic proteins. *Let-7* expression is lower in stem like cancer initiating cells (SLCICs) tumors than in normal cells, while *LIN-28* mRNA is significantly higher in tumors samples, providing a possible mechanism for *let-7* in SLCICs induced carcinogenesis. A greater understanding of what controls *let-7* expression might enable the development of treatments to fight or prevent many cancers.

Keywords: miRNAs, *Let-7*, SLCICs, CD133

1. INTRODUCTION

MicroRNA (miRNA) belongs to a class of the post transcription modulator, non-coding small RNA and contains about 22 nucleotides (Croce *et al.*, 2005). Abnormal expression of miRNA has been observed in various types of cancers (Calin *et al.*, 2006). A number of studies have demonstrated that miRNAs is able to modulate various tumorigenic processes, including antitumorigenic activity, progression and metastasis. miRNA Let-7 has been shown to be significantly correlated with the occurrence and development of cancer, suggesting it is involved in the regulation of oncogenic pathways (Lu *et al.*, 2005). Moreover, whether let-7 is involved in the development of osteosarcoma and the potential molecular mechanisms are remain unexplored (Liu *et al.*, 2014). MicroRNAs can undergo aberrant regulation during carcinogenesis, and they can act as oncogenes or tumor suppressor genes. For example, Let-7 is an important microRNA family consisting of 12 members located in genomic locations frequently deleted in human cancers. In addition, expression of let-7 RNAs is reduced in most of the cancer patients and associated with poor prognosis (Lu *et al.*, 2005). On the other hand, LIN-28 is a key inducer to reprogramme cells to augment stemness, to makes critical contributions to tumorigeneceity by suppressing Let-7 miRNA (Iliopoulos *et al.*, 2009).

ApoptomiRs including Let-7 are involved in most of carcinogenesis and apoptotic activities (Johnson *et al.*, 2007). Let-7 has also been shown to directly bind the 3'UTR of LIN28A/LIN28B and repress translation of the protein, and as these miRNAs is frequently under-expressed in malignant environment. Moreover, downregulation of let-7 promotes the expression of Bcl-xL, an anti-apoptotic gene; overexpression of Bcl-xL always induces apoptosis

resistance and reduces the sensitivity of tumor cells to drugs (Shimizu *et al.*, 2010). Lin28 is an RNA binding protein that blocks the biogenesis of let-7 by inducing terminal uridylation and degradation of let-7 precursors (Suzuki *et al.*, 2015). Collectively, over expression of LIN28 suppresses the mRNA levels of Let-7 family by induction of antiapoptotic protein Bcl-xL via intrinsic mitochondrial apoptosis pathway (Tian *et al.*, 2014).

The stem like cancer-initiating cells (SLCICs) are thought to be responsible for cancer initiation, drug resistance, recurrence and metastasis with multiple unique features which make them to be vital for tumor formation and self-renewal (Mongre *et al.*, 2015). Specific surface glycoprotein biomarkers for distinct phenotypes can be used to distinguish SLCICs from other tumor and normal stem cells. Therefore, methods to identify and targeting such cells will represent a significant advancement in cancer therapy. CD133 molecule (a trans-membrane protein Prominin 1) is a common and ubiquitous biomarker for endothelial progenitor cells, hematopoietic stem cells, glioblastoma, neuronal glial stem cells and different body organs. In addition, apart from CD133, 11 proteins have been proposed as potential differentiated biomarkers for SLCICs (Beier *et al.*, 2007). Moreover, during normal development, accumulation of let-7 can be prevented by LIN28, a promoter of pluripotency. Based on these findings, it seems that let-7 regulates ‘stemness’ by repressing self-renewal, promoting differentiation and stem like property in cancer.

The mitochondrion is the most important organelle concerned in the cellular bioenergetic and biosynthetic changes associated with cancer (Fulda *et al.*, 2010). These alterations contribute to the invasive and metastatic properties in most of typical tumors. There for mitochondria is considered as imperative target to induce apoptosis in cancer cells and numerous anticancer

drugs follows mitochondrial pathway to kill cancer cells which make their efficacy to stop cancer.

Chemopreventive potential of naturaceutical BRM270 as a zero footprint based approaches have opened a new avenue for the novel antineoplastic therapeutic strategies with no side effects in SLCICs induced carcinogenesis. BRM270 is a one of the promising anti-cancerous medicinal plant supercocktail extract. It's a well-known traditional Chinese medicine, which is used to treat a variety of diseases and cancers (Mongre *et al.*, 2016). Therefore, the current study was planned to know the efficacy of BRM270 to inhibit the tumorigenesis synergistically with Let-7. Further, the role of BRM270 in LIN-28 mediated activation of multi drug resistance (MDR) in mitochondrial dysfunction or stress mediated apoptosis pathway. There are meager works have been proposed the cellular consequence due to the targeted inactivation or expression of specific miRNA including Let-7 with phyto-drugs. Therefore, we hypothesized that alteration in the expression of Let-7 miRNAs could be achieved by treating cancer stem cells with “natural agents such as BRM270. To best of the author’s knowledge this is a one of the pioneer studies where efficacy of BRM270 as an anti-cancer natural drug that modulates Let-7 augmented mitochondrial intrinsic apoptosis pathway under *in-vitro* and *in-vivo* conditions has been studied.

2. MATERIALS AND METHODS

2. 1. *Cell lines and culture conditions*

The human cancer cell lines SaOS-2 Cal72 were purchased from ATCC (Manassas, VA). Cell lines were grown in DMEM supplemented with 10% of fetal bovine serum (FBS, Hyclone), 2 mmol/ liter glutamine, and 100 units/ml penicillin and streptomycin (complete medium). The cells were kept at 37 °C in a humidified 95% air, 5% CO₂ atmosphere incubator designated as culture at a steady-state condition.

2. 2. *Cell proliferation and colony formation assay*

Suspended cells (100µl) at a density of 4,000 cells/well were seeded in 96 - well plate (NuncTM, Wiesbaden, Germany). After 24 hours of recovery the cells were incubated in a humid atmosphere at 37°C and 5% CO₂ and treated with BRM270 and DOX. The cells were treated with varying concentrations of BRM270 (10µg-200µg) and DOX (10µM) separately. After 24 hours incubation, 25µL of PBS containing 2.5 mg/ml of MTT was added to each well. After 4 hours, the medium was discarded and 100 µL DMSO was added to dissolve the formazan crystals and then cells were incubated for 30 minutes at 37°C and 5% CO₂. The light absorbance was determined at 590 nm by the Model 680 microplate-reader (Bio-Rad, Berkeley, CA, USA).

2. 3. *Cell cycle distribution analysis*

The analysis of the cell cycle was performed by PI staining and analysis was carried out by flow cytometry using a fluorescence-activated cell sorting (FACS) caliber (Becton-Dickinson). Stem like cells treated with BRM270 (125µg) and DOX (10µM) for 24 hours then

the cells were harvested as 1×10^6 cells/ml. The cells were fixed with 70% ethanol and incubated at 4 °C overnight. The fixed cells were washed twice with cold PBS and incubated for 30 minutes with Ribonuclease A (#R-5125, Sigma, 10 µg/ml) and PI (10 µg/ml). Then, the cell samples were transferred to meshed blue capped tubes (BD Falcon™ Tubes #352235). Within 55 minutes the fluorescent signals were observed through the FL2 channel and the proportion of DNA content in the various checkpoints was analyzed using ModfitLT Version 3.0 (Verity Software House, Topsham, ME, USA).

2. 4. miRNA real-time reverse transcription-PCR

To verify the alterations in the expression of specific miRNAs Let-7, we chose representative miRNA (let-7b, let-7e) with varying expression profiles for real-time miRNA reverse transcription-PCR (RT-PCR) analysis using The Mir-X miRNA qRT-PCR SYBR® Kits (Clontech Laboratories, Inc.) following the manufacturer's protocol. Briefly, 5 ng of total RNA from each sample were subjected to reverse transcription with a specific miRNA miR-hsa-let-7a (forward primer, 5'-ACC AAG ACC GAC TGC CCT T-3' and reverse primer, 5'-CTCTGTCCACCGCAGATATT-3') and miR-hsa-let-7d (forward primer, 5'-GCCAAGTAGAAGACCAGCAAG-3') and reverse primer, 5'-CAA GGA AAC AGG TTA TCG GTG-3') were synthesized from COSMO GENETECH (Seoul, Korea). Real-time PCRs were then carried out in a total of 25µl reaction mixture. The PCR program was initiated by 10 minutes at 95°C before 40 thermal cycles, each at 15 s at 95°C and 1 minute at 60°C. Data were analyzed according to the comparative Ct method and normalized by RNU6B expression in each sample.

2. 5. Quantitative real-time polymerase chain reaction (qPCR)

The cells were detached by 0.05% trypsin-EDTA (Gibco) and total RNA was extracted by easy Blue (Intron Biotech, Seongnam-si, Gyeonggi-do, Korea). Purified RNA (1µg) was subjected to first strand cDNA synthesis using Superscript III first-strand cDNA synthesis kit and Oligo dT primer (Invitrogen). The cDNA was employed to qPCR for the quantification of the relative transcript levels of interested genes using the specific primers (Table 6.1.). β - actin opted as endogenous control.

Table 6.1. Nucleotide sequence used in quantitative real-time PCR

Gene	Sequence	T _m °C	Accession number
<i>β - actin</i>	F- GGACTTCGAGCAAGAGATGG R- AGCACTGTGTTGGCGTACAG	57.50	NM_001101
<i>NF-κB</i>	F- CTGAACCAGGGCATACTGT R- GAGAAGTCCATGTCCGCAAT	56.45	NM_001243984
<i>P⁵³</i>	F- GCCCCTCCTCAGCATCTTAT R-AAAGCTGTTCCGTCCCAGTA	56.45	NM_001126112
<i>PARP</i>	F- CCGCATACTCCATCCTCAGT R- GCTATCATCAGACCCTCCCC	61.0	XM_011538254
<i>Bcl-2</i>	F- TTCTTTGAGTTCGGTGGGGT R- TTCAGAGACAGCCAGGAGA	54.40	NM_000633
<i>Src</i>	F-TGGGTAGCAACAAGAGCAAGCCCA R- TAGAGGTTCTCCCCGGGCTGGTAC	55.45	NM_001291428
<i>LIN-28</i>	F- CGGCCAAAAGGAAAGAGCAT R- GGGTAGGGCTGTGGATTCT	56.45	NM_018947

2. 6. *Proteome Profiler*[™] *Human Apoptosis Array*

Proteome Profiler Human Apoptosis Arrays. To investigate the pathways by which BRM270 induces apoptosis, we performed a determination quantitative expression of apoptosis-related proteins using the Proteome Profiler[™] Human Apoptosis Array Kit (**R&D Systems**[™] **Human Apoptosis Array Kit (Catalog # ARY009, USA)**, according to the manufacturer's instructions. Briefly, the cells were treated with BRM270 and DOX. After 24 hours treatment of BRM270, total protein lysate extraction by RIPA lysis buffer then three hundred micrograms of protein from each sample were incubated with the human apoptosis array overnight. The apoptosis array data was quantified by scanning the membrane on a LAS4000 chemiluminescence detection machine (GE Healthcare) and analysis of the array image file was performed using image analysis software according to the manufacturer's instructions.

2. 7. *Detection of mitochondrial membrane potential ($\Delta\Psi_m$)*

Cells were initially seeded onto 35-mm dishes and allowed to grow to semiconfluence. The cells were then exposed with the addition of 100 μ g BRM270 or 10 μ M DOX as vehicle of equal volume as described previously (30, 37) to determine the state of mitochondrial membrane potential. JC-1 is a potentiometric dye that exhibits a membrane potential dependent loss as J-aggregates (polarized mitochondria) transition to JC-1 monomers (depolarized mitochondria), as indicated by a fluorescence emission shift from red to green intensity. Therefore, mitochondrial depolarization can be indicated by an increase in the green/red fluorescence intensity ratio. To stain the cells, monolayers were rinsed with DMEM without phenol red (Sigma-Aldrich). Cell monolayers were incubated with DMEM complete media and 5 μ g/ml JC-1 at 37°C for 30 min.

Cells were then rinsed two times with DMEM, and images were obtained using confocal fluorescence microscope set to excitation at 488 nm and detection at 510- to 525- (green) and 590-nm (red) channels using a dual band-pass filter. The JC-1 staining intensity was captured using a fluorescence microscope. Intensity of JC-1 is directly related to mitochondrial membrane potential. The percentage of JC-1 negative cells gives the percentage collapse of Mitochondria Membrane Permeability.

2. 8. Xenograft nude mice model and 2DG guided tumor imaging

5-week-old SPF/VAF immunodeficient nude mice were purchased from KS HI-TEC, Inc Korea. To induce A549 mediated tumorigenesis, A549 cells/ml concentrations of cells into lower right flanks of nude mouse by micro-needle syringe (29 gauge x 1/2" 12.7 mm needle, Ultra-Thin Plus™ Korea). After generation of 1x10⁶ successful tumor model CBS-1 (5 and 10mg/kg) and Doxorubicin (10mg/kg) treatment were provided up to 45 days. Then the animals sacrificed and the tumors were removed from all animals and weight.

For pre- and intraoperative tumor localization in real-time resection, we conducted *in vivo* tumor localization assay using IRDye® 800CW 2-DG (2-deoxy-D-glucose) optical probe which was purchased from LI-COR, Biosciences, USA. The probe was dissolved in phosphate buffer saline (1X PBS) and was injected into the tail vein of the tumor-bearing nude mice, then mice were observed after they were anesthetized with Zoletil 50 (Virbac, Carros, France) 1 ml/kg intraperitoneally and all surgical procedures were performed under general anesthesia at different time intervals. Metastasis were detected using optical molecular imaging, in particular near-infrared fluorescence (NIRF) range.

3. RESULTS

3.1. BRM270 inhibits colony forming efficiency of SLCICs by cells arrest at G2/M

The antitumor activity of BRM270 showed that it efficiently inhibits the tumorigenic colony formation after treatment with 125 $\mu\text{g/ml}$ (Figure 6.1A). In time lapse study also showed the significant inhibition of SLCICs cells in the treated group as compared to control (Figure 6.1C). Flowcytometric analysis showed that most of sub-populations from G1 have been transited to G2/M checkpoint, it means BRM270 significantly ($P > 0.05$) reduces the cell proliferation by arrest the cell division at G2/M (Figure 6.1C).

3.2. BRM270 activates apoptosis mediated programmed cell death

Apoptosis or programmed cell death is a key player to kill the SLCI cells. Interestingly, we showed in the Proteome microarray study, it showed that BRM270 treatment induced cellular stress and activated p53 tumor suppressor gene and enhanced the relative expression (pixel density) of apoptotic as Bad, Bax, Pro-caspase-3 by downregulating antiapoptotic proteins as Bcl-2, Survivin, XIAP, cIAP-1/2 etc (Figure 6.2A and B).

3.3. BRM270 augments mitochondrial stress and activates intrinsic apoptosis pathway

In order to mechanism action of BRM270 against SLCICs, it significantly induced the mitochondrial stress and reduces the mitochondrial membrane potential ($\Delta\Psi\text{m}$) to activate the intrinsic apoptosis pathway. Moreover, FACS study showed the after treatment with BRM270 more than 40% cells are under gone to higher to lower mitochondrial membrane potential as compared to non-treated control (Figure 6.3A and B). Apart from that we also showed that BRM270 significantly increase the ROS generations as compared to control cells.

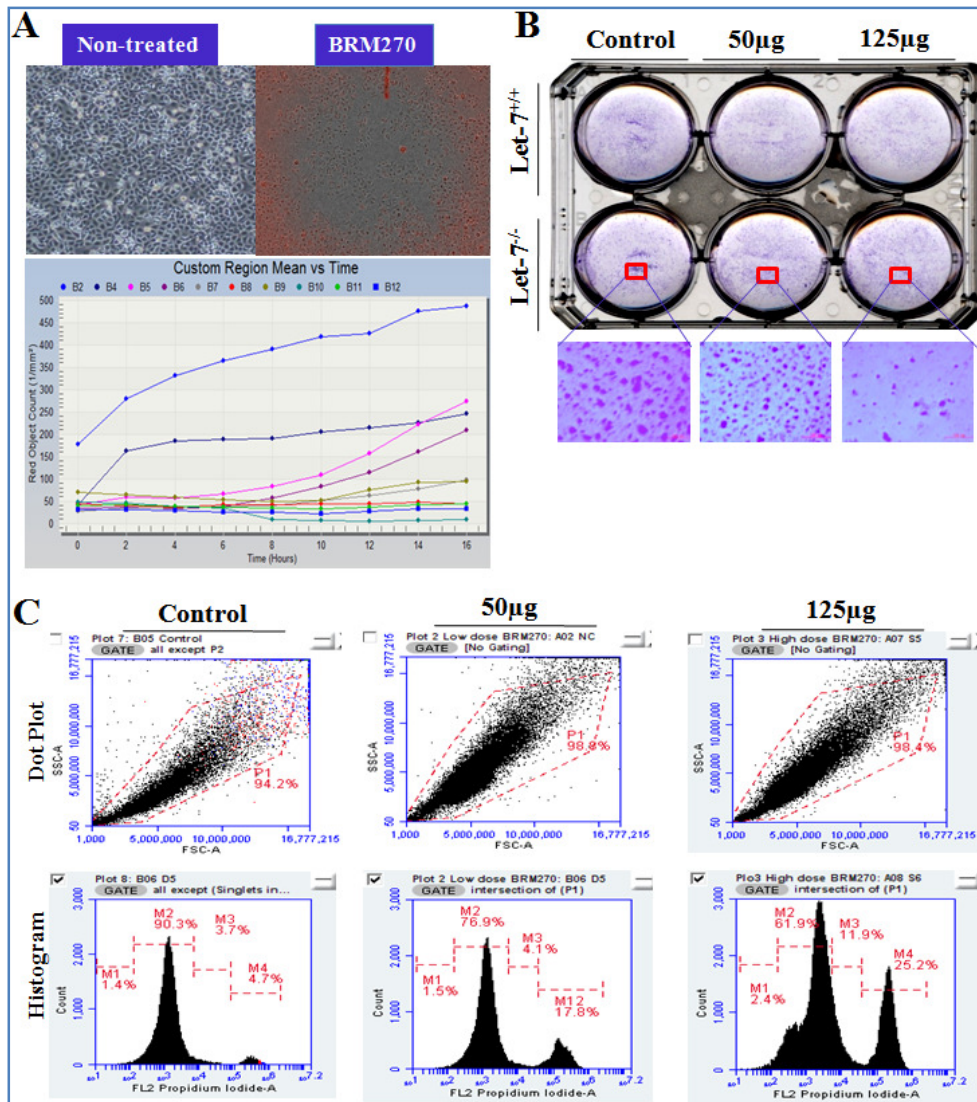


Figure 6.1. BRM270 inhibits proliferation and tumorigenic colony sphere forming capacity.

A. Time lapse study of BRM270 anticancer activity. **B.** Inhibition of colonogenic efficiency of SLCICs by BRM270. **C.** Cell cycle arrest by BRM270 in various cell cycle checkpoints.

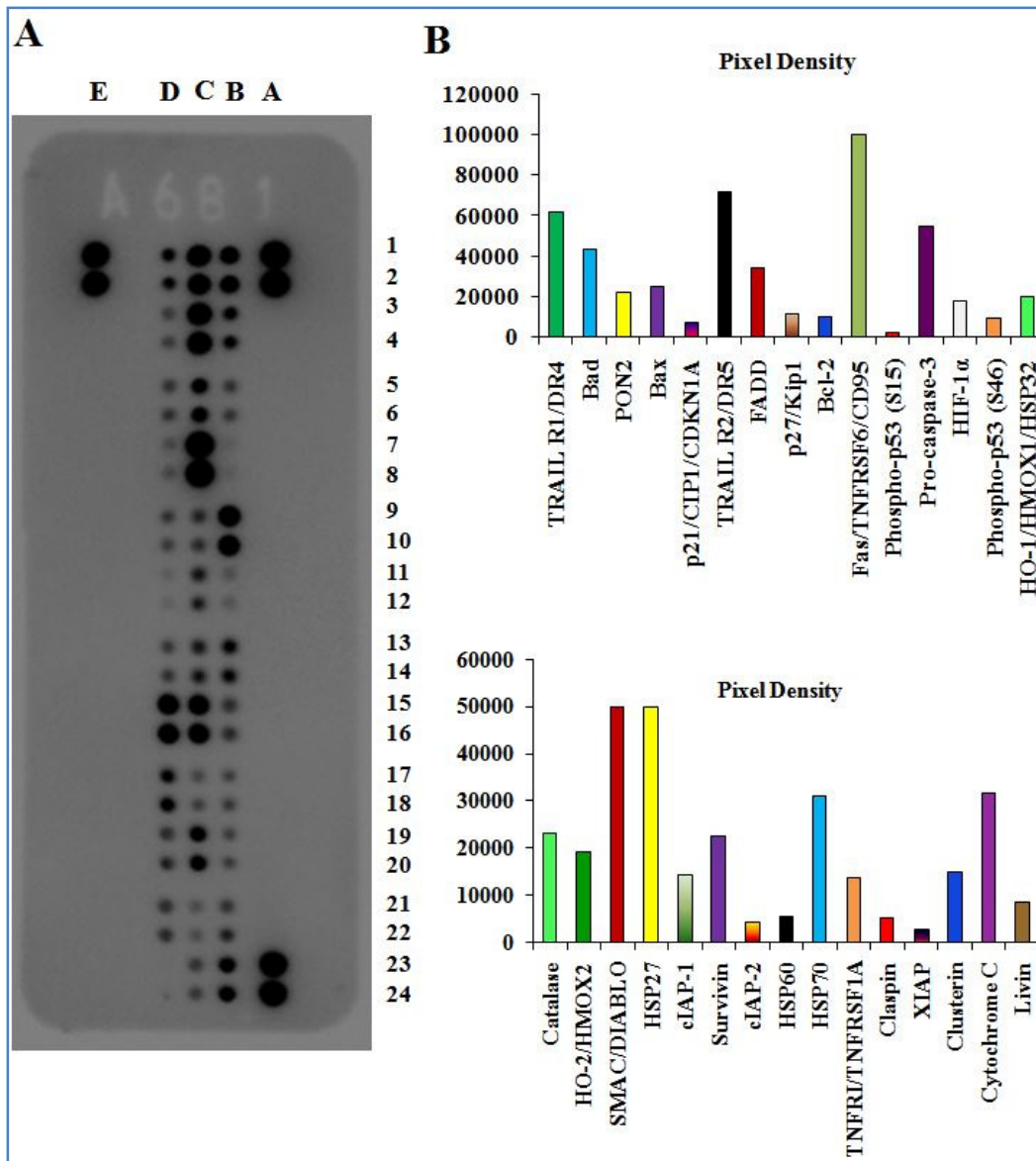


Figure 6.2. BRM270 induced apoptosis in Proteome Micro Array profiling. A. Human Osteosarcoma cancer Cal72 cells were treated with BRM270 (125 μ g/ml) or otherwise mentioned for 24 hours and cells were harvested for protein extraction and analyzed for the expression of apoptotic genes by utilizing proteome profiler apoptosis array or individual western blot analysis. B. Membrane intensity was acquired using chemiluminescence and pixel densities can be analyzed using ImageJ Analyzer software.

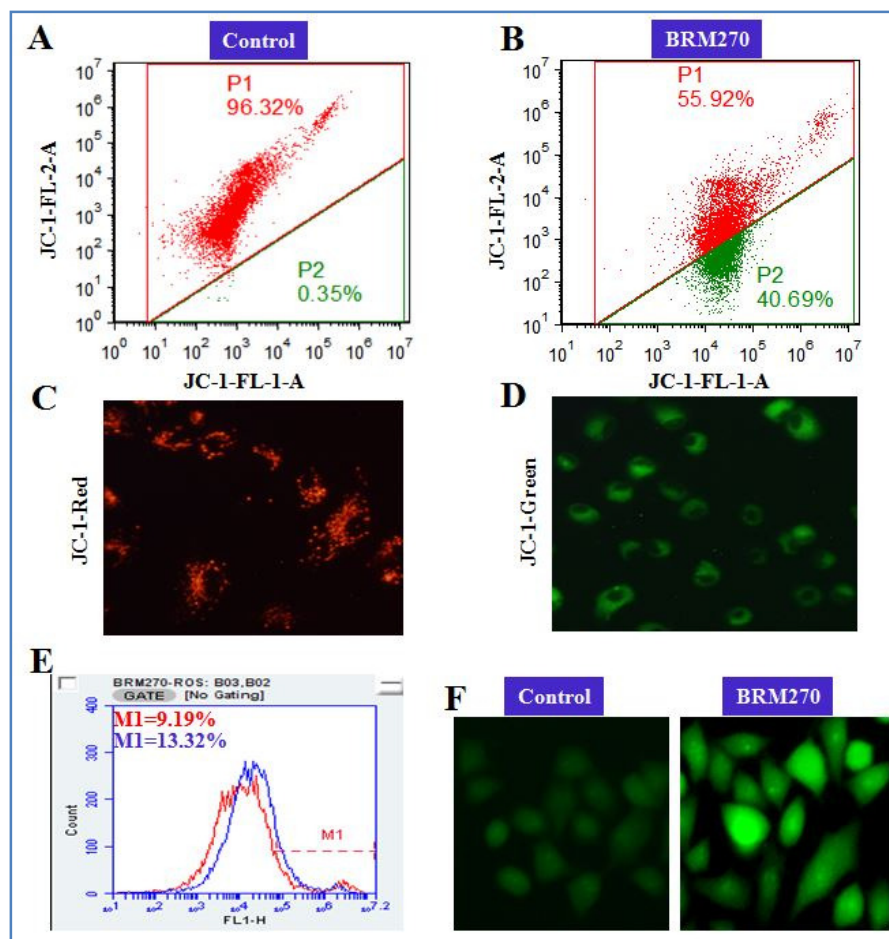


Figure 6.3. Antineoplastic efficacy of BRM270 by collapsing the mitochondrial membrane potential ($\Delta\Psi_m$) and inducing ROS generation in Cal72 cancer cells. A-D. Cal72 cells were treated with 125 μg BRM270 for 24 hours and then $\Delta\Psi_m$ was determined using JC-1 dye by flow cytometry. The JC-1 monomer was represented by green fluorescence, the JC-1 aggregate image was represented by red fluorescence, Scale bar = 100 mm. **E.** The intracellular ROS (O_2 and H_2O_2) levels were detected by flow cytometry using H2-DCFDA as fluorescent probes. Percent of cells calculated M1 gated total cell count for DCFDA positive ROS producing Cal72 cells. **F.** Intracellular ROS (O_2 and H_2O_2) levels were detected by confocal microscopy study. Values are means \pm S.E.M. for at least three independent experiments performed in triplicate (* $P < 0.05$ and ** $P < 0.01$ compared with Doxorubicin alone).

Similarly findings observed in microscopic study both $\Delta\Psi_m$ and ROS generation (Figure 6.3C-F). Although loss of $\Delta\Psi_m$ can affect the cellular proliferation efficiency by induction of apoptosis process. Interestingly, we observed that phyto-drugs BRM270 augmented intrinsic apoptosis activity by upregulation of antitumor p53 mRNA fold induction and the suppression of Bcl-2 (Figure 6.4A). In addition, transcriptomic analysis that is Heatmap demonstrated relative gene expression of PARP, NF- κ B and tumorigenic Src significantly higher than treated samples which have been analyzed using GeneEx software. It showed that BRM270 significantly downregulated the relative expression of apoptotic PARP, oncogenic NF- κ B and tumorigenic Src (Figure 6.4B).

3.4. BRM270 inhibits oncogenic LIN-28 by upregulation of Let-7 miRNA

Here we showed that BRM270 act as a suppressor of LIN-28. Simultaneously, downregulation of LIN-28 significantly upregulated the fold induction of Let-7a and Let-7d in both the Cal72 and SaOS-2 SLCICs (Figure 6.5A). Similarly, Cluster Heatmap of qPCR also showed that after treatment of BRM270 cancer cells significantly upregulated both Let-7a and Let-7d (Figure 6.5B).

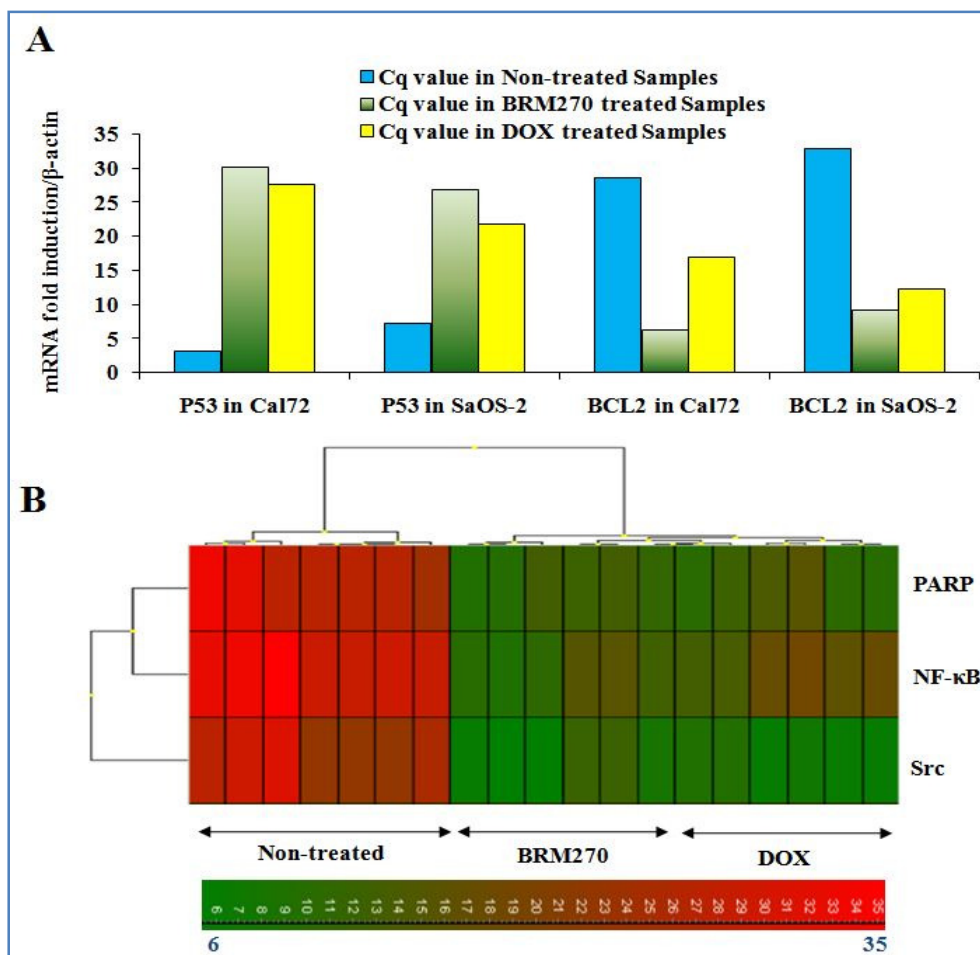


Figure 6.4. BRM270 enhanced p53 via suppression of anti-apoptotic Bcl-2. **A.** qPCR results showed significantly down regulation of Bcl-2 oncogene after treatment with BRM270 (125 μ g). Relative mRNA fold induction has been demonstrated while β - actin opted as endogenous control. **B.** Heatmap demonstrated relative gene expression of PARP, NF- κ B and tumorigenic Src. Data has been analysed using GeneEx software Ver.6.

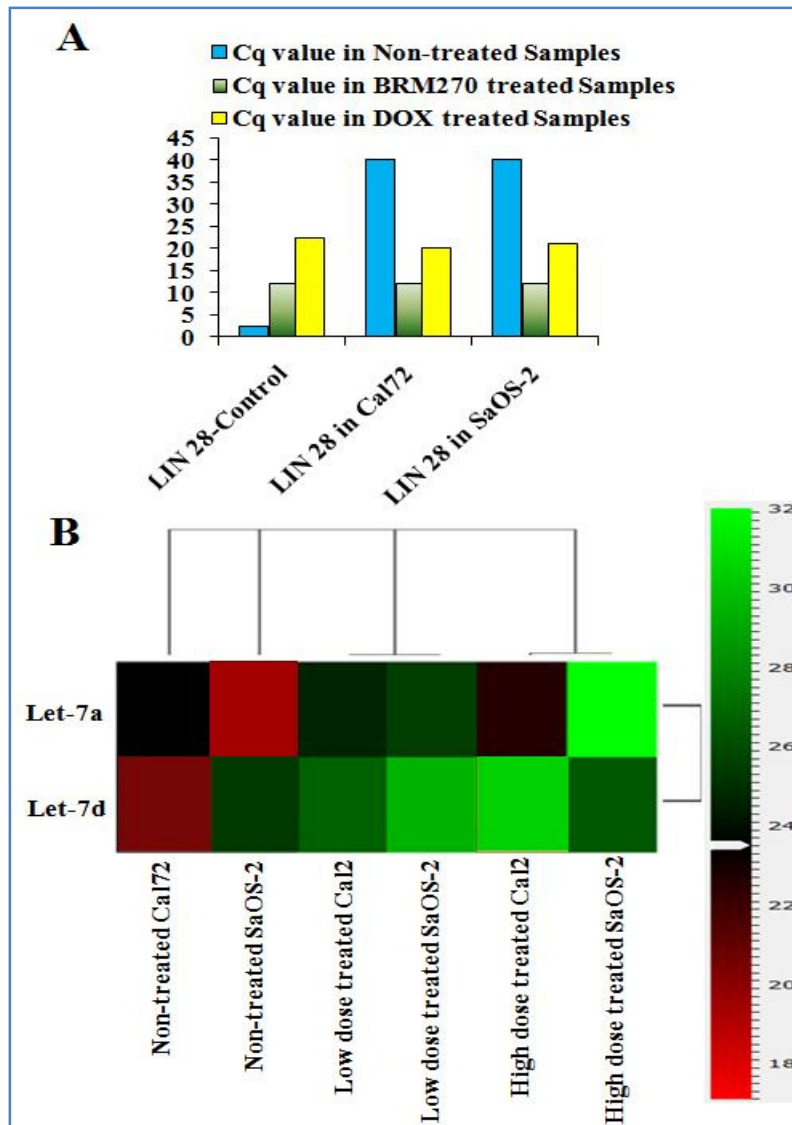


Figure 6.5. BRM270 downregulated LIN-28 by induction of Let-7. **A.** qPCR analysis showed the relative expression of LIN-28 in both treated and non-treated. **B.** Clustering Heat Map showing differentially expression of Let-7 in Cal72&SaOS-2 cancer cell line.

4. DISCUSSION AND CONCLUSION

The discovery and development of anticancer drugs, especially cytotoxic agents are a challenging task and differ drastically from the drug development process for any other diseases. Current therapy of cancer is suffering from numerous obstacles such as severe side effect, normal cell cytotoxicity as well as anticancer drug resistance. Therefore, discovery of novel phytochemical with Let-7 approaches which may provide better option to control cancer is always appreciable. In this regards, we have targeted to find the mechanism action of BRM270 in Let-7 modulated intrinsic apoptosis pathway and their extensive anticancer mechanism of action has been elucidated *in vitro*.

Hoechst 33342 staining and FACS studies revealed that BRM270 displayed excellent apoptosis in Cal72 cells (Mongre *et al.*, 2015). Spontaneous cell divisions of cancer cells are due to deregulation of cell cycle therefore inhibition of the cell cycle play an important role in treating proliferative diseases like cancer. Most of the anticancer drugs are disturb proliferation cycle of cancer cells by blocking cell cycle event led to activate checkpoints and induce apoptosis. Impact on cell cycle arresting has been assessed by FACS analysis and results showed that BRM270 arrest G2/M phase check point more efficiently as compared to DOX. In mechanistic studies, BRM270 down regulate Bcl-2 protein and up regulate Bax protein at transcriptional as well as translational level leading to deficit mitochondrial membrane potential ($\Delta\Psi_m$) and release cytochrome *C* in cytosol. Proteome microarray analysis indicates increase level of cytochrome *C* in cytosol as compared to mitochondria. This cascade changing produced by BRM270 indicative their mechanism to produced apoptosis through intrinsic pathway.

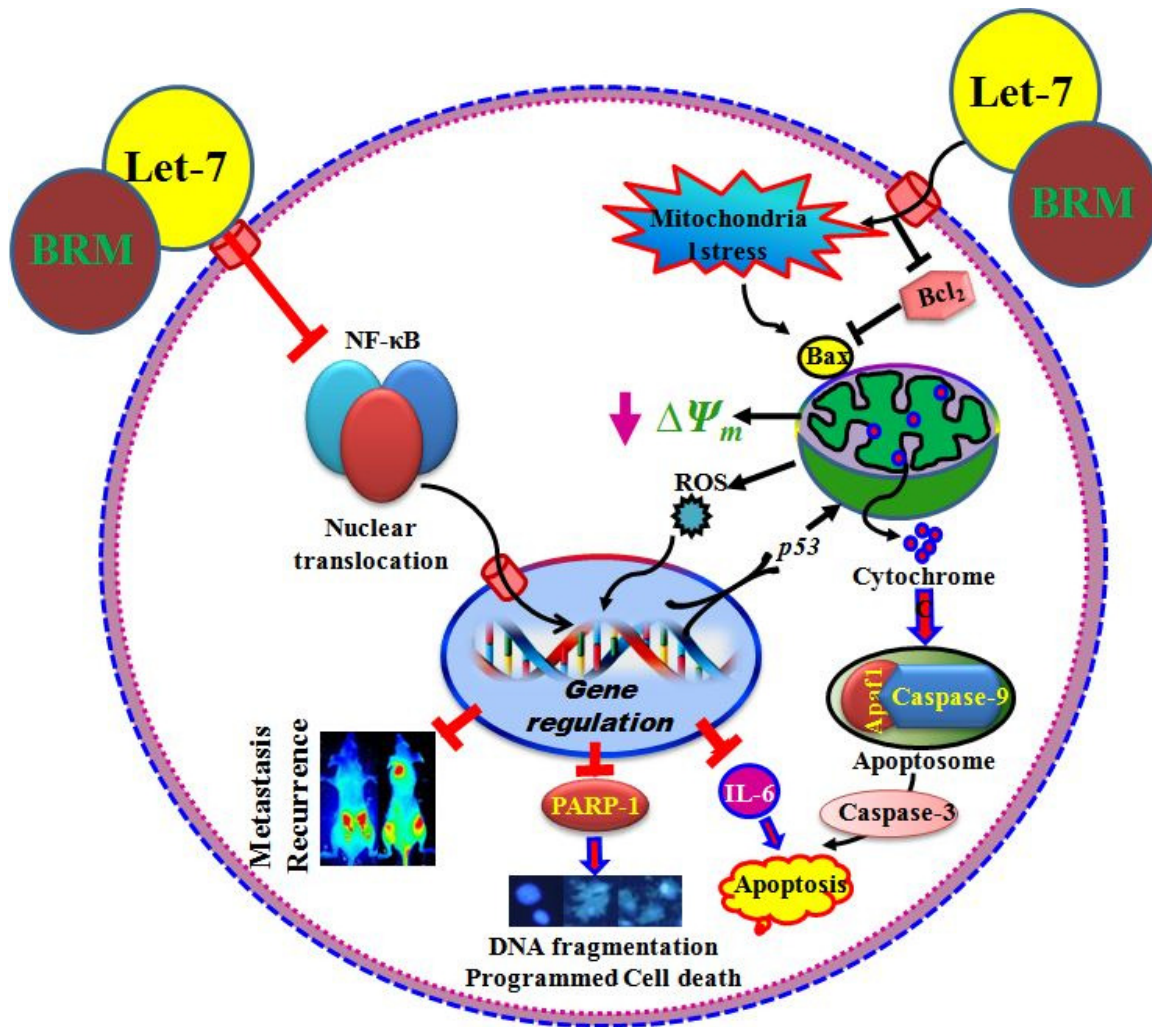


Figure 6.6. Proposed mechanism of action of BRM270 by which it produces anticancer efficacy via mitochondrial intrinsic apoptosis pathway.

BRM270 also significantly reduced mRNA level of PARP-1 as compared to untreated cells which is considered as hallmark of apoptosis. p53 serves as a controller of the apoptotic process and may modulate key control points of intrinsic pathways. p53 controls regulation of most of protein involve in apoptosis such as Bcl-2, Bax, cytochrome *C* migration and caspases. MCS-5 visibly increases p53 level at transcription as well as translational level in SLCI cells which may also warrant for activation of intrinsic pathway of apoptosis (Figure 6.6).

NF- κ B activation encourages cell proliferation and its suppression lead to stop proliferation. NF- κ B maintains the regulation of the Bcl-2 family proteins and maintains the mitochondrial integrity leads to provide suitability for the survivability of cancer cells. Hence, suppression of NF- κ B activity is helpful for induction of apoptosis and it is an important target to produce apoptosis in cancer cells. Our transcriptional and translational level of studies showed that BRM270 significantly down regulate NF- κ B and also down regulate cytokines IL-6 level which play important link between inflammation initiation and progression of oncogenesis.

ROS are a by-product of respiration and its levels are very high during cell apoptosis. Mitochondria are the major creator of ROS in mammalian cells, and its dysfunction increase high ROS level. ROS mediate mitochondrial outer membrane permeabilization which led to discharge of pro-apoptotic proteins including cytochrome *C* that begin apoptosis process through a cascade reaction. In this regards we have checked ability of BRM270 to induce ROS in SLCICs were studied. Investigation states that BRM270 remarkable induced ROS in Cal72 in dose dependent manner. Thus BRM270 triggered mitochondrial pathway of apoptosis by inducing ROS also. These extensive studies clearly indicate that BRM270 exerting apoptosis in Cal72 cells by activating mitochondrial pathway.

REFERENCES

- Akunuru S, James Zhai Q and Zheng Y: Non-small cell lung cancer stem/progenitor cells are enriched in multiple distinct phenotypic subpopulations and exhibit plasticity. *Cell Death Dis.* 3: e352, 2012.
- American Cancer Society (ACS). Side effects of targeted cancer therapy drugs. Accessed on 28, June, 2016.
- Arcaro A, Guerreiro AS. The phosphoinositide 3- kinase pathway in human cancer: genetic alterations and therapeutic implications. *Curr Genomics.* 8(5):271-306,2007.
- Auyeung KK, Ko JK. Novel herbal flavonoids promote apoptosis but differentially induce cell cycle arrest in human colon cancer cells. *Invest New Drugs.* 28(1):1-13, 2010.
- Beier D, Hau P, Proescholdt M, Lohmeier A, Wischhusen J, et al. CD133 (+) and CD133 (-) glioblastoma-derived cancer cells show differential growth characteristics and molecular profiles. *Cancer Res.* 1:67(9):4010-4015, 2007.
- Bertolini G, Roz L, Perego P, Tortoreto M, Fontanella E, et al., Highly tumorigenic lung cancer CD133+ cells display stem-like features and are spared by cisplatin treatment. *Proc Natl Acad Sci U S A* 106(38): 16281-16286, 2009.
- Bhatt AN, Mathur R, Farooque A, Verma A and Dwarakanath BS. Cancer biomarkers - Current perspectives. *Indian J Med Res* 132 :129-149, 2010.
- Blank M, Lerenthal Y, Mittelman L and Shiloh Y: Condensin I recruitment and uneven chromatin condensation precede mitotic cell death in response to DNA damage. *J Cell Biol.* 174(2): 195-206, 2006.
- Bolignano D, Donato V, Lacquaniti A, Fazio MR, Bono C, Coppolino G, et al: Neutrophil gelatinase-associated lipocalin (NGAL) in human neoplasias: a new protein enters the scene. *Cancer Lett.* 288: 10-16, 2010.

- Buss H, Handschick K, Jurrmann N, Pekkonen P, Beuerlein K, et al., Cyclin-dependent kinase 6 phosphorylates NF- κ B P65 at serine 536 and contributes to the regulation of inflammatory gene expression. *PLoS One*. 7(12): 1-13, 2012.
- Calin GA, Croce CM. MicroRNA signatures in human cancers. *Nat Rev Cancer*. 6(11):857-66, 2006.
- Cancer Research UK 2014; http://publications.cancerresearchuk.org/downloads/Product/CS_REPORT_WORLD.pdf
- Cancer statistics. Annual report 2012. Online document at <https://www.ncc.re.kr> Accessed September 19, 2015.
- Candido S, Maestro R, Polesel J, Catania A, Maira F, Signorelli SS, et al: Roles of neutrophil gelatinase-associated lipocalin (NGAL) in human cancer. *Oncotarget*. 5: 1576-1594, 2014.
- Cao Z, Lin W, Huang Z, Chen X, Zhao J, et al.: Ethyl acetate extraction from a Chinese herbal formula, JieduXiaozheng Yin, inhibits the proliferation of hepatocellular carcinoma cells via induction of G0/G1 phase arrest *in vivo* and *in vitro*. *Int J Oncol* 42, 202-210, 2013.
- Cao Z, Lin W, Huang Z, Chen X, Zhao J, et al.: JieduXiaozheng Yin, a Chinese herbal formula, inhibits tumor angiogenesis via downregulation of VEGF-A and VEGFR-2 expression *in vivo* and *in vitro*. *Oncol Rep* 29, 1080-1086, 2013.
- Casas E, Kim J, Bendesky A, Ohno-Machado L, Wolfe CJ and Yang J. Snail2 is an essential mediator of Twist1-induced epithelial mesenchymal transition and metastasis. *Cancer Res*. 71: 245-254, 2011.
- Castedo M, Perfettini JL, Roumier T, Andreau K, Medema R, et al: Cell death by mitotic catastrophe: a molecular definition. *Oncogene*. 23(16): 2825-2837, 2004.
- Castedo M, Perfettini JL, Roumier T, Valent A, Raslova H, et al., Mitotic catastrophe constitutes a special case of apoptosis whose suppression entails aneuploidy. *Oncogene*. 23(25): 4362-4370, 2004.

- Castellano E, Downward J. RAS Interaction with PI3K: More Than Just Another Effector Pathway. *Genes Cancer*. 2(3): 261-274, 2011.
- Chanchevalap S, Nandan MO, McConnell BB, Charrier L, Merlin D, et al., Kruppel-like factor 5 is an important mediator for lipopolysaccharide-induced proinflammatory response in intestinal epithelial cells. *Nucleic Acids Res*. 34(4): 1216-1223, 2006.
- Chang HY and Yang X: Proteases for Cell Suicide: Functions and Regulation of Caspases. *Microbiol Mol Biol Rev*. 64, 821-846, 2000.
- Chen D, Dou QP. The ubiquitin-proteasome system as a prospective molecular target for cancer treatment and prevention. *Curr Protein Pept Sci*. 11(6):459-70, 2010.
- Chen D, Frezza M, Schmitt S, Kanwar J, Dou QP. Bortezomib as the first proteasome inhibitor anticancer drug: current status and future perspectives. *Curr Cancer Drug Targets*. 11(3):239-53, 2011.
- Chen F, Castranova V, and Shi X. New Insights into the Role of Nuclear Factor- κ B in Cell Growth Regulation. *Am J Pathol*. 159(2): 387-397, 2001.
- Chen F: JNK-induced apoptosis, compensatory growth and cancer stem cells. *Cancer Res* 72, 379-386, 2012.
- Chen K, Huang YH and Chen JL. Understanding and targeting cancer stem cells: therapeutic implications and challenges. *Acta Pharmacol Sin*. 34(6): 732-740, 2013.
- Chen SS, Michael A and Butler-Manuel SA: Advances in the treatment of ovarian cancer: a potential role of antiinflammatory phytochemicals. *Discov Med*. 13: 7-17, 2012.
- Chen YR, Wang W, Kong AN and Tan TH: Molecular mechanisms of c-Jun N-terminal kinase-mediated apoptosis induced by anticarcinogenic isothiocyanates. *J Biol Chem*. 273, 1769-1775, 1998.
- Chinese Pharmacopoeia Commission (CPC). Pharmacopoeia of the People's Republic of China. Chinese Medical Science and Technology Press, Beijing, p263, 2010.

- Choi M, Kim W, Cheon MG, Lee CW and Kim JE: Polo-like kinase 1 inhibitor BI2536 causes mitotic catastrophe following activation of the spindle assembly checkpoint in non-small cell lung cancer cells. *Cancer Lett.* 357: 591-601, 2015.
- Chow AK, Ng L, Lam CS, Wong SK, Wan TM, et al.: The enhanced metastatic potential of hepatocellular carcinoma cells with sorafenib resistance. *PLoS One.* 8, e78675, 2013.
- Cragg GM and Pezzuto JM. Natural Products as a Vital Source for the Discovery of Cancer Chemotherapeutic and Chemopreventive Agents. *Med Princ Pract.* 1-19, 2015.
- Croce CM, Calin GA. miRNAs, cancer, and stem cell division. *Cell.* 122(1):6-7, 2005.
- de Moor JS, Mariotto AB, Parry C, Alfano CM, Padgett L, et al., Cancer Survivors in the United States: Prevalence across the Survivorship Trajectory and Implications for Care. *Cancer Epidemiol Biomarkers Prev.* 22(4): 561-570, 2013.
- De Simone V, Franzè E, Ronchetti G, Colantoni A, Fantini MC, et al., Th17-type cytokines, IL-6 and TNF- α synergistically activate STAT3 and NF- κ B to promote colorectal cancer cell growth. *Oncogene.* doi: 10.1038/onc.2014.286, 2014.
- Dean M, Fojo T and Bates S. Tumour stem cells and drug resistance. *Nat Rev Cancer.* 5(4): 275-84, 2005.
- Delbridge AR, Strasser A. The BCL-2 protein family, BH3-mimetics and cancer therapy. *Cell Death Differ.* 22(7):1071-1080, 2015.
- Demetrius LA, Coy JF, Tuszynski JA. Cancer proliferation and therapy: the Warburg effect and quantum metabolism. *Theor Biol Med Model.* 7:2: 2-18, 2010.
- DeVita VT Jr, Chu E. A history of cancer chemotherapy. *Cancer Res.* 68(21):8643-53, 2008.
- Dini L, Coppola S, Ruzittu MT and Ghibelli L. Multiple pathways for apoptotic nuclear fragmentation. *Exp Cell Res.* 223(2): 340-347, 1996.
- Dou J and Gu N. Biomarkers of Cancer Stem Cells. *Advances in Cancer Stem Cell Biology.* pp 45-67, 2012.

- Dou J and Gu N: Biomarkers of Cancer Stem Cells. *Advances in Cancer Stem Cell Biology* pp 45-67, 2012.
- Eldredge-Hindy HB, Rosenberg AL, Simone NL. Intraoperative radiotherapy for breast cancer: the lasting effects of a fleeting treatment. *Int J Breast Cancer*. 2014;214325, 2014.
- Elmore S. Apoptosis: A Review of Programmed Cell Death, *Toxicol Pathol*. 35(4): 495-516, 2007.
- Elmore S: Apoptosis: a review of programmed cell death. *Toxicol Pathol* 35, 495-516, 2007.
- El-Serag HB. Hepatocellular Carcinoma. *N Engl J Med* 365, 1118-1127, 2011.
- Fan XM, Wong BC, Wang WP, Zhou XM, Cho CH, Yuen ST, et al., Inhibition of proteasome function induced apoptosis in gastric cancer. *Int J Cancer*. 93(4):481-488, 2001.
- Ferlay J, Shin HR, Bray F, Forman D, Mathers C, Parkin DM. Estimates of worldwide burden of cancer in 2008: GLOBOCAN 2008. *International Journal of Cancer*. 127(12): 2893-2917, 2010.
- Fridman JS, Lowe SW. Control of apoptosis by p53. *Oncogene*. 22(56): 9030-9040, 2003.
- Fulda S, Debatin KM. Extrinsic versus intrinsic apoptosis pathways in anticancer chemotherapy. *Oncogene*. 25(34): 4798-4811, 2006.
- Fulda S, Galluzzi L, Kroemer G. Targeting mitochondria for cancer therapy. *Nat Rev Drug Discov*. 9(6):447-464, 2010.
- Gascoigne KE, Taylor SS. How do anti-mitotic drugs kill cancer cells? *J Cell Sci*. 122(Pt 15): 2579-85, 2009.
- Ghobrial IM, Witzig TE, Adjei AA. Targeting apoptosis pathways in cancer therapy. *CA Cancer J Clin*. 55(3): 178-94, 2005.
- Gogvadze V, Orrenius S, Zhivotovsky B. Multiple pathways of cytochrome c release from mitochondria in apoptosis. *Biochim Biophys Acta*. 1757(5-6):639-647, 2006.

- Grabacka MM, Gawin M, Pierzchalska M. Phytochemical modulators of mitochondria: the search for chemopreventive agents and supportivetherapeutics. *Pharmaceuticals (Basel)*. 7(9):913-42, 2014.
- Grimm S, Bauer MK, Baeuerle PA, Schulze-Osthoff K. Bcl-2 down-regulates the activity of transcription factor NF-kappaB induced upon apoptosis. *J Cell Biol*. 134(1):13-23, 1996.
- Gullett NP, Ruhul Amin AR, Bayraktar S, Pezzuto JM, Shin DM, et al., Cancer prevention with natural compounds. *Semin Oncol*. 37(3):258-81, 2010.
- Hahn WC and Weinberg RA: Modelling the molecular circuitry of cancer. *Nat Rev Cancer*. 2: 331-341, 2002.
- Handschiek K, Beuerlein K, Jurida L, Bartkuhn M, Müller H, et al., Cyclin-dependent kinase 6 is a chromatin-bound cofactor for NF-κB-dependent gene expression. *Mol Cell*. 53(2): 193-208, 2014.
- Haupt S, Berger M, Goldberg Z, Haupt Y. Apoptosis - the p53 network. *J Cell Sci*. 116(20): 4077-4085, 2003.
- Hennessy EJ, Sheedy FJ, Santamaria D, Barbacid M and O'Neill LA: Toll-like receptor-4 (TLR4) down-regulates microRNA-107, increasing macrophage adhesion via cyclin-dependent kinase 6. *J Biol Chem*. 286(29): 25531-25539, 2011.
- Hoesel B, Schmid JA. The complexity of NF-κB signaling in inflammation and cancer. *Mol Cancer*. 2: 12-86, 2013.
- Holohan C, Van Schaeybroeck S, Longley DB, Johnston PG. Cancer drug resistance: an evolving paradigm. *Nat Rev Cancer*. 2013 Oct;13(10):714-26.
- Horn PA, Tesch H, Staib P, Kube D, Diehl V et al., Expression of AC133, a novel hematopoietic precursor antigen, on acute myeloid leukemia cells. *Blood*. 93(4): 1435-1437, 1999.
- Hortobágyi GN. Anthracyclines in the treatment of cancer. An overview. *Drugs*. 54(4):1-7, 1997.

- Hou Y, Zou Q, Ge R, Shen F and Wang Y: The critical role of CD133⁽⁺⁾ CD44^(+/high) tumor cells in hematogenous metastasis of liver cancers. *Cell Res* 22, 259-272, 2012.
- Huber MA, Azoitei N, Baumann B, Grünert S, Sommer A, Pehamberger H, *et al*: NF-kappaB is essential for epithelial-mesenchymal transition and metastasis in a model of breast cancer progression. *J Clin Invest* 114: 569-581, 2004.
- Hwang YJ, Lee EJ, Kim HR and Hwang KA. In vitro antioxidant and anticancer effects of solvent fractions from *Prunella vulgaris* var. *lilacina*. *BMC Complement Altern Med* 13, 310, 2013.
- Iannetti A, Pacifico F, Acquaviva R, Lavorgna A, Crescenzi E, Vascotto C, *et al*: The neutrophil gelatinase-associated lipocalin (NGAL), a NF-κB-regulated gene, is a survival factor for thyroid neoplastic cells. *Proc Natl Acad Sci U S A* 105: 14058-14063, 2008.
- Iliopoulos D, Hirsch HA and Struhl K: An epigenetic switch involving NF-kappaB, Lin28, Let-7 MicroRNA, and IL6 links inflammation to cell transformation. *Cell* 139(4): 693-706, 2009.
- Johnson CD, Esquela-Kerscher A, Stefani G, Byrom M, Kelnar K, *et al*. The let-7 microRNA represses cell proliferation pathways in human cells. *Cancer Res.* 67(16):7713-22, 2007.
- Joo M, Kang YK, Kim MR, Lee HK and Jang JJ: Cyclin D1 overexpression in hepatocellular carcinoma. *Liver* 21(2), 89-95, 2001.
- Jordan CT, Guzman ML and Noble M: Cancer stem cells. *N Engl J Med* 355: 1253-1261, 2006.
- Kalimuthu S, Se-Kwon K. Cell survival and apoptosis signaling as therapeutic target for cancer. Marine bioactive compounds. *Int J Mol Sci.* 14(2):2334-2354, 2013.
- Kallenberger SM, Beaudouin J, Claus J, Fischer C, Sorger PK, *et al*., Intra- and interdimeric Casp-8 self-cleavage controls strength and timing of CD95-induced apoptosis. *Sci Signal.* 7(316): ra23. doi: 10.1126/scisignal.2004738. 2014.

- Karin M. Nuclear factor-kappaB in cancer development and progression. *Nature*. 441(7092): 431-436, 2006.
- Kathiravan MK, Khilare MM, Nikoomanesh K, Chothe AS, Jain KS. Topoisomerase as target for antibacterial and anticancer drug discovery. *J Enzyme Inhib Med Chem*. 28(3):419-35, 2013.
- Kaur S, Sharma N, Krishn SR, Lakshmanan I, Rachagani S, Baine MJ, *et al*: MUC4-mediated regulation of acute phase protein lipocalin-2 through HER2/AKT/NF-κB signaling in pancreatic cancer. *Clin Cancer Res*. 20: 688-700, 2014.
- Kerr JF, Wyllie AH and Currie AR: Apoptosis: a basic biological phenomenon with wide-ranging implications in tissue kinetics. *Br J Cancer*. 26(4): 239-257, 1972.
- Khan Z, Shervington A, Munje C and Shervington L. The complexity of identifying cancer stem cell biomarkers. *Cancer Invest*. 31(6): 404-411, 2013.
- Kitamura H, Okudela K, Yazawa T, Sato H and Shimoyamada H: Cancer stem cell: implications in cancer biology and therapy with special reference to lung cancer. *Lung Cancer*. 66: 275-281, 2009.
- Kitanaka C, Sato A and Okada M: JNK Signaling in the Control of the Tumor-Initiating Capacity Associated with Cancer Stem Cells. *Genes Cancer* 4, 388-396, 2013.
- Kovar JL, Volcheck W, Sevick-Muraca E, Simpson MA and Olive DM: Characterization and performance of a near-infrared 2-deoxyglucose optical imaging agent for mouse cancer models. *Anal Biochem*. 384: 254-262, 2009.
- Kowalczyk E, Krzesiński P, Kura M, Niedworok J, Kowalski J, *et al.*, Pharmacological effects of flavonoids from *Scutellaria baicalensis*. *Przegl Lek* 63(2): 95-6. 2006.
- Kowalczyk E, Krzesiński P, Kura M, Niedworok J, Kowalski J, *et al.*: Pharmacological effects of flavonoids from *Scutellaria baicalensis*. *Przegl Lek* 63, 95-96, 2006.

- Krysan K, Cui X, Gardner BK, Reckamp KL, Wang X, Hong L, *et al*: Elevated neutrophil gelatinase-associated lipocalin2 contributes to erlotinib resistance in non-small cell lungcancer. *Am J Transl Res.* 5: 481-496, 2013.
- Lee AY, Han YA, Kim JE, Hong SH, Park EJ, *et al.*: Saururus chinensis Baill induces apoptosis through endoplasmic reticulum stress in HepG2 hepatocellular carcinoma cells. *Food Chem Toxicol* 83, 183-92, 2015.
- Lee JJ, Kim HJ, Yang CS, Kyeong HH, Choi JM, *et al.*, A high-affinity protein binder that blocks the IL6/STAT3 signaling pathway effectively suppresses non-small cell lung cancer. *Mol Ther.* 22(7): 1254-1265, 2014.
- Leung L, Radulovich N, Zhu CQ, Organ S, Bandarchi B, Pintilie M, *et al*: Lipocalin-2 promotes invasion, tumorigenicity and gemcitabine resistance in pancreatic ductal adenocarcinoma. *PLoS One.* 7: 1-10, 2012.
- Levêque D. Use of body weight and body surface area in dosing of anticancer agents in adult patients. *Bull Cancer.* 94(7): 647-51, 2007.
- Li CW, Xia W, Huo L, Lim SO, Wu Y, Hsu JL, *et al*: Epithelial-mesenchymal transition induced by TNF- α requires NF- κ B-mediated transcriptional upregulation of Twist1. *Cancer Res.* 72: 1290-1300, 2012.
- Li PF, Dietz R, von Harsdorf R. p53 regulates mitochondrial membrane potential through reactive oxygen species and induces cytochrome c-independent apoptosis blocked by Bcl-2. *EMBO J.* 18(21):6027-6036, 1999.
- Lin CW, Tseng SW, Yang SF, Ko CP, Lin CH, Wei LH, *et al*: Role of Lipocalin2 and its complex with matrix metalloproteinase-9 in oral cancer. *Oral Dis.* 18: 734-740, 2012.
- Liu JM, Long XH, Zhang GM, Zhou Y, Chen XY *et al.*, Let-7g reverses malignant phenotype of osteosarcoma cells by targeting Aurora-B. *Int J Clin Exp Pathol.* 7(8):4596-606, 2014.

- Lu J, Getz G, Miska EA, Alvarez-Saavedra E, Lamb J, et al., MicroRNA expression profiles classify human cancers. *Nature*. 435(7043):834-8, 2005.
- Lu L, Kanwar J, Schmitt S, Cui QC, Zhang C, Zhao C, Dou QP. Inhibition of tumor cellular proteasome activity by triptolide extracted from the Chinese medicinal plant 'thunder god vine'. *Anticancer Res*. 31(1): 1-10, 2011.
- Luk SC, Siu SW, Lai CK, Wu YJ and Pang SF: Cell Cycle Arrest by a Natural Product via G2/M Checkpoint. *Int J Med Sci*. 2(2): 64-69, 2005.
- Mannelqvist M, Stefansson IM, Wik E, Kusonmano K, Raeder MB, Øyan AM, et al: Lipocalin-2 expression is associated with aggressive features of endometrial cancer. *BMC Cancer*. 12: 1-7, 2012.
- Mantena SK, Sharma SD and Katiyar SK: Berberine, a natural product, induces G1-phase cell cycle arrest and caspase-3-dependent apoptosis in human prostate carcinoma cells. *Mol Cancer Ther*. 5: 296-308, 2006.
- McFarland BC, Hong SW, Rajbhandari R, Twitty GB Jr, Gray GK, et al., NF- κ B-induced IL-6 ensures STAT3 activation and tumor aggressiveness in glioblastoma. *PLoS One*. 8(11): doi: 10.1371/journal.pone.0078728, 2013.
- McMillan SC. Carcinogenesis. *Semin Oncol Nurs*. 8(1):10-9, 1992.
- Mizrak D, Brittan M and Alison M. CD133 molecule of the moment. *J Pathol*. 214(1):3-9, 2008.
- Mizrak D, Brittan M and Alison M: CD133 molecule of the moment. *J Pathol*. 214(1):3-9, 2008.
- Molina JR, Yang P, Cassivi SD, Schild SE, Adjei AA. Non-Small Cell Lung Cancer: Epidemiology, Risk Factors, Treatment, and Survivorship. *Mayo Clin Proc*. 83(5): 584-594, 2008.
- Mongre RK, Sodhi SS, Sharma N, Ghosh M, Kim JH, et al.: Epigenetic induction of epithelial to mesenchymal transition by LCN2 mediates metastasis and tumorigenesis, which is abrogated by NF- κ B inhibitor BRM270 in a xenograft model of lung adenocarcinoma. *Int J Oncol* 48, 84-98, 2016.

- Mongre RK, Sodhi SS, Ghosh M, Kim JH, Kim N. The novel inhibitor BRM270 downregulates tumorigenesis by suppression of NF- κ B signaling cascade in MDR-induced stem like cancer-initiating cells. *Int J Oncol*. 46(6):2573-85, 2015.
- Nagai T, Arao T, Matsumoto K, Sakai K, Kudo K, Kaneda H, *et al*: Impact of TJP-1 and TWIST expression on post-operative prognosis in hepatocellular carcinoma, Proceedings of the 103rd Annual Meeting of the AACR. *Cancer Res*. 72: Abstract no: 3406, 2012.
- Nakamura I, Hama S, Itakura S, Takasaki I, Nishi T, Tabuchi Y, *et al*: Lipocalin-2 as a plasma marker for tumors with hypoxic regions. *Nature Sci Rep*. 4: 1-8, 2014.
- NIH 2007, Understanding Cancer, <http://www.ncbi.nlm.nih.gov/books/NBK20362/#A318>.
- Lodish H, Berk A, Zipursky SL, *et al*. Molecular Cell Biology. 4th edition. New York: W. H. Freeman; 2000.
- Nikoletopoulou V, Markaki M, Palikaras K, Tavernarakis N. Crosstalk between apoptosis, necrosis and autophagy. *Biochim Biophys Acta*. 1833(12):3448-3459, 2013.
- Nitiss JL. Targeting DNA topoisomerase II in cancer chemotherapy. *Nat Rev Cancer*. 9(5):338-50, 2009.
- Pal D, Sur S, Mandal S, Das A, Roy A, *et al*.: Prevention of liver carcinogenesis by amarogentin through modulation of G1/S cell cycle check point and induction of apoptosis. *Carcinogenesis* 33, 2424-2431, 2012.
- Panieri E, Santoro MM. ROS homeostasis and metabolism: a dangerous liason in cancer cells. *Cell Death Dis*. 7(6):e2253, 2016.
- Park CY, Tseng D and Weissman IL. Cancer stem cell-directed therapies: recent data from the laboratory and clinic. *Mol Ther* 17, 219-230, 2009.
- Parrish AB, Freel CD, Kornbluth S. Cellular mechanisms controlling caspase activation and function. *Cold Spring Harb Perspect Biol*. 5(6): pii: a008672, 2013.

- Peickert S, Waurig J, Dittfeld C, Dietrich A, Garbe Y, et al., Rapid re-expression of CD133 protein in colorectal cancer cell lines *in-vitro* and *in-vivo*. *Lab Invest.* 92(11): 1607-1622, 2012.
- Peter ME, Krammer PH. The CD95(APO-1/Fas) DISC and beyond. *Cell Death Differ.* 10(1): 26-35, 2003.
- Pommier Y, Leo E, Zhang H, Marchand C. DNA topoisomerases and their poisoning by anticancer and antibacterial drugs. *Chem Biol.* 17(5):421-33, 2010.
- Pommier Y. Topoisomerase I inhibitors: camptothecins and beyond. *Nat Rev Cancer.* 6(10): 789-802, 2006.
- Prince ME, Sivanandan R, Kaczorowski A, Wolf GT, Kaplan MJ, Dalerba P, Weissman IL, Clarke MF and Ailles LE: Identification of a subpopulation of cells with cancer stem cell properties in head and neck squamous cell carcinoma. *Proc Natl Acad Sci U S A.* 104(3): 973-978, 2007.
- Reimer RR, Hoover R, Fraumeni JF Jr, Young RC. Acute leukemia after alkylating agent therapy of ovarian cancer. *N Engl J Med.* 297(4): 177-81, 1977.
- Ricci MS, Zong WX. Chemotherapeutic approaches for targeting cell death pathways. *Oncologist.* (4):342-57, 2006.
- Rich JN and Bao S: Chemotherapy and cancer stem cells. *Cell Stem Cell.* 1: 353-355, 2007.
- Rodvold JJ, Mahadevan NR and Zanetti M: Lipocalin-2 in cancer: when good immunity goes bad. *Cancer let.* 316: 132-138, 2012.
- Roninson IB, Broude EV and Chang BD: If not apoptosis, then what? Treatment-induced senescence and mitotic catastrophe in tumor cells. *Drug Resist Updat.* 4: 303-313, 2001.
- Roti G and Stegmaier K. Genetic and proteomic approaches to identify cancer drug targets. *Br J Cancer.* 106(2): 254-261, 2012.

- Ruiz-Morales JM, Dorantes-Heredia R, Arrieta O, Chávez-Tapia NC, Motola-Kuba D, *et al*: Neutrophil gelatinase-associated lipocalin (NGAL) and matrix metalloproteinase-9 (MMP-9) prognostic value in lung adenocarcinoma. *Tumour Biol.* 36: 3601-3610, 2014.
- Saeed AM, Toonkel R, Glassberg MK, Nguyen D, Hu JJ, Zimmers TA, *et al*: The influence of Hispanic ethnicity on nonsmall cell lung cancer histology and patient survival: an analysis of the Survival, Epidemiology, and end Results database. *Cancer.* 118: 4495-4501, 2012.
- Saelens X, Festjens N, Vande Walle L, van Gorp M, van Loo G, Vandenabeele P. Toxic proteins released from mitochondria in cell death. *Oncogene.* 23(16): 2861-2874, 2004.
- Salem MSZ. Cancer: Some genetic considerations, *Egyptian Journal of Medical Human Genetics.* 16(1): 1-10, 2015.
- Sanai N, Alvarez-Buylla A and Berger MS. Neural stem cells and the origin of gliomas. *N Engl J Med.* 353(8): 811-822, 2005.
- Sansone P and Bromberg J: Targeting the interleukin-6/Jak/stat pathway in human malignancies. *J Clin Oncol.* 30(9): 1005-1014. 2012.
- Sarvi S, Mackinnon AC, Avlonitis N, Bradley M, Rintoul RC, *et al.*, CD133+ cancer stem-like cells in small cell lung cancer are highly tumorigenic and chemoresistant but sensitive to a novel neuropeptide antagonist. *Cancer Res.* 74(5): 1554-1565, 2014.
- Schober M and Fuchs E. Tumor-initiating stem cells of squamous cell carcinomas and their control by TGF- β and integrin/focal adhesion kinase (FAK) signaling. *PNAS.* 108(26): 10544-10549, 2011.
- Shi H, Gu Y, Yang J, Xu L, Mi W and Yu W: Lipocalin-2 promotes lung metastasis of murine breast cancer cells. *J Exp Clin Cancer Res.* 27: 1-9, 2008.
- Shibata T and Aburatani H: Exploration of liver cancer genomes. *Nat Rev Gastroenterol Hepatol* 11, 340-349, 2014.

- Shiiba M, Saito K, Fushimi K, Ishigami T, Shinozuka K, Nakashima D, *et al*: Lipocalin-2 is associated with radioresistance in oral cancer and lung cancer cells. *Int J Oncol.* 42: 1197-1204, 2013.
- Shimizu S, Takehara T, Hikita H, Kodama T, Miyagi T, *et al.*, The let-7 family of microRNAs inhibits Bcl-xL expression and potentiates sorafenib-induced apoptosis in human hepatocellular carcinoma. *J Hepatol.* 52(5):698-704, 2010.
- Shmelkov SV, Butler JM, Hooper AT, Hormigo A, Kushner J, *et al.*, CD133 expression is not restricted to stem cells, and both CD133+ and CD133- metastatic colon cancer cells initiate tumors. *J Clin Invest.* 118(6): 2111-2120, 2008.
- Shmelkov SV, St Clair R, Lyden D and Rafii S. AC133/CD133/Prominin-1. *Int J Biochem Cell Biol.* 37(4): 715-719, 2005.
- Shrivastava S, Steele R, Sowadski M, Crawford SE, Varvares M *et al.*, Identification of molecular signature of head and neck cancer stem-like cells. *Sci Rep.* 5: 7819, 2015.
- Siegel RL, Miller KD, Jemal A. Cancer Statistics, 2015. *CA Cancer J Clin.* 65:5–29, 2015.
- Siegel RL, Miller KD and Jemal A. Cancer statistics, 2016. *CA Cancer J Clin.* 66(1):7-30, 2016.
- Signore M, Ricci-Vitiani L, De Maria R. Targeting apoptosis pathways in cancer stem cells. *Cancer Lett.* 332(2):374-82, 2013.
- Soufizomorrod M, Soleimani M, Hajifathali A, Mohammadi MM and Abroun S: Expansion of CD133⁺ Umbilical Cord Blood Derived Hematopoietic Stem Cells on a Biocompatible Microwells. *Int J Hematol Oncol Stem Cell Res.* 7(1): 9-14, 2013.
- Suzuki HI, Katsura A, Miyazono K. A role of uridylation pathway for blockade of let-7 microRNA biogenesis by Lin28B. *Cancer Sci.* 106(9):1174-1181, 2015.
- Szczepanski MJ, Czystowska M, Szajnik M, Harasymczuk M, Boyiadzis M, *et al.*, Triggering of Toll-like receptor 4 expressed on human head and neck squamous cell carcinoma promotes

- tumor development and protects the tumor from immune attack. *Cancer Res.* 69(7): 3105-3113. 2009.
- Tai P. A practical update of surgical management of merkel cell carcinoma of the skin. *ISRN Surg.* 2013;2013:850797.
- Thorat RM, Gaikwad DD, Jadhav SL and Kokate ST. Oncogene: The Dominant Evil. *Int J of Pharm and Chem Sci.* 1(2): 570-583, 2012.
- Tian N, Han Z, Li Z, Zhou M, Fan C. Lin28/let-7/Bcl-xL pathway: the underlying mechanism of drug resistance in Hep3B cells. *Oncol Rep.* 32(3):1050-6, 2014.
- Tong M, Fung TM, Luk ST, Ng KY, Lee TK, et al.: ANXA3/JNK Signaling Promotes Self-Renewal and Tumor Growth, and Its Blockade Provides a Therapeutic Target for Hepatocellular Carcinoma. *Stem Cell Reports* 5, 45-59, 2015.
- Torre LA, Bray F, Siegel RL, Ferlay J, Lortet-Tieulent J and Jemal A: Cancer incidence and mortality worldwide: sources, methods and major patterns in GLOBOCAN 2012. *CA Cancer J Clin.* 65: 87-108, 2015.
- Tsai JH and Yang J: Epithelial-mesenchymal plasticity in carcinoma metastasis. *Genes Dev.* 27: 2192-2206, 2013.
- Tung MC, Hsieh SC, Yang SF, Cheng CW, Tsai RT, Wang SC, et al: Knockdown of lipocalin-2 suppresses the growth and invasion of prostate cancer cells. *Prostate.* 73: 1281-1290, 2013.
- Urashima M, Teoh G, Chauhan D, Hoshi Y, Ogata A, et al., Interleukin-6 overcomes p21WAF1 upregulation and G1 growth arrest induced by dexamethasone and interferon-gamma in multiple myeloma cells. *Blood.* 90(1): 279-89, 1997.
- van der Heijden M, Zimmerlin CD, Nicholson AM, Colak S, Kemp R. Bcl-2 is a critical mediator of intestinal transformation. *Nat Commun.* 7:10916, 2016.

- Venook AP, Papandreou C, Furuse J and de Guevara LL: The incidence and epidemiology of hepatocellular carcinoma: a global and regional perspective. *Oncologist*. 4: 5-13, 2010.
- Vermeulen K, Van Bockstaele DR and Berneman ZN: The cell cycle: a review of regulation, deregulation and therapeutic targets in cancer. *Cell Prolif* 36, 131-149, 2003.
- Vogelstein B and Kinzler KW: Cancer genes and the pathways they control. *Nat Med*. 10(8):789-99, 2004.
- Vriesendorp HM, Vriesendorp R, Vriesendorp FJ. Prediction of normal tissue damage induced by cancer chemotherapy. *Cancer_Chemother Pharmacol*. 19(4):273-276, 1987.
- Wang P, Gao Q, Suo Z, Munthe E, Solberg S, Ma L, *et al*: Identification and characterization of cells with cancer stem cell properties in human primary lung cancer cell lines. *PLoS One*. 8: e57020, 2013.
- Wang Y, Thakur A, Sun Y, Wu J, Biliran H, *et al*: Synergistic effect of cyclinD1 and c-Myc leads to more aggressive and invasive mammary tumors in severe combined immunodeficient mice. *Cancer Res*. 67(8): 3698-707, 2007.
- Warwick GP. The mechanism of action of alkylating agents. *Cancer Res*. 23:1315-33, 1963.
- Weinberg SE, Chandel NS. Targeting mitochondria metabolism for cancer therapy. *Nat Chem Biol*. 11(1):9-15, 2015.
- Woodward WA and Sulman EP. Cancer stem cells: markers or biomarkers? *Cancer Metastasis Rev*. 27: 459-470, 2008.
- Wu XZ. A new classification system of anticancer drugs - based on cell biological mechanisms. *Med Hypotheses*. 66(5):883-887, 2006.
- Xiong W, Luo G, Zhou L, Zeng Y and Yang W. In vitro and in vivo antitumor effects of acetylshikonin isolated from *Arnebia euchroma* (Royle) Johnston (Ruanzicao) cell suspension cultures. *Chin Med*. 4:14, 1-7, 2009.

- Xue Y, Ren H, Xiao W, Chu Z, Lee JJ and Mao L: Antitumor activity of AZ64 via G2/M arrest in non-small cell lung cancer. *Int J Oncol.* 41(5): 1798-808, 2012.
- Yamashita T and Kaneko S: Orchestration of hepatocellular carcinoma development by diverse liver cancer stem cells. *J Gastroenterol.* 49, 1105-11010, 2014.
- Yamashita T and Wang XW: Cancer stem cells in the development of liver cancer. *J Clin Invest.* 123, 1911-1918, 2013.
- Yan HQ, Huang XB, Ke SZ, Jiang YN, Zhang YH, et al., Interleukin 6 augments lung cancer chemotherapeutic resistance via ataxiatelangiectasia mutated/NF-kappaB pathway activation. *Cancer Sci.* 105(9): 1220-1227, 2014.
- Yang J and Moses MA: Lipocalin 2: a multifaceted modulator of human cancer. *Cell Cycle.* 8: 2347-2352, 2009.
- Yang J, Bielenberg DR, Rodig SJ, Doiron R, Clifton MC, Kung AL, et al: Lipocalin-2 promotes breast cancer progression. *Proc Natl Acad Sci U S A.* 106: 3913-3918, 2009.
- Yokota J. Tumor progression and metastasis. *Carcinogenesis.* 21(3): 497-503, 2000.
- Yonehara A, Tanaka Y, Kulkeaw K, Era T, Nakanishi Y, et al.: Aloe vera Extract Suppresses Proliferation of Neuroblastoma Cells In Vitro. *Anticancer Res.* 35, 4479-85, 2015.
- Yoon CH, Kim MJ, Kim RK, Lim EJ, Choi KS, et al.: c-Jun N-terminal kinase has a pivotal role in the maintenance of self-renewal and tumorigenicity in glioma stem-like cells. *Oncogene.* 31, 4655-4666, 2012.
- Zhai L, Wang T, Kang K, Zhao Y, Shrotriya P and Nilsen-Hamilton M: An RNA aptamer-based microcantilever sensor to detect the inflammatory marker, mouse lipocalin-2. *Anal Chem.* 84: 8763-8770, 2012.

- Zhang B, Yuan Q, Huang L, Liu X, Li X, et al., Locality identification of Chinese medicinal plant *Scutellaria baicalensis* (Lamiaceae) population-level DNA barcoding. *Zhongguo Zhong Yao Za Zhi*. 37(8): 1100-1106. 2012.
- Zhang YX, Kong CZ, Wang HQ, Wang LH, Xu CL, et al.: Phosphorylation of Bcl-2 and activation of caspase-3 via the c-Jun N-terminal kinase pathway in ursolic acid-induced DU145 cells apoptosis. *Biochimie*. 91, 1173-1179, 2009.
- Zhao P, Elks CM and Stephens JM: The induction of lipocalin-2 protein expression *in vivo* and *in vitro*. *J Biol Chem*. 289: 5960-5969, 2014.
- Zhao R, Gao X, Cai Y, Shao X, Jia G, et al.: Antitumor activity of *Portulaca oleracea* L. polysaccharides against cervical carcinoma *in vitro* and *in vivo*. *Carbohydr Polym*. 96, 376-83, 2013.